TEMPORAL AND SPATIAL VARIATIONS OF HYDRAULIC CONDUCTIVITY IN A STREAM BED IN GOLDEN COLORADO

by

Steven R. Hannula and Eileen Poeter

April 11, 1995

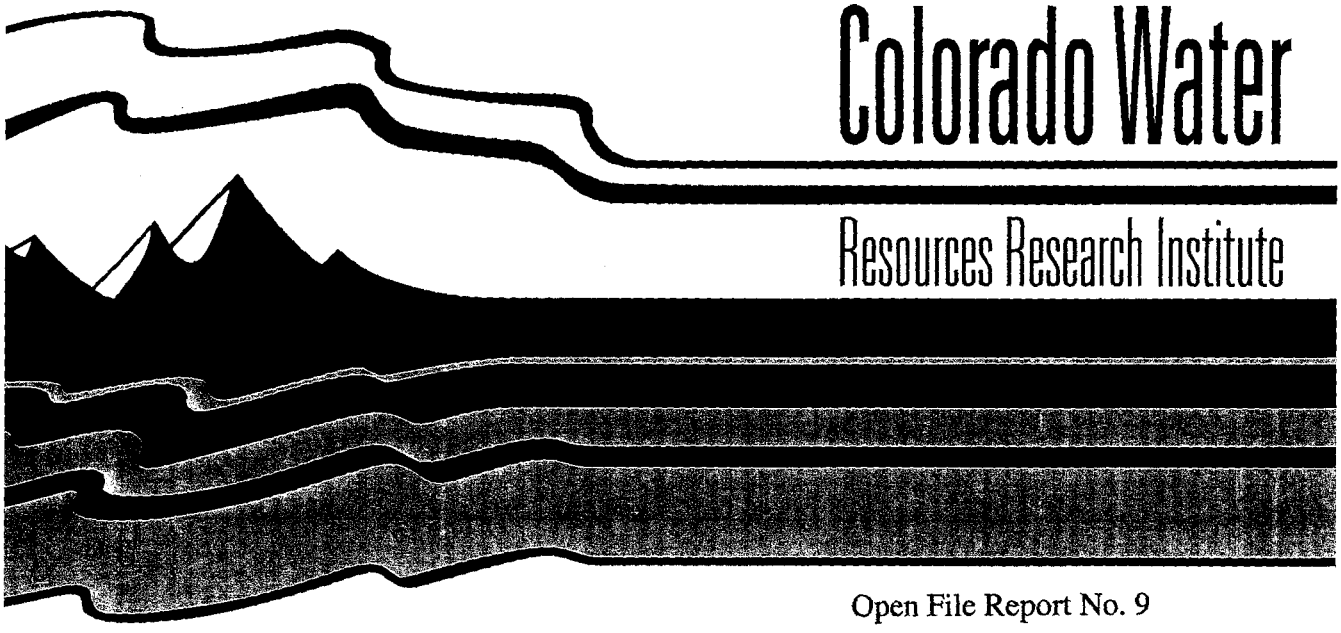

Open File Report No. 9

Colorado State University

TEMPORAL AND SPATIAL VARIATIONS OF HYDRAULIC CONDUCTIVITY IN A STREAM BED IN GOLDEN COLORADO

by

Steven R. Hannula and Eileen P. Poeter

Geology and Geological Engineering
Colorado School of Mines

April 11, 1995

Grant No. 14-08-0001-G2008/3
Project No. 07

The research on which this report is based was financed in part by the U.S. Department of the Interior, Geological Survey, through the Colorado Water Resources Research Institute; and the contents of this publication do not necessarily reflect the views and policies of the U.S. Department of the Interior, nor does mention of trade names of commercial products constitute their endorsement by the United States Government.

COLORADO WATER RESOURCES RESEARCH INSTITUTE
Colorado State University
Fort Collins, Colorado 80523

Robert C. Ward, Director

ABSTRACT

Temporal and spatial variations of hydraulic conductivity were measured along a stream bed, located on the Colorado School of Mines survey field in Golden Colorado. A portable, in-situ, constant head permeameter was built to measure hydraulic conductivity. Hydraulic conductivity of the stream bed ranged from 9×10^{-4} to 2×10^{-2} cm/sec. Two V-notched weirs were used to measure stream discharge and a network of fifty five piezometers was used to monitor hydraulic gradient in the stream bed. Piezometer measurements defined a gaining and losing section in the stream. The period of study included changing hydraulic conditions in the stream bed. Hydraulic conductivity varied in time as hydraulic conditions changed. The temporal and spatial variations of hydraulic conductivity were used in conjunction with other hydraulic parameters to estimate the flow rate between the stream and the underlying aquifer. The data were also used to develop several conceptual models to illustrate the uncertainty of hydrologic conditions observed at the site.

TABLE OF CONTENTS

LIST OF FIGURES

LIST OF TABLES

Chapter 1. INTRODUCTION

1.1 Background

Quantifying the interaction between surface water and ground water is challenging because heterogeneities within the soil and rock can create a large spatial variability in the hydraulic parameters. Furthermore, parameters such as the hydraulic conductivity of a stream bed, K, and vertical gradient have both spatial and temporal variability that add challenges to characterizing stream/aquifer interaction. These spatial and temporal variations of hydraulic parameters are best characterized through a well timed and placed sampling program. Single values of hydraulic conductivity and gradient are of limited value to understanding stream/aquifer interaction. Confidence in the measurement of these hydraulic parameters increases when the number of samples increases. For example, the seepage rate between a stream and the underlying aquifer depends upon several factors, two of which are stream stage and the hydraulic conductivity of the stream bed. These two factors change with time and a single measurement may not be representative, which affects the accuracy of the seepage calculation.

The quality of stream/aquifer characterization hinges on accurate measurements of the variable hydraulic parameters. A model that includes stream/aquifer interaction is affected by inaccuracies of stream characterization to different degrees depending on the relative scale of the model and the stream. A small stream's changes throughout the year may be insignificant to the accuracy of a large basin model, but for a focused study on that small stream, the temporal variations can be significant to the accuracy of the model. When variability of hydraulic parameters of a stream is thought to be significant, an effort should be made to quantify that variability.

This project includes quantifying the temporal and spatial variability of several hydraulic parameters along a stream bed through a sampling program specifically designed for this variability. Measuring the changing hydraulic parameters requires several in-situ techniques. Field measurements include: in-situ hydraulic conductivity of the stream bed, near-surface head measurements to establish hydraulic gradients, stream flow at both ends of the field site, and head measurements in piezometers located in the alluvium adjacent to the stream. To observe changes in sediment composition, grain-size analyses of sediment taken from the stream bottom at various times are performed. The study began in February, 1994, when stream discharge was low, continued through the spring during high flow periods and finished in July 1994 when the stream went dry.

1.2 Objective and Purpose

The purpose of this project is to understand the nature of stream/aquifer interactions. The methods and interpretation techniques used in this project are applicable to many

hydrogeologic studies. For example, projects that assess the impact of polluted stream wat on nearby ground water or determine impacts of pumping ground water to stream flow require an understanding of stream/aquifer interaction. The nature of stream/aquifer interaction is an important influence on the quality of ground water or surface water when pollutants are nearby.

To identify the nature of the stream/aquifer interaction at the site, three objectives a defined:

1) Quantify the temporal and spatial variations of the hydraulic conductivity and the vertical hydraulic gradient within a stream bed.

2) Use these temporal values to calculate the net volumetric flow rate between the stream and the underlying aquifer.

3) Develop several conceptual models of stream/aquifer interactions at the site.

1.3 Location and Description of Site

The site consists of 200 feet of an intermittent stream on the Colorado School of Mines (CSM) survey field in Golden, Colorado about one mile southwest of the CSM camp (Figure 1.1). This stream is part of a primary drainage path for Lookout Mountain and is tributary to Kenney's Creek and Clear Creek. The local groundwater system consists of a shallow, alluvial aquifer. The water table and the paleo-topography of the underlying bedrock control the thickness and the lateral extent of the alluvial aquifer. The bedrock is 0 to 25 feet below land surface and is assumed to be relatively impermeable compared to the alluvium. Peak discharge of the stream is approximately 1.2 cubic feet per second (cfs).

Hydrologic conditions along the stream define the extent of the site. The upstream boundary is placed at the upper end of a section of stream that gains in the spring; the downstream boundary is downgradient of a section of stream that loses in the spring. The gaining and losing sections are obvious when the stream is almost dry. During these times c transition, the upper end of the gaining section is marked by a spring, and the lower end of the site is marked by a dry stream bed. At other times these boundaries are not obvious. The lateral boundaries are defined parallel to the stream path and away from influences of th stream near possible contacts between alluvium, bedrock, and the water table.

The small size, accessible location, and changing hydrologic characteristics of the stream make this field site ideal for this study. The disturbances to the stream are the weirs and piezometers installed in a previous study (Anderman, 1993). Boreholes for the nested piezometers are the only disturbance to the alluvium. An average annual precipitation of 18 to 23 inches falls on the site (Anderman, 1993). A large portion of the streams' discharge occurs from melting snow, which abates in the month of May. The large changes in the stream discharge create a dynamic environment in the stream bed.

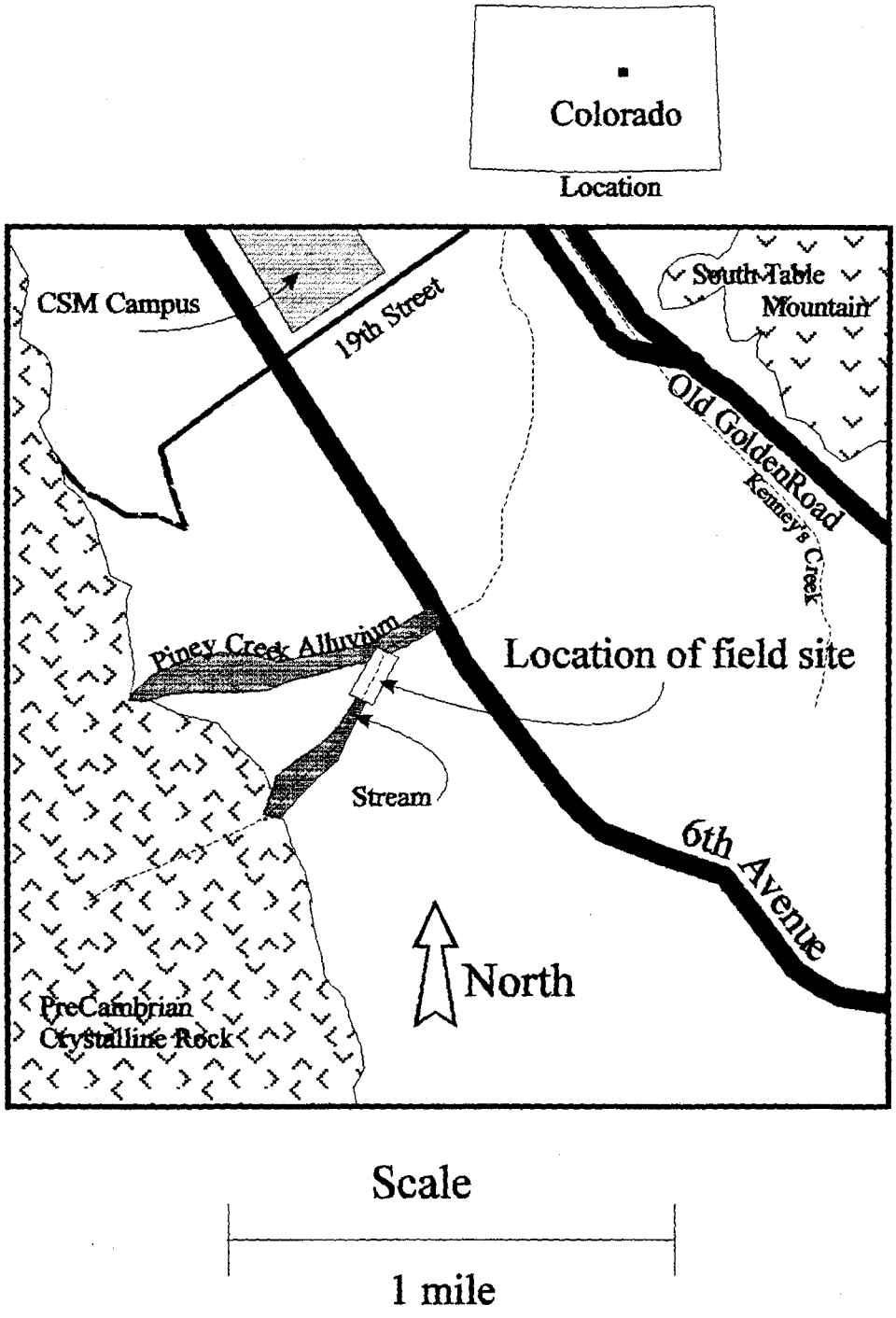

Figure 1.1 Location map of field site.

1.4 Geology of Site

The geology of the site consists of 0 to 25 feet of Piney Creek alluvium overlying nearly vertical to overturned layers of bedrock. A geologic outcrop near the field site is used along with a published geologic map of the Morrison Quadrangle (Scott, 1972), to develop maps presented in Figure 1.2a and 1.2b. There are three units underlying the site: the Strain Shale Member (LeRoy, 1946) (Triassic? and Permian), the Ralston Creek Formation (Upper Jurassic), and the Morrison Formation (Upper Jurassic). The Piney Creek Alluvium (Upper Holocene) is a dark-gray to reddish-brown humic clayey silt and sand containing layers of pebbles and gravel (Scott, 1972). The orientation of the bedrock layers is approximately N50W dipping 70°E. The proliferation of cobbles and boulders along the stream bottom can be explained by the proximity of the Precambrian crystalline rocks comprising the foothills. The Golden Fault strikes roughly north-northwest near the east end of the site. A conceptualization of the geologic cross section as interpreted from the surface expression is presented in Figure 1.3. The distribution of material types along the stream bed is presented in Figure 1.4.

Conditions in the underlying geologic units are important to the understanding of the stream/aquifer interaction. Information such as; depth to bedrock, permeability relative to the overlying alluvium, and the nature of the bedrock surface is important for conceptualization of the hydrogeology.

1.5 Previous Work

In a field study by Anderman (1993), a network of piezometers and weirs was established to study the hydraulic properties of the stream at the field site. That work established a basis for interpretations of the stream/aquifer interactions.

Bissett (1994) used geophysical methods to determine the depth to the bedrock unit that was then used to construct a MODFLOW model simulating this site. Lack of data prevented this attempt to accurately model the site. Conclusions from both Anderman and Bissett suggested that the underlying geology of the site and spatial and temporal variations in the hydraulic parameters must play an important role in this hydrologic system and that more data were required for an accurate interpretation.

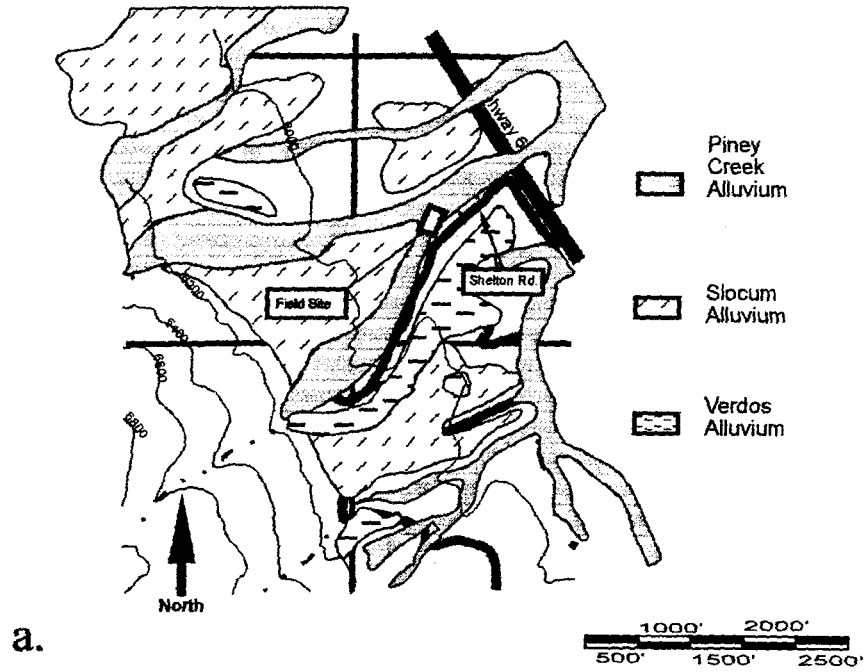

a.

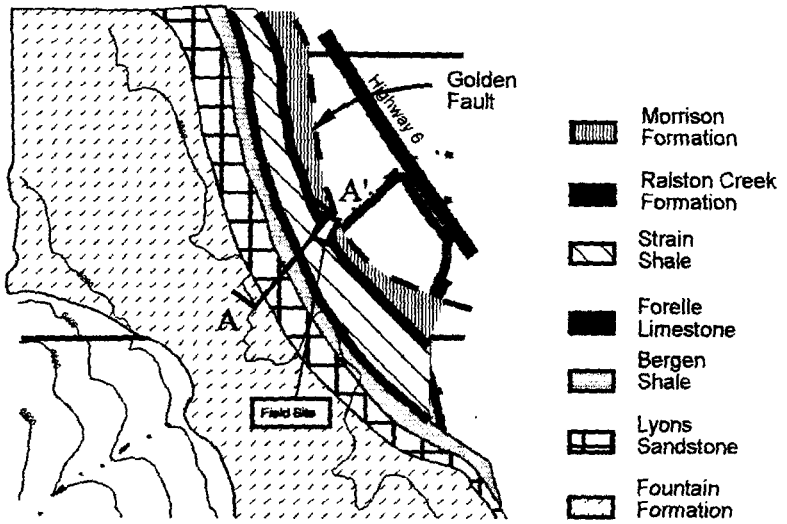

b.

Figure 1.2 a,b Surface and subsurface geology in the vicinity of the field site.

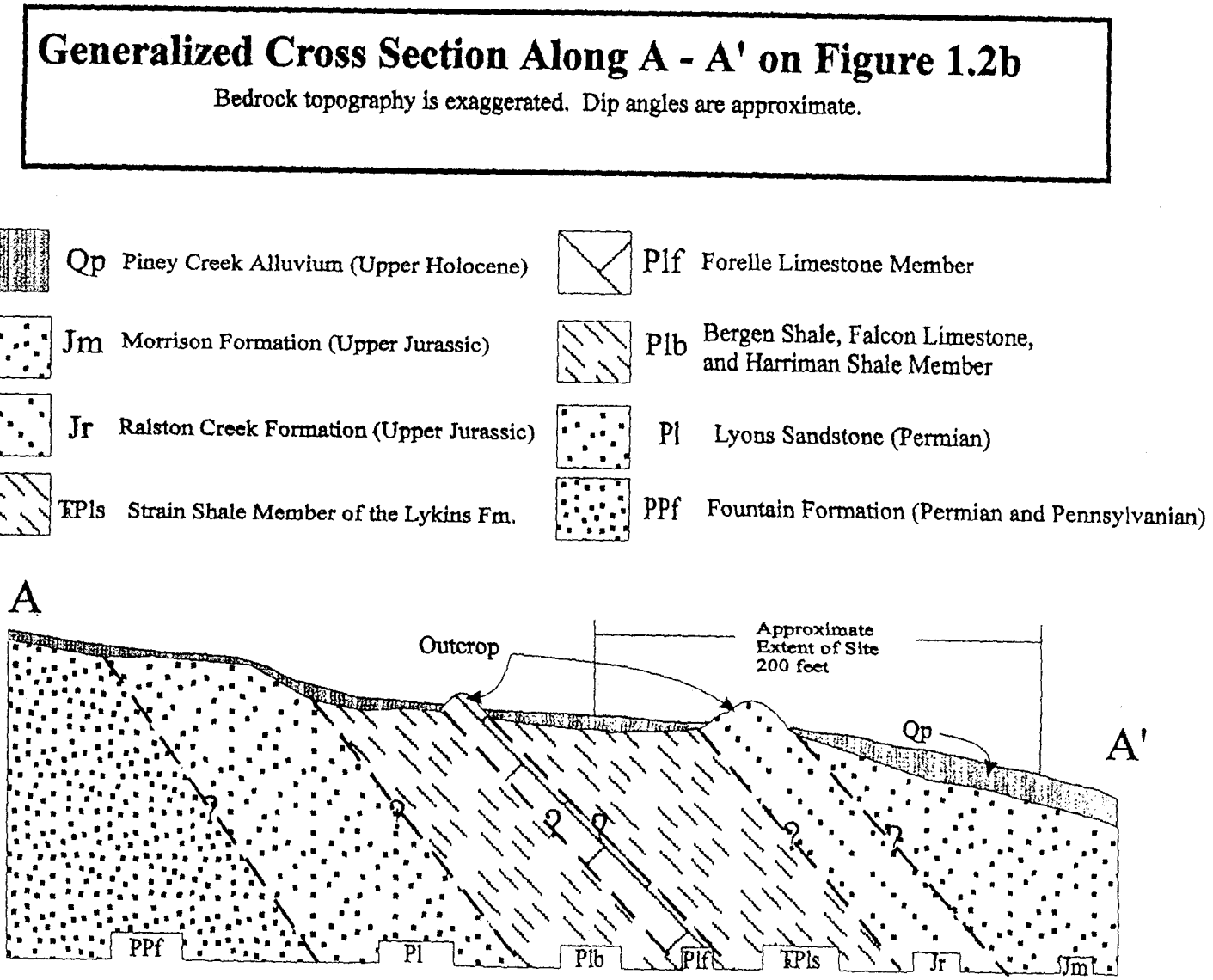

Figure 1.3 Cross section of the field site.

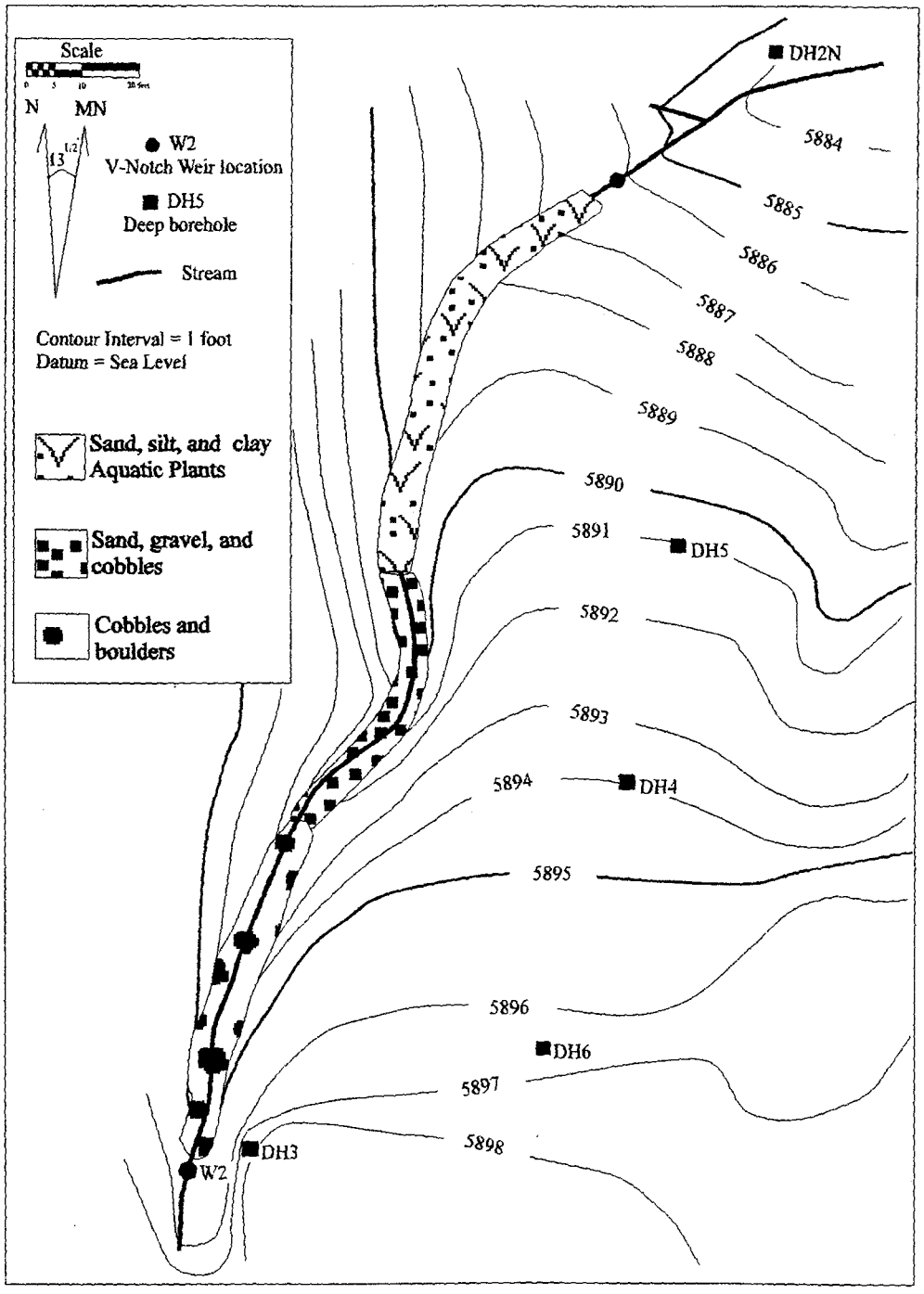

Figure 1.4 Topographic map with stream bed description.

Chapter 2. FIELD METHODS, DATA COLLECTION, INTERPRETATION

2.1 The Constant Head Permeameter

To satisfy the first objective, in-situ measurements of hydraulic conductivity made with minimal disturbance to the stream bed are needed. Several locations along the stream channel are established that can be revisited several times throughout the season. A consta head permeameter is used for measuring hydraulic conductivity of the stream bed, and is based on an experiment by Amoozegar (1989). Amoozegar constructed a compact constan head permeameter for measuring field saturated hydraulic conductivity within a borehole. similar device is the commercially available Guelph Permeameter developed by Reynolds e al. (1983, 1984). An adaptation to the permeameter by Amoozegar is made to operate in a stream bottom as described in Appendix A. The Mariotte principle is used to maintain a constant head of water inside a cylinder as described below, see Appendix B for details.

The major adaptation from Amoozegar's design is the utilization of the Mariotte principle with a cylinder permeameter. A cylinder permeameter is a cylinder driven into th soil about 15 cm, with tensiometers placed close to the cylinder at a depth of approximately 20 cm. Water is maintained in the cylinder until saturation is achieved. Saturation has bee achieved when the tensiometers register a zero pressure head. Infiltration rate is then measured and hydraulic conductivity is calculated using Darcy's Law.

A modified cylinder permeameter is used in conjunction with the Mariotte principle for this project. A schematic of the cylinder construction is presented in Figure 2.1. A sharp metal edge is attached to the cylinder to slice down into the soil to a depth of about o inch, rather than being driven to a depth of 15 cm. The thin metal edge can be removed from the soil easily which results in minimal damage to the bed. Saturation of the stream bed is assumed to prevail at all times since the stream of interest is flowing. The head in th cylinder is maintained constant by the Mariotte principle. Perforated tubes, or piezometers are used in place of tensiometers. Two piezometers are placed into the stream bed to measure the head beneath the cylinder. The piezometers indicate a stabilized head level in the tube when steady state conditions are achieved. A schematic of the constant head permeameter cylinder and piezometers is presented in Figure 2.2.

2.1.1 Use of the Constant Head Permeameter

Weekly field measurements of saturated hydraulic conductivity (Ksat) were made at 1 stations along the stream, beginning in March 1994, and continued through June 1994. Temporal variations were detected by returning to identical stations several times throughout the season. Spatial variations were detected by operating the permeameter at the 11 stations. Stations were chosen primarily on whether the cylinder could actually be inserted into the soil. Stony soil was not suitable for the constant head permeameter. Ksat was expected to b

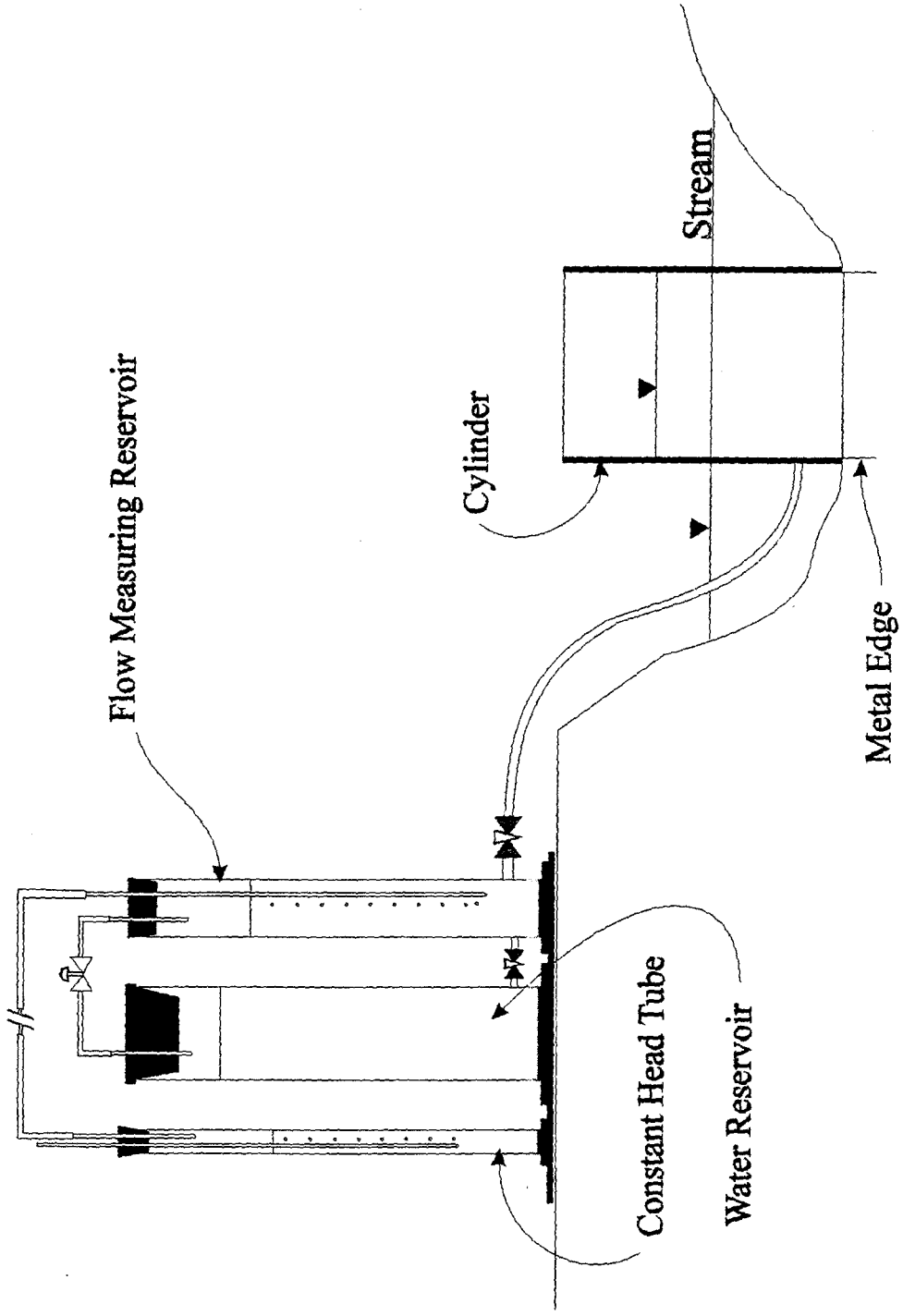

Figure 2.1 Constant head permeameter.

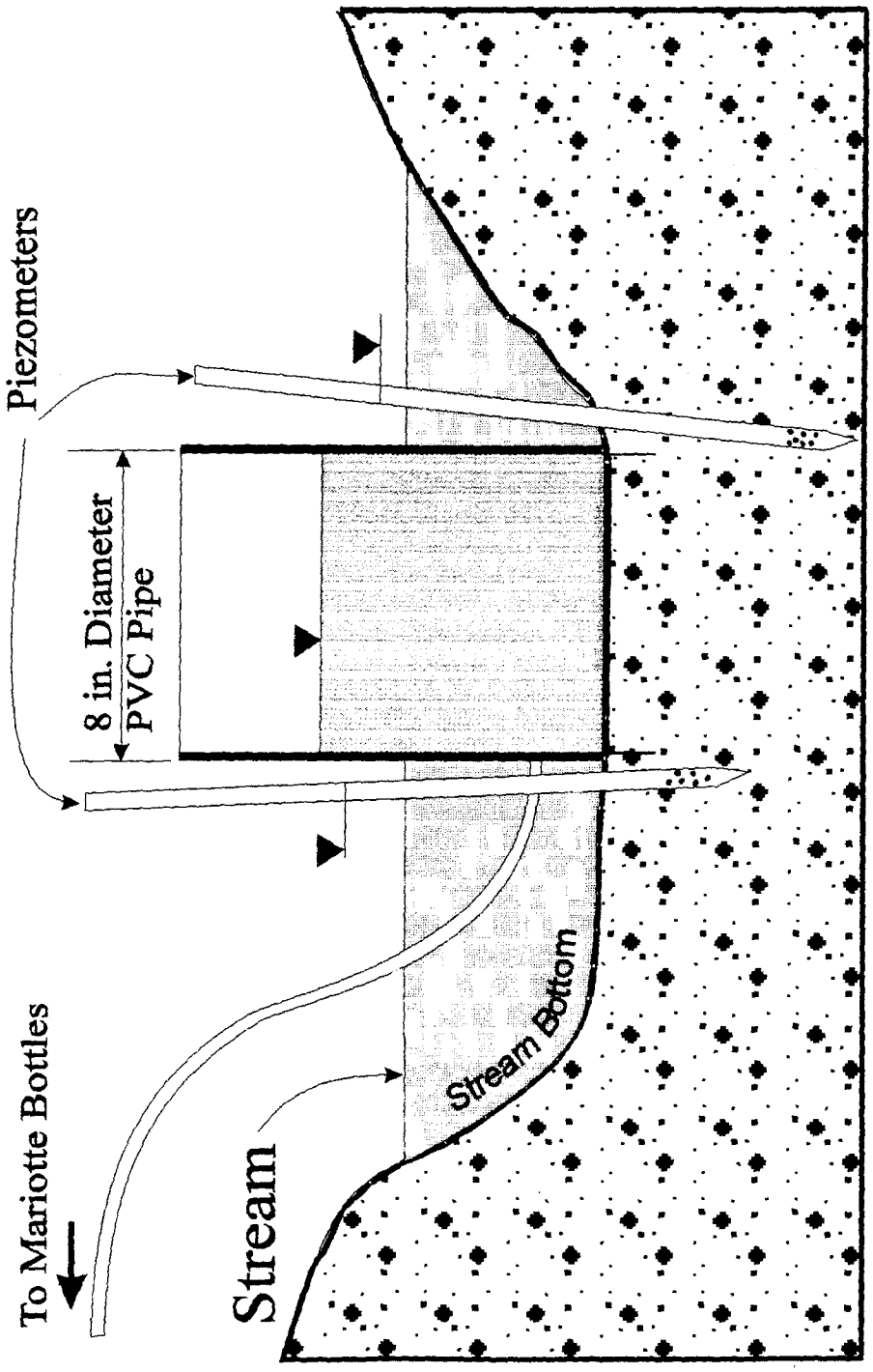

Figure 2.2 Layout of the constant head permeameter cylinder and piezometers.

affected by two factors: the seasonal variations in stream discharge, and the direction and magnitude of vertical gradients.

2.1.2 Considerations in the Permeameter Design

Amoozegar's permeameter is designed to measure hydraulic conductivity in a variably-saturated borehole (Amoozegar, 1989). The application for this project is different in two ways: 1) the permeameter is used on a stream bottom, not in a borehole; and 2) the stream bottom is assumed to be fully saturated. These differences require changes in the design of the permeameter from Amoozegar's version. Considerations addressed in the design of the permeameter include: minimizing the disturbance to the stream bed, ensuring a good seal between the cylinder and the stream bed material, incorporating a large enough area of the stream bottom to be representative, and the ability to impose a gradient downward yet keep the head in the cylinder a minimum.

The seal between the cylinder and the soil is critical for consistent results. Finer material forms a better seal against the permeameter than coarse material. This technique is not suitable for stony soil. If cobbles and gravel are present, the metal edge on the cylinder cannot penetrate completely and open channels may occur between the gravel particles and the permeameter, thus the flow rate is not representative of the soil's hydraulic conductivity. A smaller cylinder is easier to insert into the ground, but may not encompass a representative area. An eight-inch diameter cylinder is chosen for portability, ease of inserting into the soil, and a large surface area of measurement.

The gradient beneath the cylinder is controlled by operating the Mariotte Bottles as described in Appendix B. Edge effects are reduced by maintaining a low gradient beneath the cylinder. An extreme example of this problem is a critical gradient condition. A critical gradient condition is such that if the difference in head between the cylinder and the outside is sufficient, the flow of water actually suspends the sediments, creating a boiling condition. If boiling occurs, the water flows through the soil in a turbulent fashion and Darcy's Law cannot apply. The gradient between the head in the cylinder and the stream has to be kept small to ensure flow is laminar.

For a description of the construction of the constant head permeameter, see Appendix A. A discussion on the Mariotte bottles is provided in Appendix B.

2.1.3 Observations Required

The principle of the permeameter is based on the continuity equation ($flow_{in}$ - $flow_{out}$ = Δstorage). The constant head permeameter has a zero Δstorage term. This means, the amount of water flowing out of the cylinder into the stream bed is exactly replaced by water flowing from the reservoir of the permeameter. By recording the volume of water that flows out of the reservoir as a function of time, the volumetric flow rate into the ground is known.

The field observations required to determine the temporal variability of permeability using the constant head permeameter are: 1) volume of water lost from the reservoir(s), 2) elapsed time, 3) head maintained, 4) piezometer levels, 5) stream stage, and 6) date of test.

Interpretation of these data is based upon Darcy's Law and the geometry of the flow field beneath the cylinder as described in section 2.1.6 and 2.1.7 (Demir and Narasimhan, 199 Hvorslev, 1951; Taylor, 1946).

2.1.4 Limitations and Errors With the Constant Head Permeameter

The constant head permeameter has several limitations. The seal between the met edge on the cylinder and the stream bottom is critical for accurate and consistent results. this seal is poor, water can short circuit around the natural material thus producing errone results. Fine sands, silt, and clay provide the best seal, while coarse sand, gravel, and cobbles make poor seals. Operator judgement is required to decide whether the seal is sufficient.

In tight soils, the rate of flow through the permeameter is small, especially when t is little difference between the head in the cylinder and the piezometers. Consequently, th bubbles that form to pass air from the atmosphere through the Mariotte bottles and into th reservoir have sufficient resistance to impede flow. This resistance is overcome when a sufficient pressure imbalance develops in the Mariotte bottles and a volume change is registered. This resistance and resulting pressure imbalance can cause fluctuations in flow These fluctuations in flow are averaged out and become negligible over the length of a tes Additional perturbations in flow rate are observed which are attributed to subtle changes i atmospheric pressure and amount of direct sunlight hitting the Mariotte bottles, which war both the air and water causing them to expand.

Despite the shortcomings, this device proves to be easy to use, portable and consistent. However, a different permeameter design is needed for material with a hydrau conductivity less than approximately $1x10^{-5}$ cm/sec. Head loss in the current permeameter design may cause significant errors at low flow rates. Also, for material with a hydraulic conductivity greater than approximately $1x10^{-2}$ cm/sec, a constant head is difficult to maint with this permeameter design. When testing high K materials, the rate of infiltration is greater than the rate at which the reservoirs can replace the water in the cylinder, thus the constant head is lost. A taller cylinder and an anchoring device is required to use the curr permeameter design in a deep stream. Although the permeameter may not provide a meas of absolute values of K, relative values of hydraulic conductivity can be measured with thi device, because the errors that prevent the results from being absolute, are consistent.

The procedure used for obtaining a representative measurement of the gradient imposed by the constant head permeameter is incorrect. The gradient is determined by dividing the distance between the water level inside of the cylinder and the water level in t adjacent piezometer by the distance from the stream bed surface to the center of the open interval of the piezometer. However, field measurements to obtain head in the piezometer reference the top of the piezometer, which is fixed relative to the datum used to establish t elevations at the site. The reference for the head in the cylinder is the elevation of the stre bed, which is not fixed, but is assumed fixed for the calculations. Furthermore, within the eight-inch diameter cylinder, the surface of the stream bed is not always level. Using the stream bed surface is a poor choice of datum to reference the elevation of the constant hea

By not having a stable datum, the resulting elevation of the constant head is not consistent. The fluctuations of the stream bed elevation relative to the fixed value in the calculations of gradient are significant enough to reverse the direction of gradient, which results in some negative values for K.

2.1.5 Operation of Permeameter

Undisturbed piezometer water levels are measured before installing the permeameter at a site to determine the natural gradient. The installation of the constant head permeameter begins by inserting the cylinder vertically into the stream bottom sediments. A downward gradient is imposed by filling the cylinder higher than the stage of the stream. Care must be taken when filling the cylinder not to agitate the sediment of the stream bed. An equilibrium is established between the flow of water from the reservoirs to the cylinder and into the stream bed by adjusting the brass rod on bottle 1 as described in Appendix B. The Mariotte bottles are illustrated in Figure 2.3. While the permeameter is running, piezometer levels are monitored to establish when steady state conditions are approached, which usually occurs within 10 minutes. When the water levels in the piezometers no longer fluctuate, the levels are recorded, which establishes the hydraulic head at a depth of 4 and 7 inches below the stream bottom. The gradient term of Darcy's Law is evaluated as the difference between the head inside the cylinder and the head 4 inches below the stream bottom. The chance of erroneous measurements is reduced by conducting two tests with different constant heads in the cylinder.

2.1.6 Analysis of Permeameter Data using Darcy's Law

Using the data from the permeameter, hydraulic conductivity can be calculated using Darcy's equation,

$$Q = KiA \tag{2.1}$$

or rearranging:

$$K = \frac{Q}{iA} \tag{2.2}$$

where:

Q= volumetric flow (L^3/T)
K= Hydraulic Conductivity (L/T)
i = Gradient (unitless)
A= Cross Sectional Area (L^2).

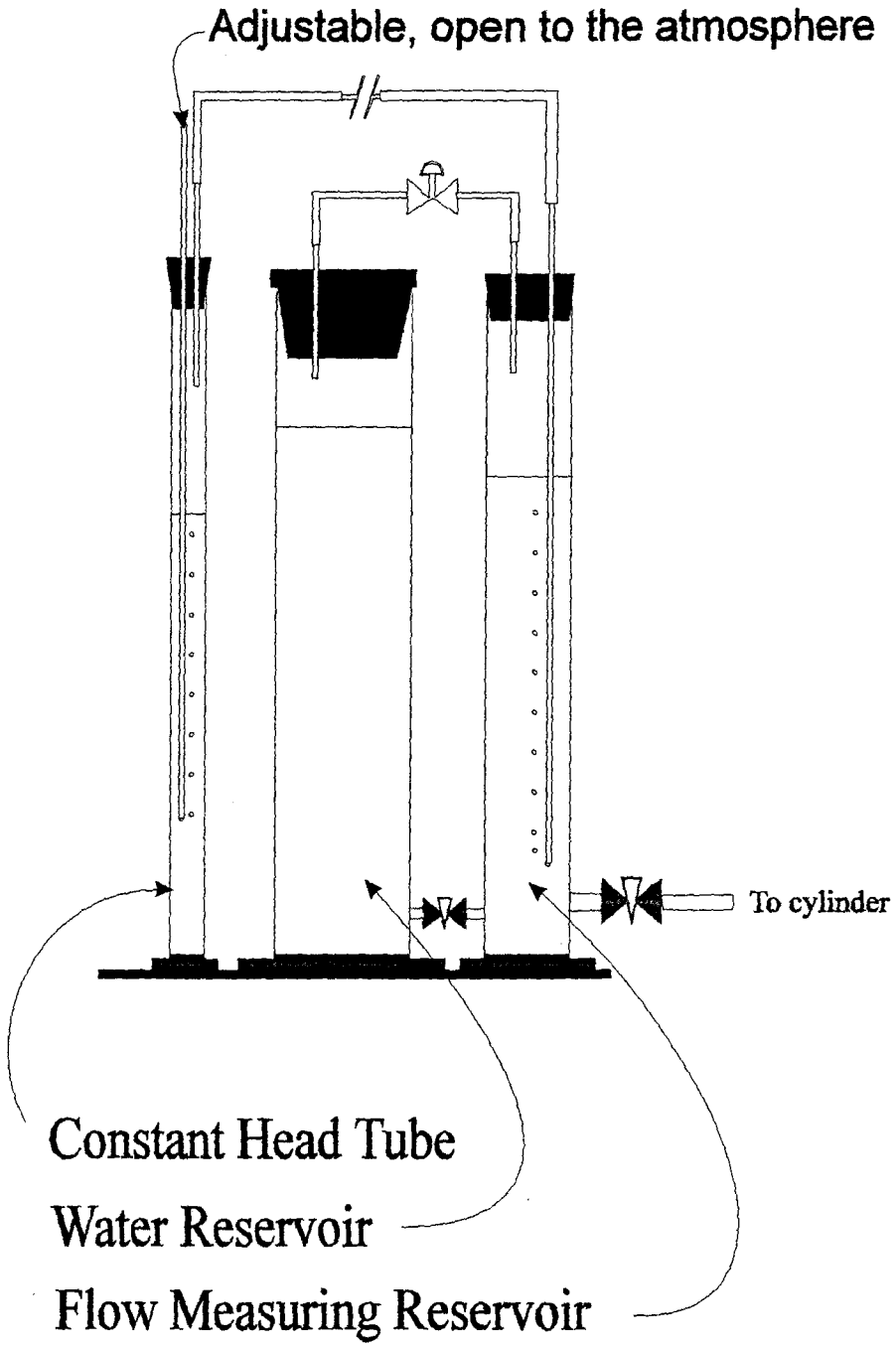

Figure 2.3 The Mariotte Bottles.

Q is the quotient of the volume drained from the reservoir of the permeameter and the time period during which that volume accumulates. A is the cross sectional area of the cylinder. Gradient, i, is determined by dividing the difference between the head in the cylinder and the head in the adjacent piezometer by the distance between the stream bottom elevation and the elevation of the open interval of the piezometer.

2.1.7 Geometry Based Analysis of Permeameter Data using Darcy's Law

An option to solving for saturated hydraulic conductivity (Ksat) with Darcy's Law is to use an empirical solution given by Hvorslev (1951). Hvorslev bases his formula on experiments by Harza (1935) and a graphical solution through radial flow nets by Taylor (1948). Taylor's radial flow net solution uses Darcy's Law and flow net techniques to get an empirical solution for flow through a circular well point where the flow is the same for all radial cross sections through a given axis. To verify the solution is applicable to the constant head permeameter, a flow net is constructed as shown in Figure 2.4.

To construct a radial flow net, several assumptions are made. First, the flow in each flow tube remains the same throughout the flow path, meaning that there is no transverse flow between tubes. Second, the total flow through the cylinder is equally divided between the flow tubes, as shown in equation 2.3. The third assumption is that the cross sectional area of flow increases as a function of radius. Also, Darcy's Law is valid and the soil is homogeneous.

$$Q = \Delta Q \, n_f \tag{2.3}$$

where:

ΔQ = Flow through one flow tube.
n_f = Total number of flow tubes.
Q = Total flow through cylinder.

The construction of the flow net is drawn on a plane of axial symmetry. Darcy's Law can be rewritten for a single element of the flow net with the following substitutions; where an element is defined as the volume between two adjacent flow lines and two successive equipotentials. The area of flow can be described as the area of the base of a cylindrical wall with an inner radius of r_1 and an outer radius of r_2, (Figure 2.4).

$$Area = \pi(r_2^2 - r_1^2) \tag{2.4}$$

The gradient term can be described as the change in head over the length of one element of the flow net.

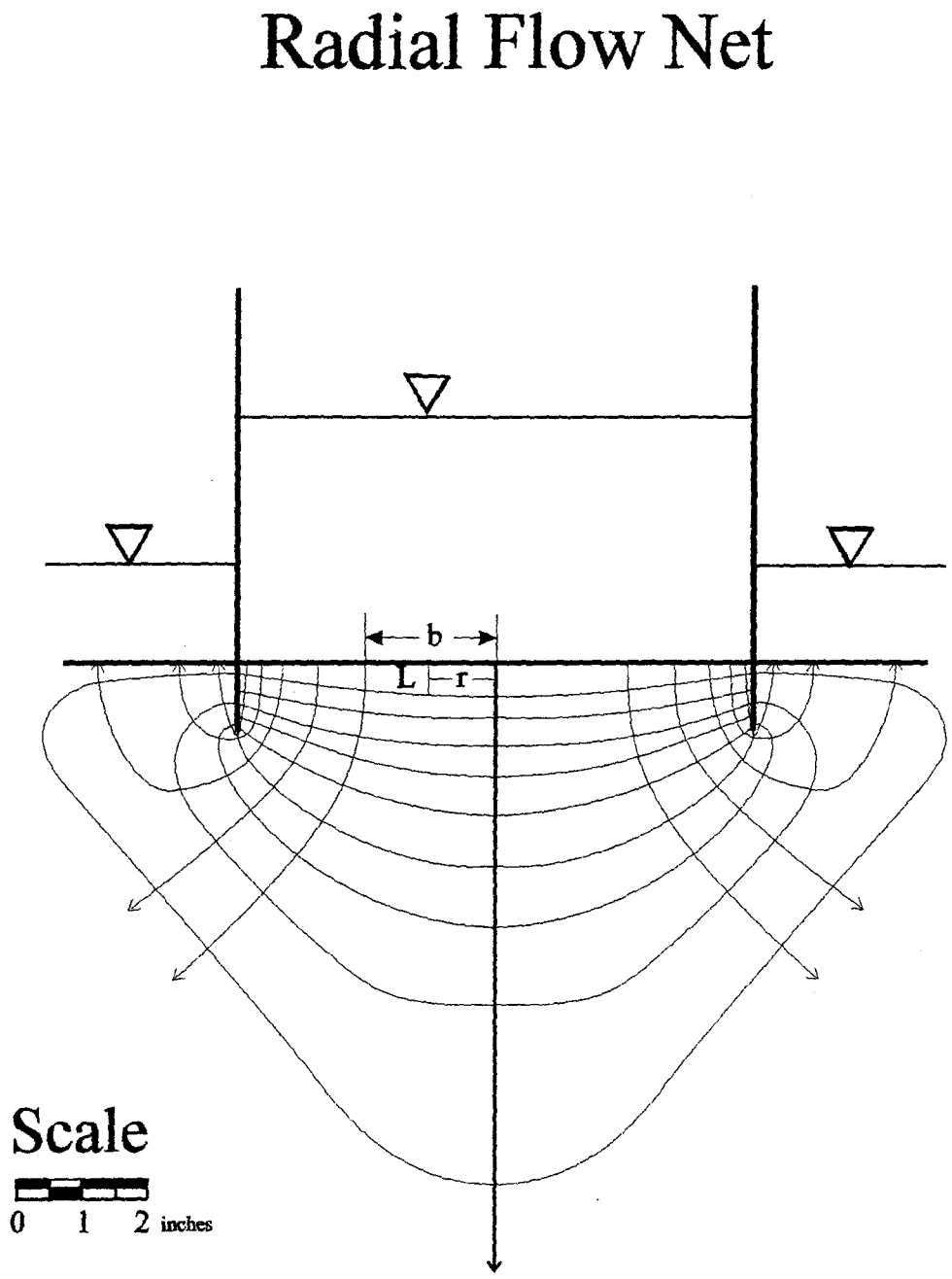

Figure 2.4 Radial flow net for interpretation of permeameter data.

$$Gradient = i = \frac{\Delta h}{l} \tag{2.5}$$

If Darcy's Law is written for flow through only one tube, ΔQ, then:

$$\Delta Q = \frac{K \Delta h \pi (r_2^2 - r_1^2)}{l} \tag{2.6}$$

The difference of two squares, r_2^2-r_1^2, can be written as $(r_2-r_1)(r_2+r_1)$. If average radius, r, equals $(r_2+r_1)/2$ and the width of an element, b, is (r_2-r_1), then Darcy's Law is:

$$\Delta Q = \frac{K \Delta h 2 \pi r b}{l} \tag{2.7}$$

If the total flow through the system is Q, and the total head drop across the system is H, then the flow through one tube and head drop across one element can be rewritten as:

$$\begin{aligned} Q &= \Delta Q n_f \\ H &= \Delta h n_d \end{aligned} \tag{2.8}$$

where:

n_f= The number of flow tubes,
n_d= The number of equipotential drops.

For a constant head permeameter, the total flow, Q, is constant, the total head change across the system, H, is constant, and hydraulic conductivity, K, is constant. Consequently, the ratio of rb/l is constant. The final form of Darcy's Law for a radial flow scenario is:

$$Q = KH 2\pi \frac{rb}{l} \frac{n_f}{n_d} \tag{2.9}$$

From Figure 2.4, the average ratio of rb/l is approximately 5.23 inches, or 13.28 cm. The number of flow tubes, n_f is 6. The number of equipotential drops, n_d, is 9.1, considering the final drop to be one tenth of a full drop. Notice that the symmetric appearance of the flow net shows the flow tubes twice. Using these numbers, the following equation is solved for hydraulic conductivity:

$$K\left(\frac{cm}{\sec}\right)=\frac{Q\left(\frac{cm^3}{\sec}\right)\ 9.1(drops)}{H(cm)\ 2\pi\ 13.28(cm)\ 6(tubes)} \tag{2.10}$$

2.2 Hydraulic Conductivity In Gravel

A different permeameter is installed to obtain a value of hydraulic conductivity in the gravelly section toward the upstream end of the field site. A six-inch diameter PVC pipe is cemented vertically onto the stream bed. A concrete apron around the pipe creates an impermeable boundary along the stream bed surface. This prevents water from flowing vertically upwards right next to the pipe. A piezometer is inserted into the soil at the center of the pipe for measuring the head below ground surface during falling head and constant head permeameter tests (Figure 2.5).

This construction was done after the stream had dried up, so to perform the tests, the volume below the pipe had to be artificially saturated. The pipe was continuously filled with water until a large volume of soil was assumed to be saturated. Saturation was assumed when the rate at which the water level fell in the pipe was roughly constant between trials.

Once field saturation was assumed, several falling head permeameter tests and a constant head test was performed. The data from these tests were analyzed using Hvorslev's case B method as was illustrated in his figure 18 (Hvorslev, 1951). The flow field is diagramed in Figure 2.5. Although the boundary conditions were not identical to Hvorslev's, this method provided a rough estimate of K. The formula used was:

$$K=\frac{\pi D}{8(t_2-t_1)}\ln\left(\frac{H_1}{H_2}\right) \tag{2.11}$$

where:

D = Diameter of pipe, (cm)

H_1, H_2 = Head at time = t_1 and t_2 respectively.

2.3 Piezometers

Piezometers were used to determine the direction and magnitude of the vertical gradients. The piezometers monitor head at a specific depth below ground surface. Regular monitoring of piezometers began in late March 1994 and continued into the winter of 1995. Three sets of piezometers were used and are described in the following three sections.

Distance from the top of the piezometer to the water level inside the perforated pipe was measured. This measurement is converted to an elevation of the static water level. The elevation to which water rises into the piezometer corresponds to the head at the center of the

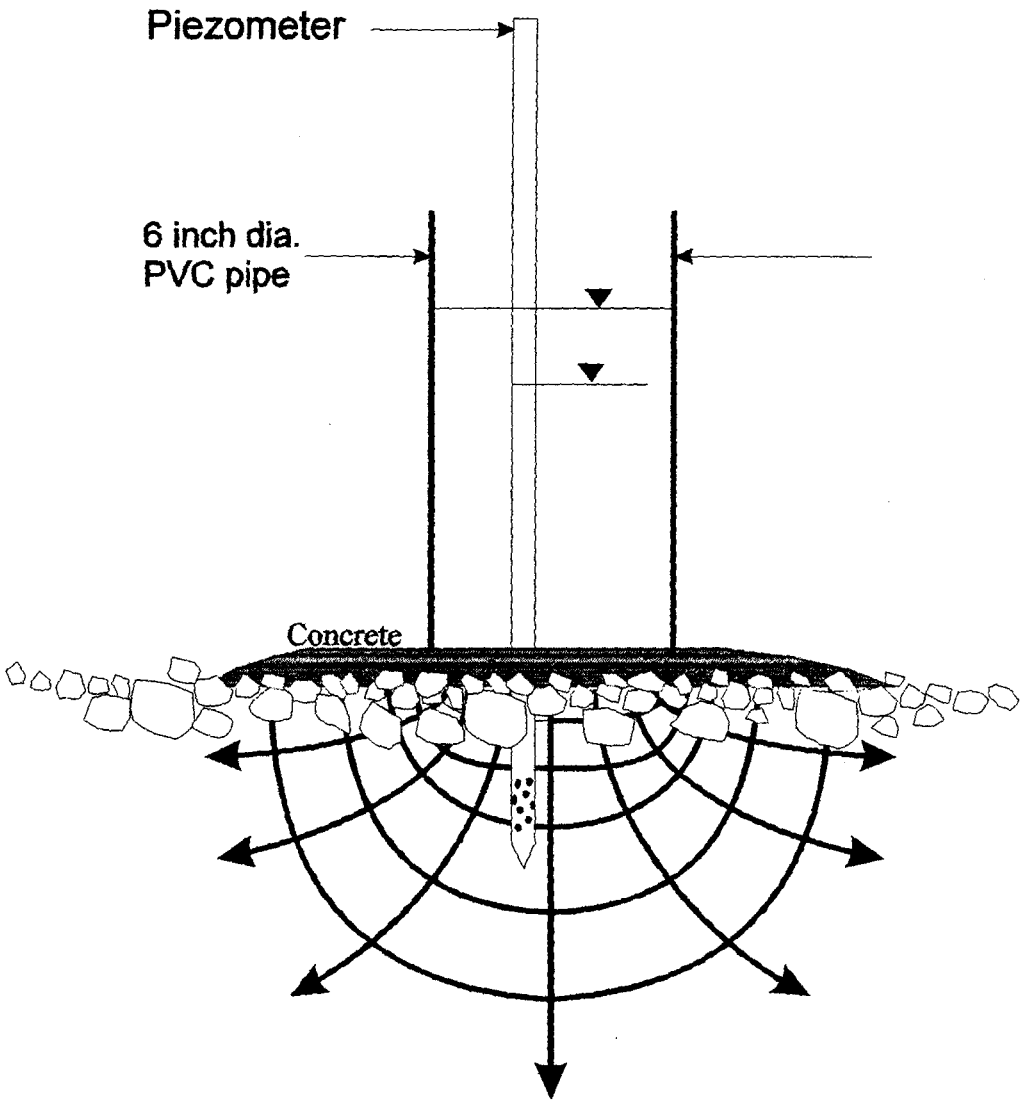

Figure 2.5 Permeameter used in rocky soils.

open interval, which is buried at depth in the soil. For piezometers at the same locatio with different depths of open intervals, the difference in water level elevation between piezometers divided by the difference in the elevation of the open intervals is the vertic gradient.

2.3.1 Shallow Monitoring Piezometers

Fifteen piezometers installed during a previous study (Anderman, 1993) are avail These are constructed of 1/2 inch diameter electrical conduit, cut to lengths of 3, 4, and feet. One end is crimped shut with several small holes drilled through a short zone abo crimp. These holes are the openings through which water can flow. The tubes are then driven into the stream bed to depths of approximately 1, 2, and 3 feet at seven locations along the stream reach. These piezometers are identified by the following pattern: the number is approximately the distance upstream from weir #1 in feet, piezometers driven approximately three feet deep are colored orange and are sufficed with the letter 'O', thc buried approximately two feet deep are colored blue and labeled with the suffix 'BL', an those buried approximately one foot deep are black and suffixed with 'BK'. The elevatic of the piezometer tops and angles from vertical are listed in Table 2.1 and their locations shown in Figure 2.6.

2.3.2 Shallow Permeability Testing Piezometers

Two 20-inch piezometers are installed at eleven stations to measure head during permeability tests. Piezometer names begin with the distance in feet upstream from weir Piezometer names that end with a letter 'N' are buried approximately four inches and are painted. Those suffixed with a 'W' are driven approximately seven inches deep and are colored white. For example, piezometer 42W is located 42 feet upstream of weir #1 and painted white. This piezometer set is constructed of 1/2 inch diameter electric conduit, ct 20 inch lengths with a 2-inch zone of small holes drilled near the bottom. The bottom en are crimped shut over a bead of caulk to prevent water from entering the bottom and to provide a leading edge for driving into the ground. The purpose of these shallow piezometers is to measure the near surface gradient, so the open intervals had to be close t the stream bed surface, yet deep enough not to get knocked over. Besides measuring the head at depth, these piezometers mark each permeameter station so that consistent placeme of the cylinder can be made.

Installation of these piezometers resulted in silt being forced into the open interval. This silt was removed using a shop-vac prior to the field measurements and did not contin to be a problem.

Location	Angle (degrees)	Piezometer Elevation (feet)	Elevation of Open Interval (feet)	Location	Angle (degrees)	Piezometer Elevation (feet)	Elevation of Open Interval (feet)
30N	0	5889.53	5888.03	DH2S	0	5885.53	5871.53
30W	0	5889.27	5887.77	DH2N	0	5886.17	5875.44
35O	0	5890.74	5885.44	DH3-16	0	5900.26	5882.86
35BL	0	5890.81	5886.51	DH3-12	0	5900.55	5888.95
35BK	0	5890.54	5887.24	DH3-7	0	5900.76	5893.46
42N	0	5889.98	5888.48	DH4-16	0	5896.20	5880.60
42W	0	5889.68	5888.18	DH4-13	0	5896.40	5883.60
48N	0	5889.95	5888.45	DH4-8	0	5896.52	5889.02
48W	0	5889.79	5888.29	DH5-17	0	5893.44	5877.04
58BL	0	5889.77	5885.47	DH5-14	0	5893.57	5880.07
58BK	0	5889.62	5886.32	DH5-9	0	5893.76	5887.76
65N	0	5890.39	5888.89	DH6-25	0	5898.17	5874.57
65W	0	5890.10	5888.60	DH6-20	0	5898.35	5878.75
71O	0	5890.96	5886.10	DH6-15	0	5898.56	5884.56
71BL	0	5891.14	5886.75				
71BK	0	5891.17	5888.05				
80N	0	5890.42	5888.92				
80W	0	5890.22	5888.72				
95N	20	5891.67	5890.80				
95W	10	5891.44	5890.47				
106N	17	5891.90	5890.99				
106W	9	5891.68	5890.70				
108O	15	5894.19	5894.01				
108BL	13	5893.19	5892.61				
108BK	5	5892.71	5891.75				
111N	15	5892.25	5891.33				
111W	6	5892.05	5891.06				
128N	15	5893.34	5892.41				
128W	9	5893.06	5892.09				
133N	10	5893.45	5892.48				
133W	13	5893.19	5892.25				
133BK	10	5894.21	5893.36				
173N	40	5894.65	5894.15				
173W	10	5894.66	5893.69				
179O	12	5896.23	5895.78				
179BL	10	5896.03	5895.31				
179BK	10	5895.81	5894.96				

Table 2.1 Piezometer elevations.

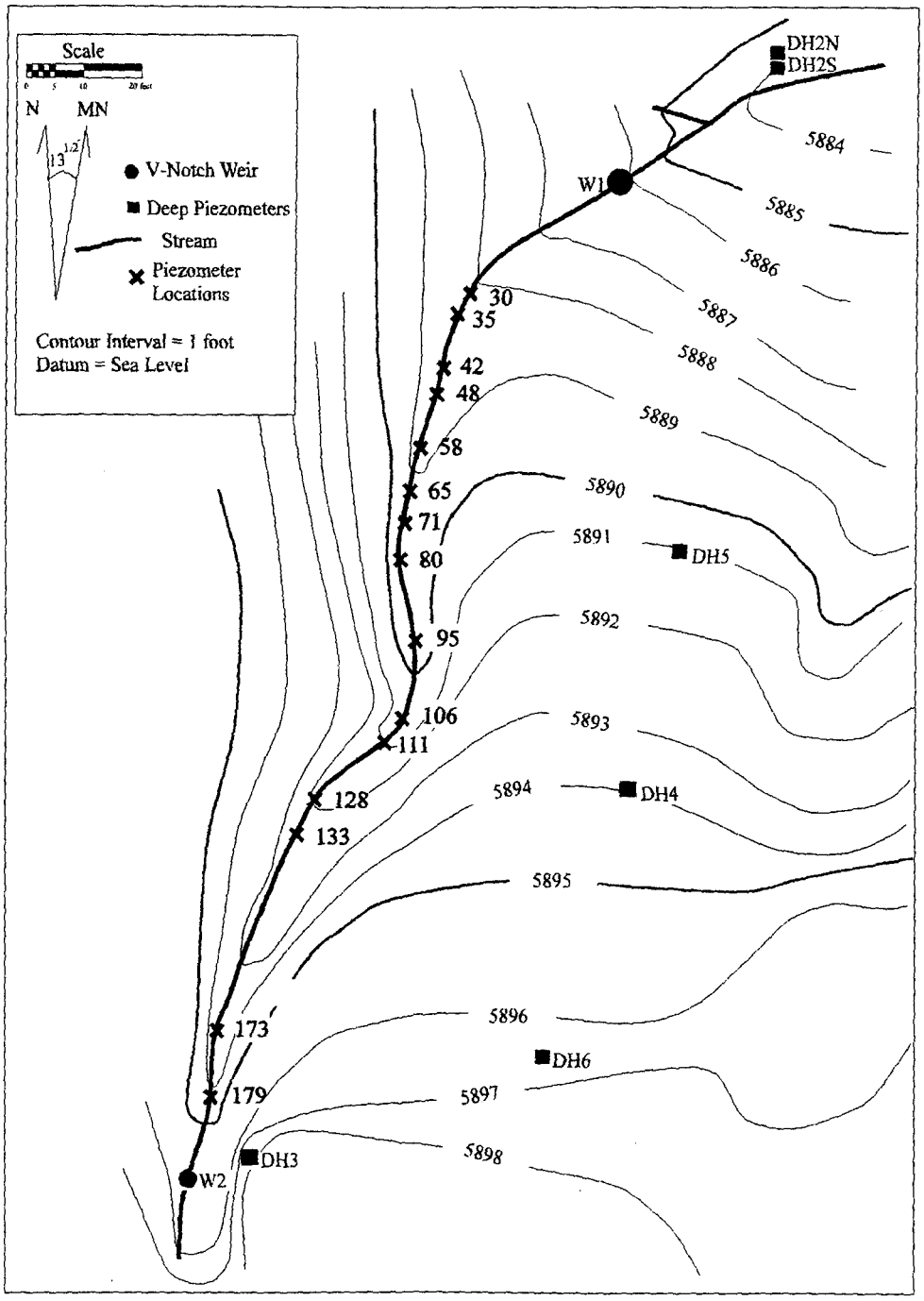

Figure 2.6 Location map of piezometers.

2.3.3 Deep Piezometers

In March 1994, four auger holes were drilled to bedrock and completed with three nested piezometers. Labels for these piezometers begin with 'DH', and are followed by the hole number and the depth of open interval. For example, DH3-16 means "drill hole 3" with the open interval about 16 feet below ground surface. The location of these piezometers are shown in Figure 2.6. Depth to bedrock ranges between 17 and 25 feet below ground surface. Piezometers DH2N and DH2S are single piezometers completed to depths of 12 and 15 feet respectively. Completion diagrams are found in Appendix C. The open intervals range between 7 and 25 feet below ground surface. The deepest piezometer in these deep holes is a two-inch diameter PVC pipe with an open interval approximately six inches in length near the bottom. The slots are placed slightly above the bedrock surface. The other two piezometers in each hole are one inch diameter PVC pipes. The open intervals of the multiple piezometers are placed to monitor the top, middle, and bottom of the alluvial aquifer. Both shallow and deep gradients can be interpreted from these piezometers.

Well rehabilitation was required to improve the efficiency of the sand pack around the deep piezometers. The sand pack lost efficiency from the void spaces being clogged by silt. A 15 foot hose attached to a shop-vac can remove silt from a depth up to the maximum extension of the hose. This method pulled the silt from the bore, but did not clean out the sand pack well. To reach deeper, a positive displacement hand pump was used to surge the water and to pump the silt out. This method worked well for the 2-inch piezometers, but the pump was too large for the 1-inch diameter piezometers. To clean the one inch piezometers, a one-way foot valve was constructed and mounted on the end of a length of stiff nylon tubing. By surging this pump up and down, much of the silt was removed.

2.4 Weirs

To measure stream discharge, all of the water in the stream is funnelled through two V-notch weirs. The weir construction is shown in Figure 2.7. A rubberized canvas apron is laid out upstream of the weirs to prevent water from infiltrating and flowing underneath. To prevent water from bypassing around the V-notch, dirt banks are built-up on the sides of the weir. A metal plate forms the V to provide a clean break over which the water can flow.

Location of the weirs is shown in Figure 2.6. Weir #1 is installed at the downstream boundary of the field site, and weir #2 is placed at the upstream boundary. Anderman (1993) constructed and installed the weirs.

Field measurements at the weirs are taken as the distance from the bottom of the V to the backwater level on the upstream side. For this to be an accurate measurement, the water has to be flowing cleanly over the metal edge of the V and not dribbling over. The expected result from the weir measurements is to show changes in flow rate over the length of the study area. The measurements indicate a net change of discharge, but do not resolve the extent of gaining and losing reaches.

Stream discharge is solved for by the following equation (Fetter, 1988):

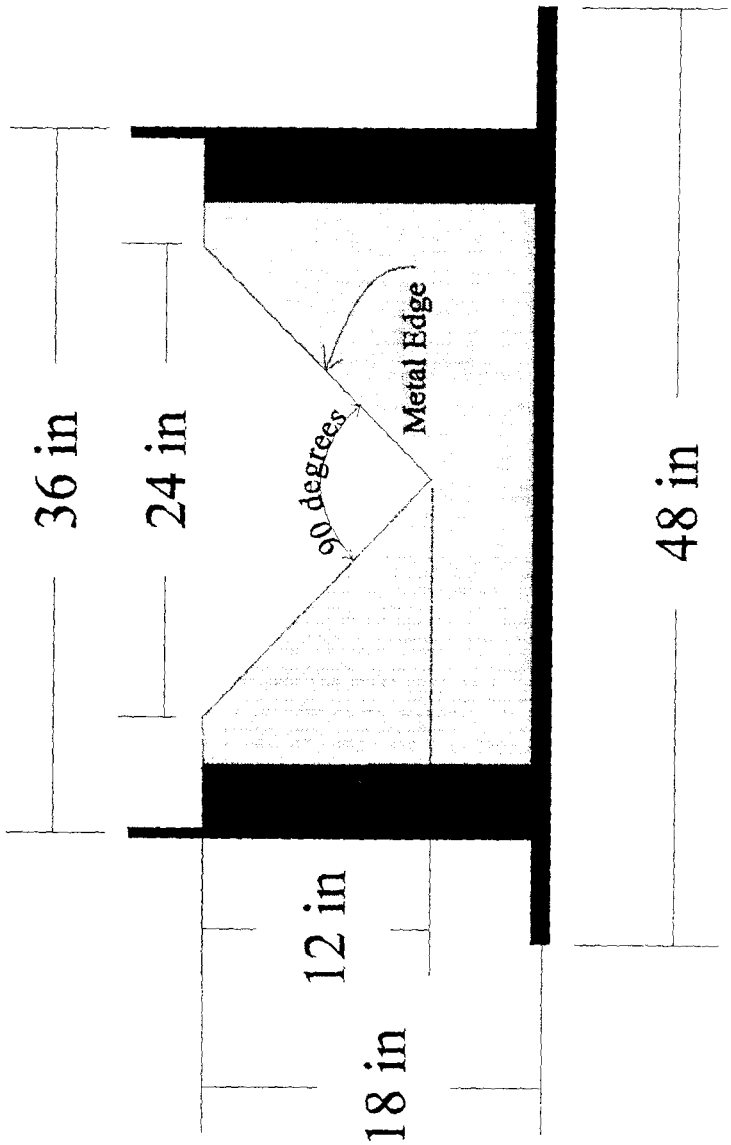

Figure 2.7 Construction of the V-notch weir built by Anderman (1993).

$$Q = 2.5H^{\frac{5}{2}} \tag{2.12}$$

where:

Q = Stream discharge (cubic feet per second)
H = Head of the backwater above the weir crest (feet)

Field measurements for the weirs are presented in Table 2.2, and plotted on Figure 2.8. The area between the curves for weir #1 and #2 represents the amount of water the stream gained over the 200 foot reach during the period of measurement.

2.5 Slug Tests

Saturated hydraulic conductivity is determined by performing slug tests in each piezometer within the deep holes. With slug test information at several depths in different holes, a spatial distribution of hydraulic conductivity is generated to investigate heterogeneity within the alluvium.

Slug tests are performed by measuring the initial water level in the piezometer, then instantaneously raising the water level. The initial rise in the water level is recorded. The rate at which the water level returns to the static water level is monitored at timed intervals. The instantaneous change in water level is made by quickly pouring water into the piezometer. Wellbore geometry is illustrated in the wellbore completion diagrams in Appendix C.

Empirical equations for water table aquifer slug test interpretation have long been available from Hvorslev (1951) and more recently by Bouwer and Rice (1976, 1989). These two slug test interpretation methods are used in this report.

2.5.1 Hvorslev Method

To use the Hvorslev method, the following assumptions must be made; Darcy's Law must be assumed valid, both water and soil are incompressible, the added water does not cause perceptible increase of the groundwater level, and the hydraulic losses in the pipe and well screen are negligible. The derivation of Hvorslev's variable head permeameter equation for a screened interval in homogeneous soil is similar to that for a laboratory falling head permeameter.

The flow through the screened interval, q, can be expressed by Darcy's Law as:

$$q = FKH = FK(z - y) \tag{2.13}$$

Date	Weir 1 Flow *(cfs)*	Weir 2 Flow *(cfs)*	Date	Weir 1 Flow *(cfs)*	Weir 2 Flow *(cfs)*
3/18	0.10	Dry	5/1	0.67	0.54
3/24	0.06	0.00	5/2	0.71	0.56
3/29	0.08	0.01	5/3	0.70	0.55
3/30	0.08	0.02	5/3	0.67	0.52
3/31	0.09	0.03	5/4	0.56	0.42
3/31	0.10	0.03	5/5	0.59	0.44
4/4	0.13	0.06	5/10	0.44	0.30
4/5	0.17	0.09	5/12	0.34	0.22
4/6	0.16	0.07	5/16	0.23	0.14
4/7	0.22	0.14	5/20	0.14	0.05
4/8	0.17	0.10	5/25	0.05	0.02
4/8	0.20	0.11	5/26	0.15	0.09
4/14	1.08	0.92	5/31	0.09	0.02
4/15	0.99	0.80	6/2	0.10	0.02
4/19	0.64	0.37	6/3	0.10	0.02
4/21	0.48	0.20	6/7	0.09	0.02
4/21	0.45	0.40	6/8	0.09	0.02
4/22	0.44	0.39	6/9	0.09	0.01
4/23	0.40	0.34	6/10	0.08	0.01
4/23	0.37	0.30	6/11	0.08	0.01
4/26	0.43	0.36	6/13	0.07	0.00
4/27	0.41	0.34	6/14	0.06	0.00
4/29	0.42	0.36	6/16	0.06	0.00
4/30	0.42	0.34	6/20	0.03	Dry
4/30	0.61	0.52	6/23	0.03	Dry
4/30	0.76	0.70	6/27	0.02	Dry
4/30	0.84	0.71	6/28	0.01	Dry
			7/2	0.00	Dry
			7/7	0.00	Dry

Table 2.2 Weir measurements.

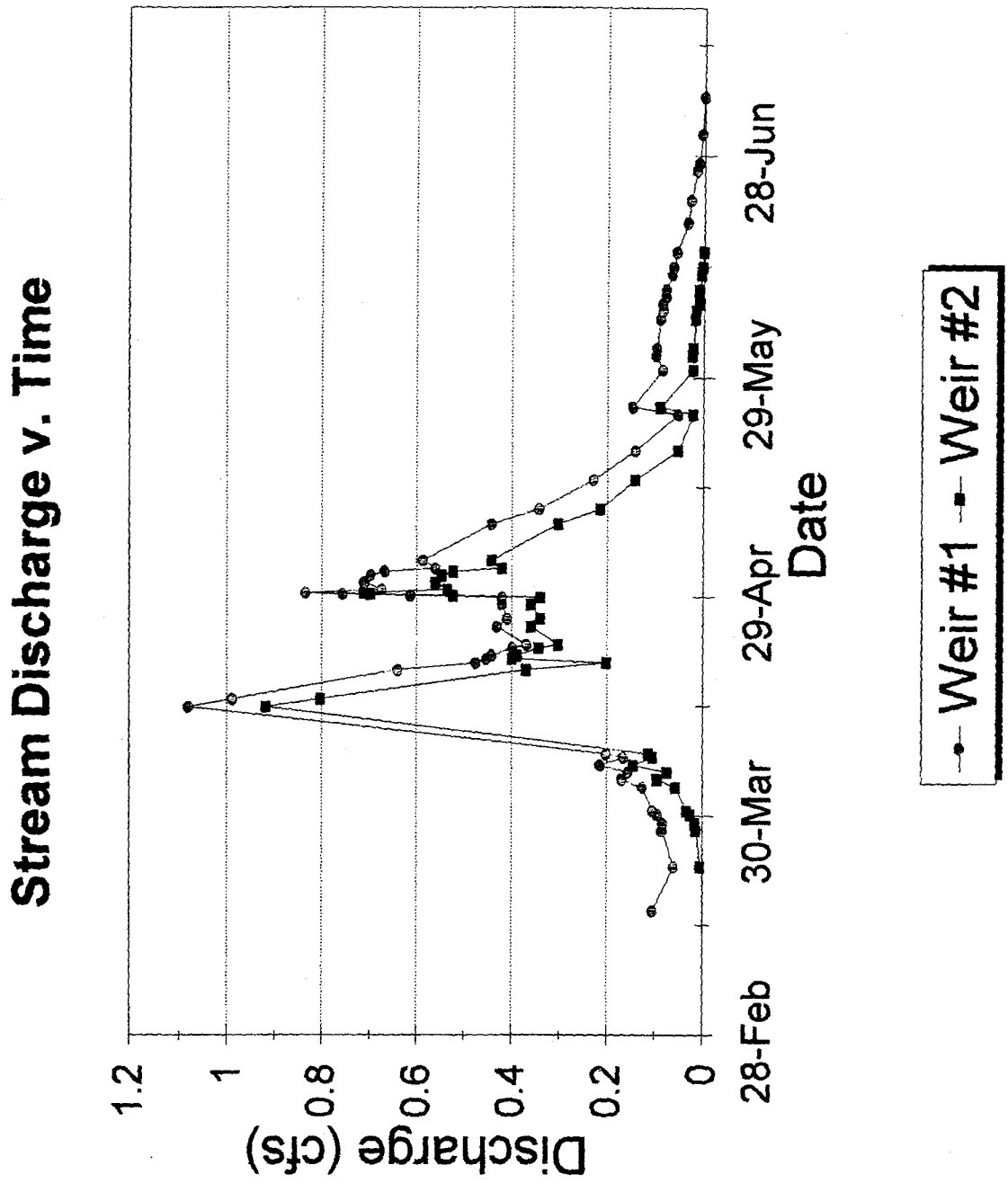

Figure 2.8 Stream discharge.

where F is a shape factor and H is the head at time t above or below the equilibrium v level, and y is the head above z, which is the head at t= 0 (Hvorslev, 1951). These parameters are illustrated in Figure 2.9. The volume of flow during time dt, is,

$$q\ dt = A\ dy \qquad (2.13)$$

where A is the cross sectional area of the observation well with diameter d (Figure 2.9 Substituting equation 2.13 into equation 2.14 gives,

$$\frac{dy}{(z-y)} = \frac{FK}{A}\ dt \qquad (2.14)$$

If the total volume of flow for pressure equalization is V=AH, then the total time for equalization, T, is,

$$T = \frac{V}{q} = \frac{AH}{FKH} = \frac{A}{FK} \qquad (2.15)$$

which leads to,

$$\frac{dy}{(z - y)} = \frac{dt}{T} \qquad (2.16)$$

Then, if z= H_0= head at t=0, and y= 0 at t= 0, the solution is,

Substituting for T and rearranging gives,

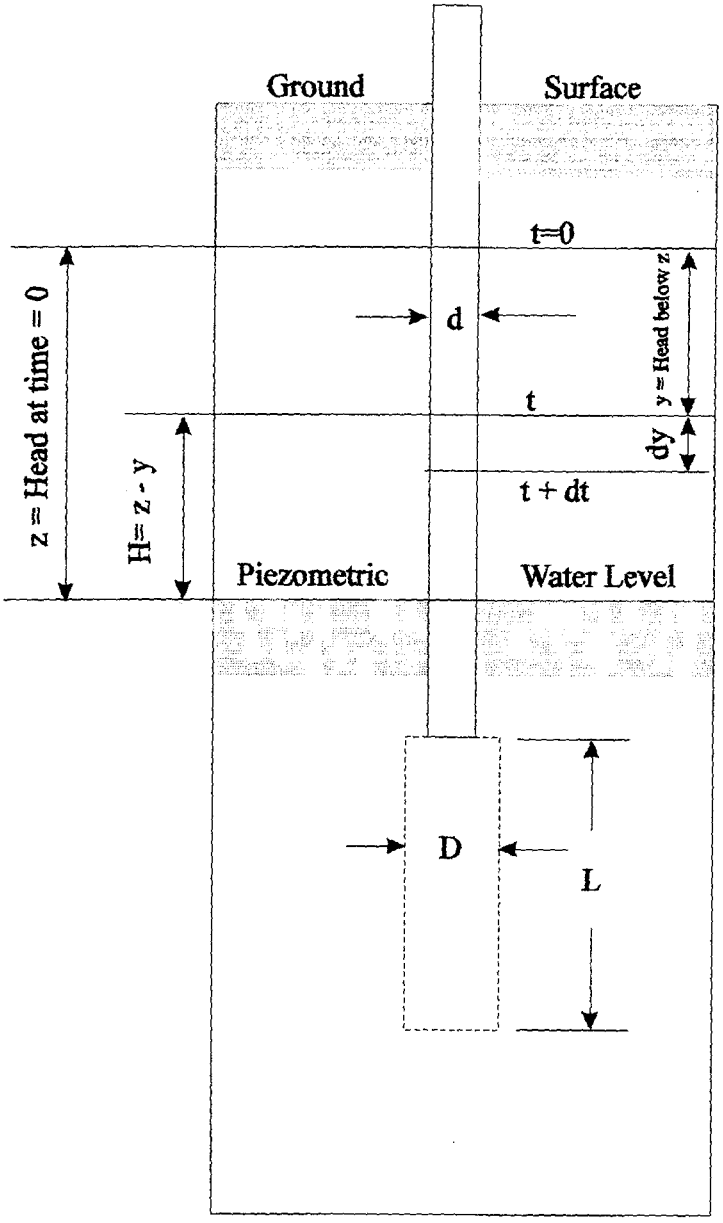

Figure 2.9 Geometry used in Hvorslev's analysis.

$$K = \frac{A}{(t_2 - t_1)F}\ln\left(\frac{H_0}{H}\right) \qquad (2$$

For the geometry of the screened intervals used, the shape factor is (Hvorslev, 1951):

$$F = \frac{2\pi L}{\ln\left[\frac{L}{D} + \sqrt{\left(\frac{L}{D}\right)^2 + 1}\right]} \qquad (2$$

Substituting the shape factor into equation 2.19 gives Hvorslev's equation for hydraulic conductivity for a well-point in uniform soil with the assumption that vertical and horizo hydraulic conductivity is equal. The formula is written as,

$$K = \frac{d^2 \ln\left[\frac{L}{D} + \sqrt{\left(\frac{L}{D}\right)^2 + 1}\right]}{8\,L\,(t_2 - t_1)}\ln\left(\frac{H_1}{H_2}\right) \qquad (2.$$

where K = Hydraulic conductivity (L/T).
d = Inside diameter of observation well (L).
D = Diameter of screened interval = borehole diameter (L).
L = Length of screened interval (L).
H_1 = Head for $t = t_1$ (L).
H_2 = Head for $t = t_2$ (L).

2.5.2 Bouwer and Rice Slug Test Analysis

The basis for the Bouwer and Rice method of slug test analysis is the Thiem equat written as (Bouwer and Rice, 1976):

$$Q = 2\pi K L_e \frac{y}{\ln(R_e/r_w)} \tag{2.22}$$

where Q = volumetric rate of flow into well.
K = Hydraulic conductivity of the aquifer around the well.
L_e = Length of screened interval of well.
y = Vertical distance between water level inside well and static water table outside well.
R_e = Effective radial distance over which y is dissipated.
r_w = Radius of boring including disturbed zone.

Values of R_e were determined by Bouwer and Rice with an electrical resistance network analog for different values of r_w, L_e, L_w, and H. The geometry and symbols used are presented in Figure 2.10 (Bouwer and Rice, 1976). These results are expressed in terms of the dimensionless ratio $\ln(R_e/r_w)$. The data are fit to two equations depending upon the geometry of the well bore. For partially penetrating well, $\ln(R_e/r_w)$ is expressed as:

$$\ln\left(\frac{R_e}{r_w}\right) = \left[\frac{1.1}{\ln(L_w/r_w)} + \frac{A + B\ln[(H-L_w)/r_w]}{L_e/r_w}\right]^{-1} \tag{2.23}$$

For a fully penetrating well, $\ln(R_e/r_w)$ is expressed as:

$$\ln\left(\frac{R_e}{r_w}\right) = \left[\frac{1.1}{\ln(L_w/r_w)} + \frac{C}{L_e/r_w}\right]^{-1} \tag{2.24}$$

where A, B, C are dimensionless numbers and are plotted on Figure 2.11 as a function of L_e/r_w (Bouwer and Rice, 1976).

Then, if dy/dt is the rate of rise of the water level during the slug test, this analogy can be made:

$$\frac{dy}{dt} = -\frac{Q}{\pi r_c^2} \tag{2.25}$$

where r_c is the radius of the casing where the rise of the water level is measured.

Solving equation 2.25 for Q, setting the resulting expression equal to equation 2.22, then separating variables for integration, yields an expression for K as:

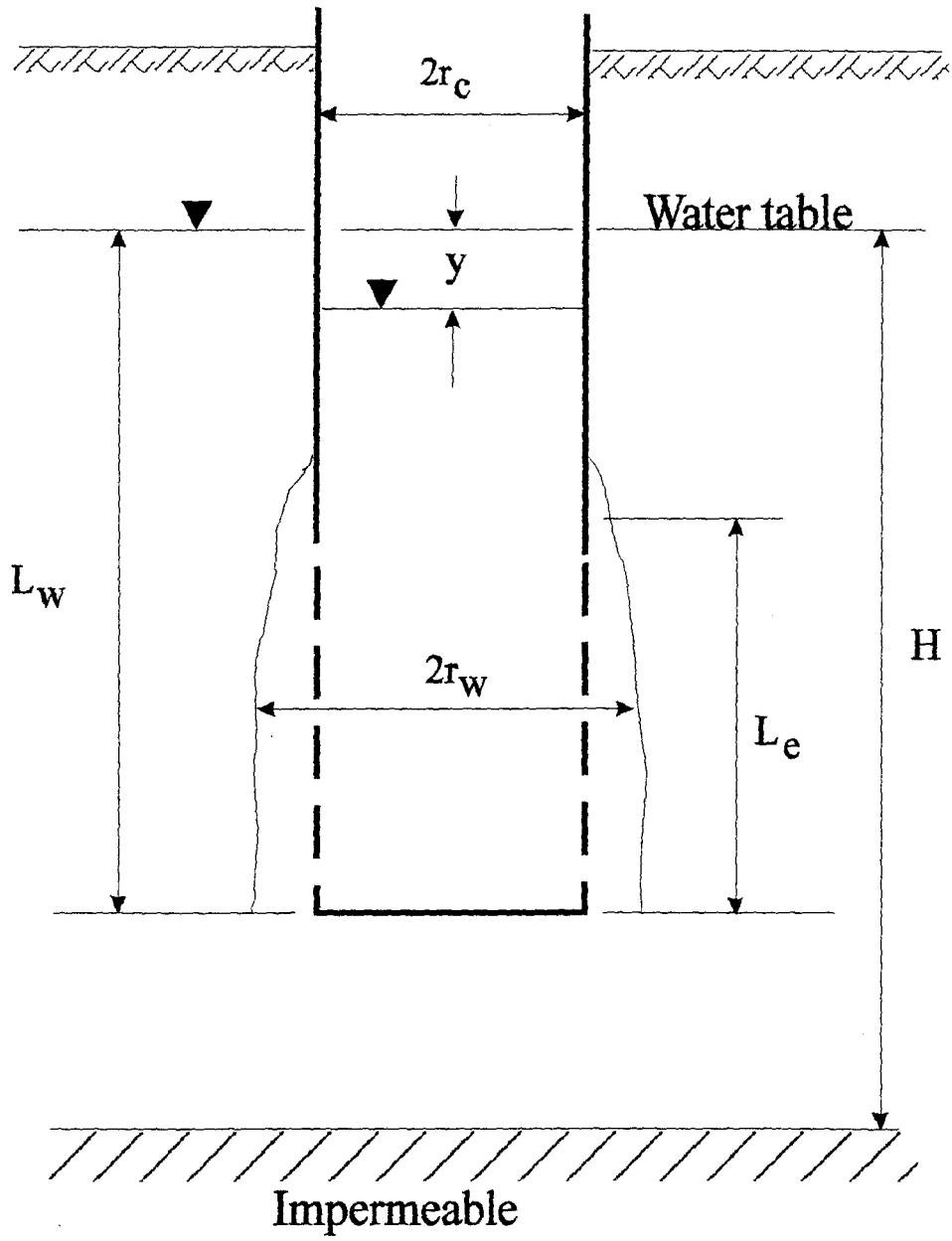

Figure 2.10 Geometry used in Bower and Rice analysis.

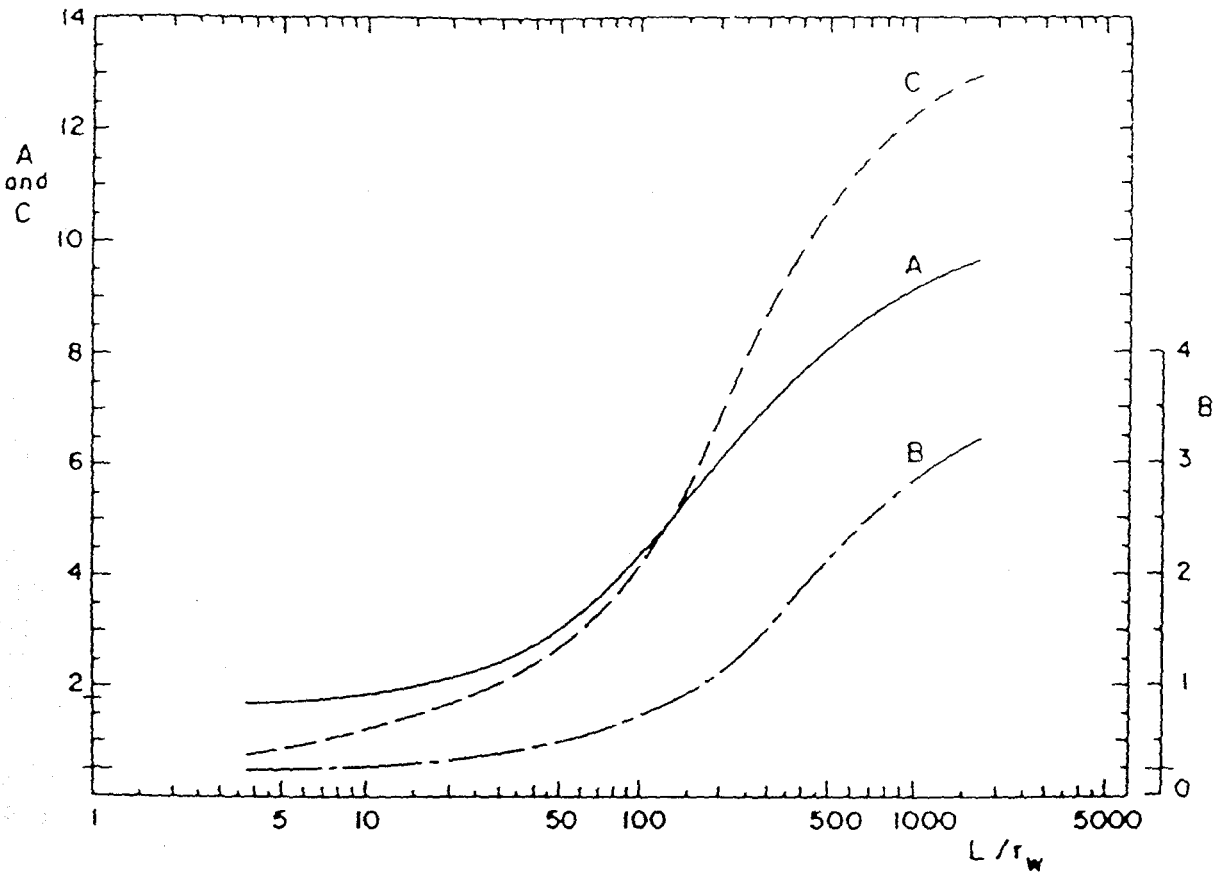

Figure 2.11 Parameters A, B, and C used in Bower & Rice analysis (Bower & Rice, 1976).

$$K = \frac{r_c^2 \ln(R_e/r_w)}{2L_e} \frac{1}{t} \ln\frac{y_0}{y_t} \qquad (2$$

where y_0 = y at time zero; and y_t = y at time t.

Slug test data are plotted on semilog paper with time along the abscissa and head above static water level along the ordinate. Values for t and y_t are taken from the straig line portion of the graph. The term y_0 is taken as the head above the static water level a instant the slug of water was inserted into the well. Hydraulic conductivity is then calcu using equation 2.26. The Bouwer and Rice method works equally well for rising head s tests as falling head slug tests.

2.6 Sediment Sampling

To measure the physical changes in stream bed composition, samples were taken several locations along the reach of study at various times throughout the season. These samples were taken to determine if the grain-size distribution has changed with changing hydrologic events. Samples were taken from locations at which the permeameter was us the results could be correlated to hydraulic conductivity. However, sampling destroyed t natural condition of the stream bed and possibly affected the future consistency of the permeameter data. Therefore, to reduce the destruction of the stream bottom, sampling w limited. To further reduce the destruction of the stream bottom, areas with plants growir were not sampled. With these restrictions, only seven samples were taken, with three of samples from one station, station 106. Although other stations were sampled, subsequent samples were not taken because of the slow rate at which new material was being deposit Station 106 was noted to be changing rapidly in both shape and rates of deposition, so removal of a small sample did not have substantial impact on the character of the stream

Grab samples were taken during the drilling of the deep wells to identify changes the composition of the alluvium with depth. Samples were taken every five feet, corresponding to each auger flight added to the drill stem. However, an interpretation of these grab samples was difficult because the material coming from the borehole during drilling was a well mixed slurry. This mixing obliterated the correlation between depth o the auger and the sample.

A mechanical sieve analysis was performed on the samples from station 106. The grain size distribution curve is shown on Figure 2.12. The shift in curve represents a coarsening of sediments at the station.

2.7 Topographic Survey

Two surveys were performed by the author to generate a detailed topographic map absolute elevations of the piezometers. The topographic map was based on a plane table a

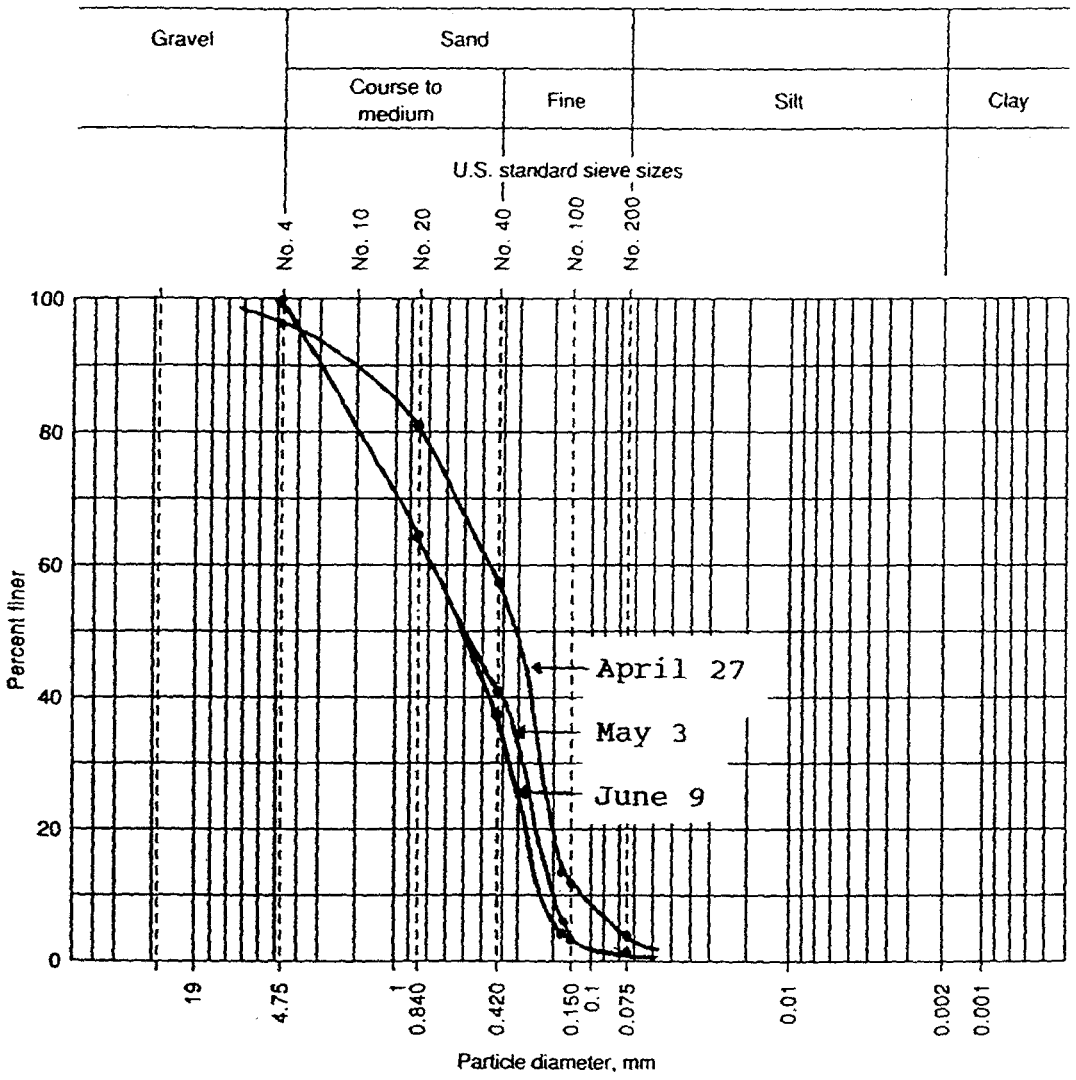

Figure 2.12 Grain-size distribution of station 106 samples.

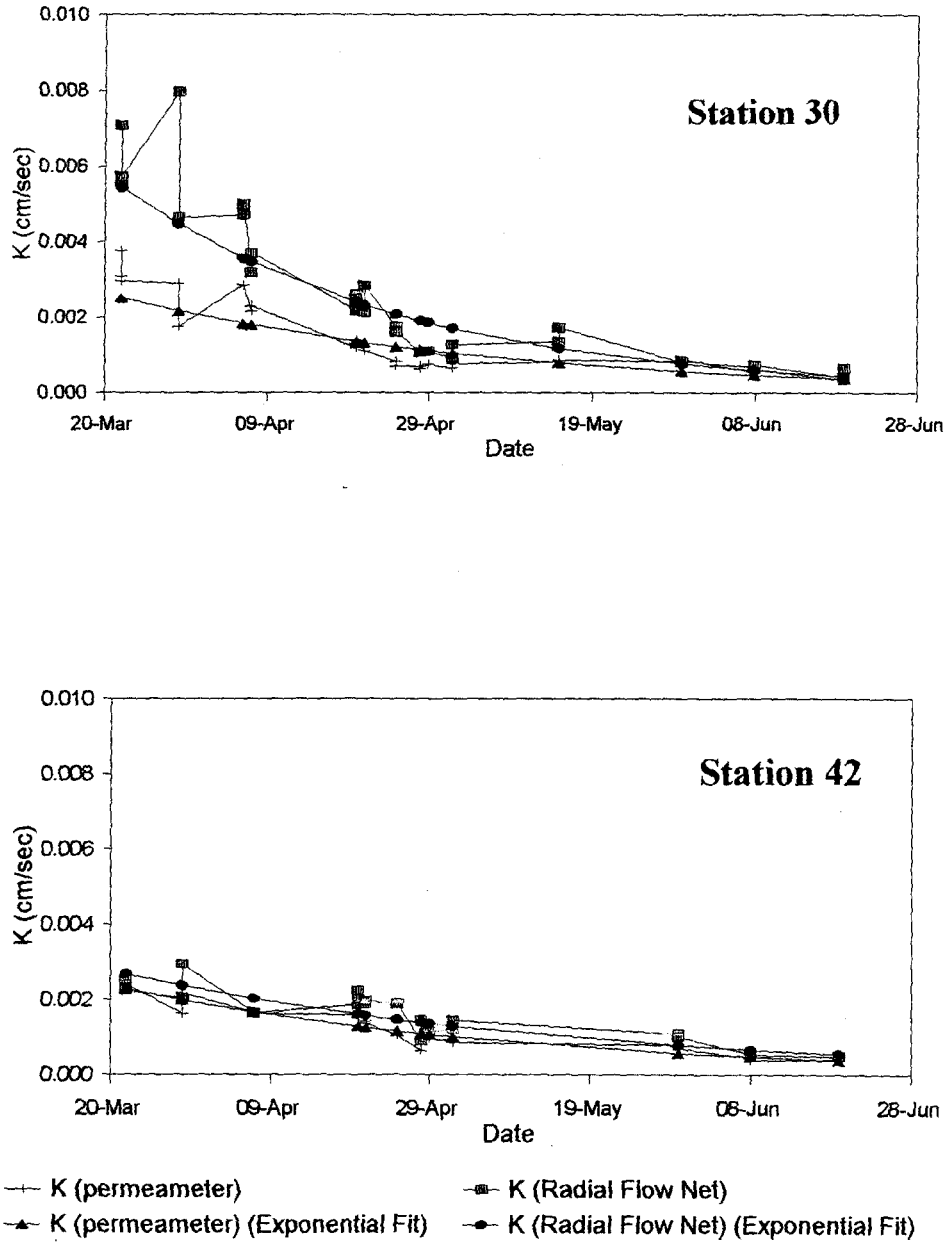

Figure 3.1 Temporal variations of hydraulic conductivity.

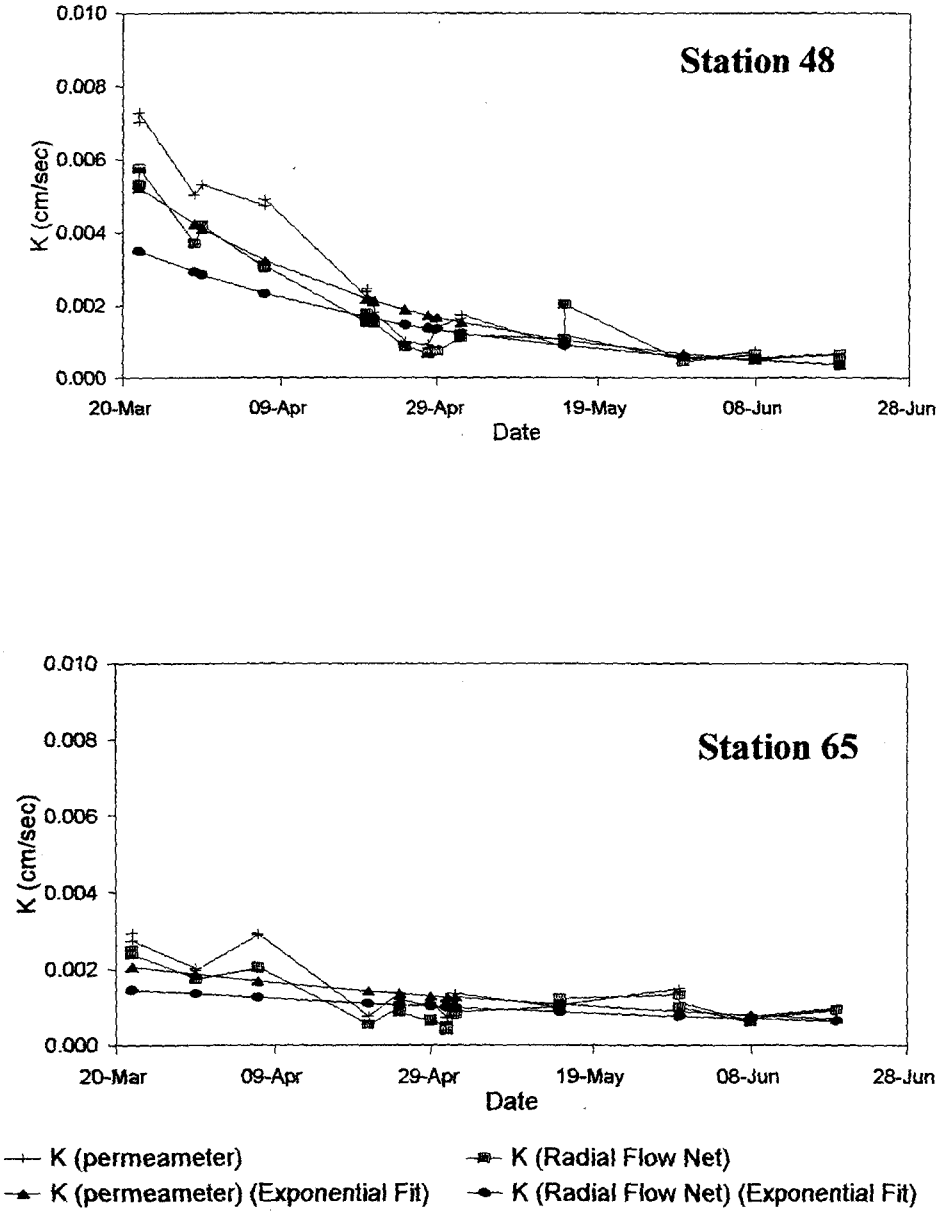

Figure 3.1 (continued) Temporal variations of hydraulic conductivity.

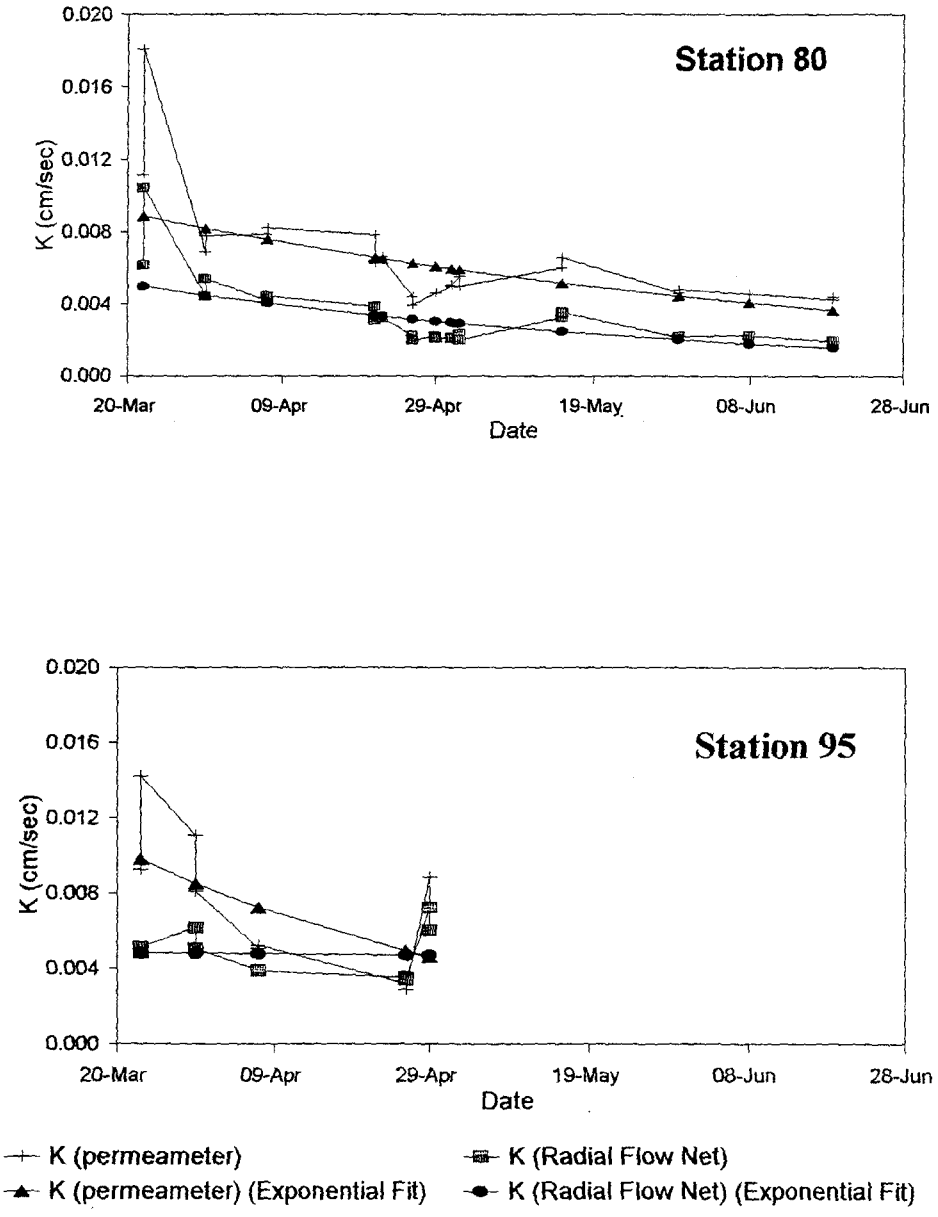

Figure 3.1 (continued) Temporal variations of hydraulic conductivity.

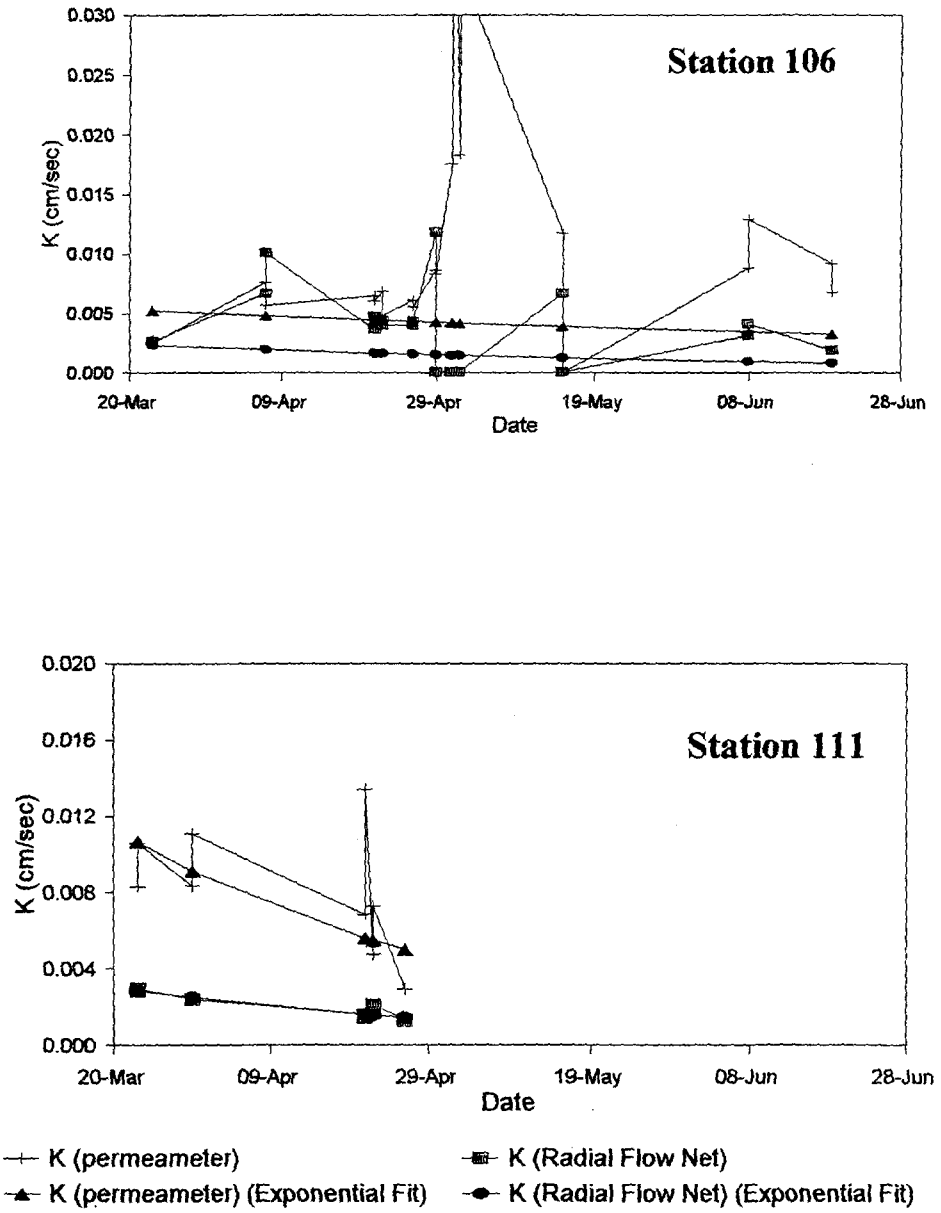

Figure 3.1 (continued) Temporal variations of hydraulic conductivity.

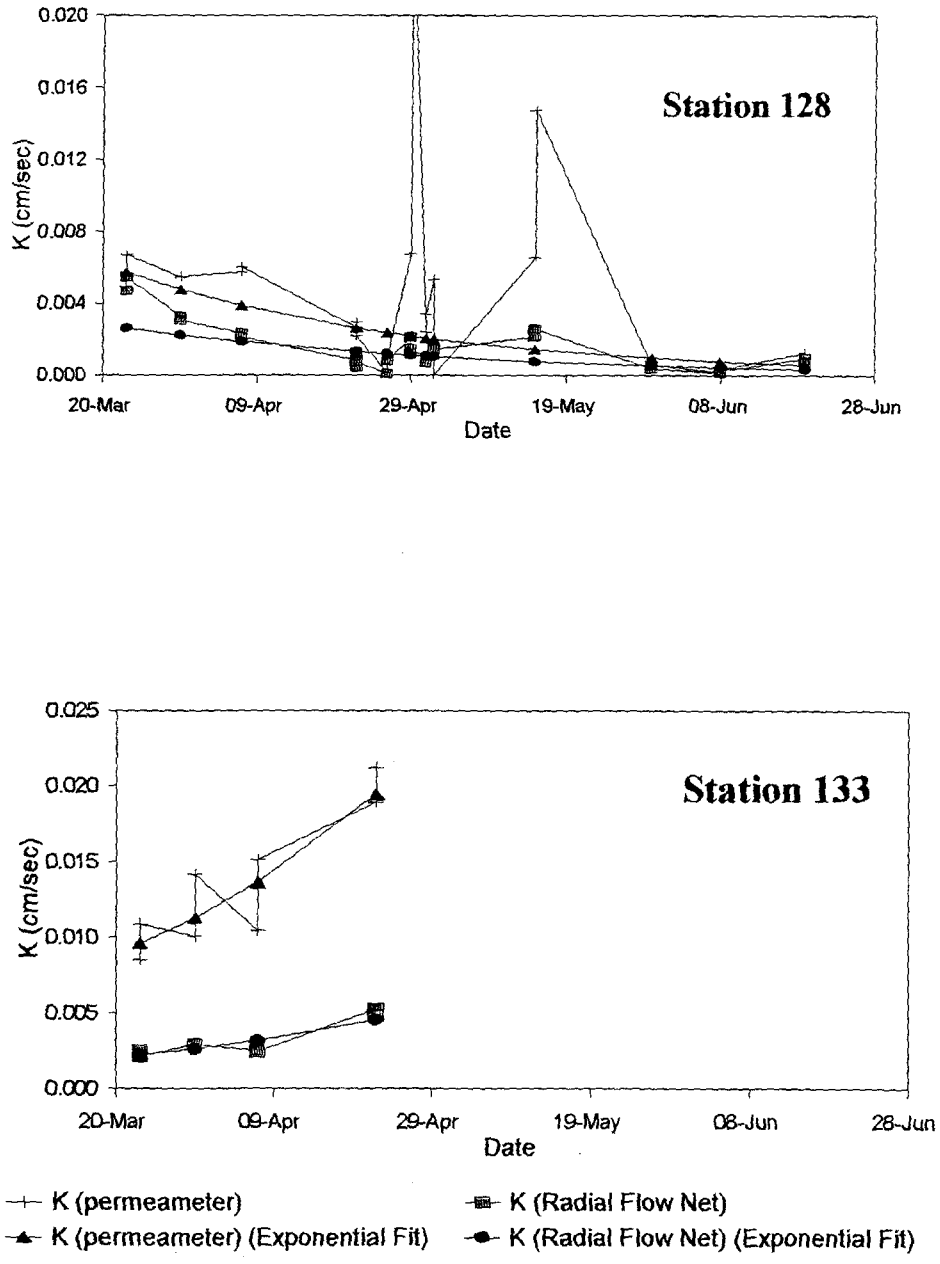

Figure 3.1 (continued) Temporal variations of hydraulic conductivity.

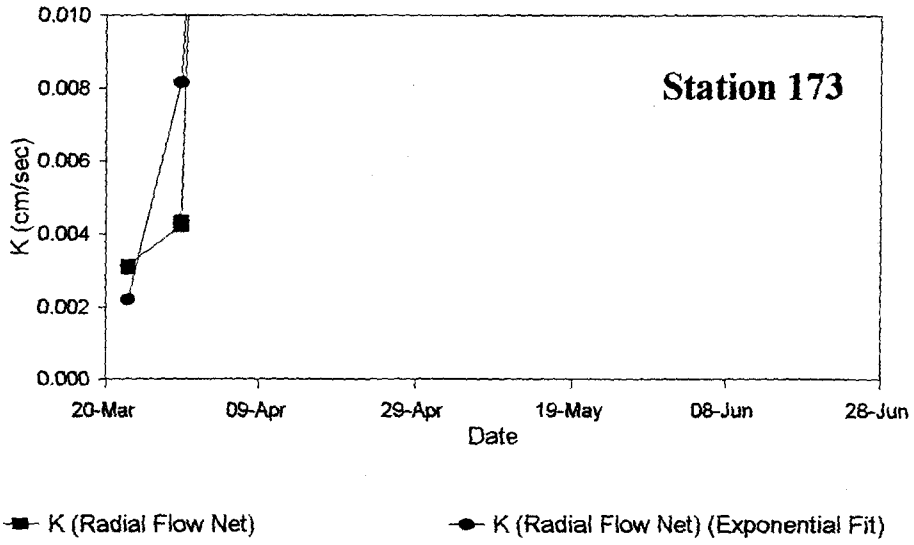

Figure 3.1 (continued) Temporal variations of hydraulic conductivity.

3.1 Effects of Plant Growth on Hydraulic Conductivity

Plant growth is a factor to the temporal changes of hydraulic conductivity of the stream bed. This growth could have four effects. One is that as the plants grow larger, plant has a larger surface area through which water can be filtered. Although the strean flowing in a turbulent fashion, the water between the stems and leaves of the plants is m relatively slower. This slower velocity allows the fine particles to settle out of suspensic As these fines settle, they create a seal at the sediment-water interface. As the plants continue to grow, more fines could accumulate thus decreasing the observed hydraulic conductivity. Another possible effect from plant growth is the formation of a thick mat vegetation on the stream bottom. This mat of plant material may be so dense as to limit flow of water through it, thus lowering the hydraulic conductivity.

A third effect from plant growth is the change in the shape of the stream bed. Tl changing of shape was not measured with this project, but was observed during the field study. As the plants grew, they created barriers, diverting flow. These diversions create small channels through which water flows. These changes in flow path also result in cha of flow velocity. The shifting channels suggest a dynamic stream bed, which supports th idea that the corresponding hydraulic parameters like Ksat also changes with time.

A fourth effect of plant growth is the compression of the soil from the growth of roots. As the roots begin transporting water, the structure may swell and compress the sc If new roots are generated, then pore spaces may be filled with the new growth. Howeve contrary effect could also result from the roots creating new openings for water to flow through.

Distinguishing between these possible effects is not part of the project. The above discussion revolves around the plants when they are growing, after the stream dries up however, these plants go dormant until the next growing season. As the plants and soil d the structure of the root zone must change, which changes the hydraulic conductivity. Th change affects the flow rate between the stream and the aquifer when water flows in the channel again. This change in the root zone is a difficult parameter to quantify.

3.2 Effects of Stream Velocity on Hydraulic Conductivity

Stream bottom composition is primarily changed by the flow rate of water and the direction of vertical gradients. Assuming there is always a source of sediment available, tl distribution of these sediments is primarily controlled by stream flow rate.

Water velocity along the stream bottom can change in time and in space. At any particular location, the velocity changes depending upon the characteristics of the stream channel. Spatially, sections of the stream channel that are narrow have a higher velocity tl sections that are relatively wide. In areas where the stream channel widens, the velocity is visibly slower and the stream bed is lined with a layer of fine material. Where the stream channel narrows, the stream bed material is coarse.

The ability of water to transport sediments is a function of velocity. As water veloc increases, larger the grains of sediment are able to be transported. When the water velocit

slows and loses energy, the largest of the moving grains come to rest. Based on this principle, fine material on the stream bottom is scoured away during high flow periods resulting in an increase in hydraulic conductivity.

Hydraulic conductivity of soil is controlled by the sorting and grain size. By removing the fine portion from the sediments, the sorting is improved and the average grain size is increased, thus raising Ksat (Fetter, 1988). Areas along the stream bed that are lacking plant life are more susceptible to this scouring process. The increase in hydraulic conductivity of the stream bed above station 128 could be a function of these principles.

3.3 Effects of Vertical Gradients on Hydraulic Conductivity

Sediment transport is also controlled by the direction and magnitude of the vertical gradients within the stream bed. Many factors such as; flow turbulence, sediment size and shape distribution, and transverse seepage velocity affect the onset of particle motion (Watters and Rao, 1971). Seepage can be either influent, water seeping into the bed from the stream, or effluent, water seeping from the bed into the stream. Seepage rate and direction affect the lift and drag forces on the unconsolidated material along the stream bed.

> First is the direct effect of the seepage flow which results in a dynamic force in the direction of the seepage velocity. Second is the indirect effect of the seepage, which is to alter the main channel flow conditions which in turn alters the force on the particles. This second effect of seepage is manifested in several ways. In general, it can be said: 1) It changes the angle of attack at which the main channel flow attacks the bed particle; 2) it flushes the dead water out of the bed (or into the bed) from the porous regions of the top bed layer, thereby exposing more of the particle surface to active fluid action; and 3) it alters the wake behind the particle which not only affects the particle under study, but the other particle just downstream on which the wake impinges. The relative importance, direction, and the extent of the effects depends on the bed configuration, the flow configuration before seepage and the direction of seepage. (Watters and Rao, 1971).

Watters and Rao conclude that the drag forces on the particles are reduced during effluent seepage (Figure 3.2) and increased during influent seepage. However, the lift forces depend on both flow direction and particle position. The stream at the field site has a complex bed configuration, variable direction and magnitude of seepage, and variable stream velocity. These variable parameters affect the importance of the drag and lift forces acting on the bed particles.

An interpretation of the compositional differences along the stream bed can be made. In the areas of a strong effluent seepage velocity, such as the areas above station 95, the upward lift forces, which promote particle motion, are increased, while drag forces are reduced, which inhibits particle motion. The bed along the upstream end is composed of

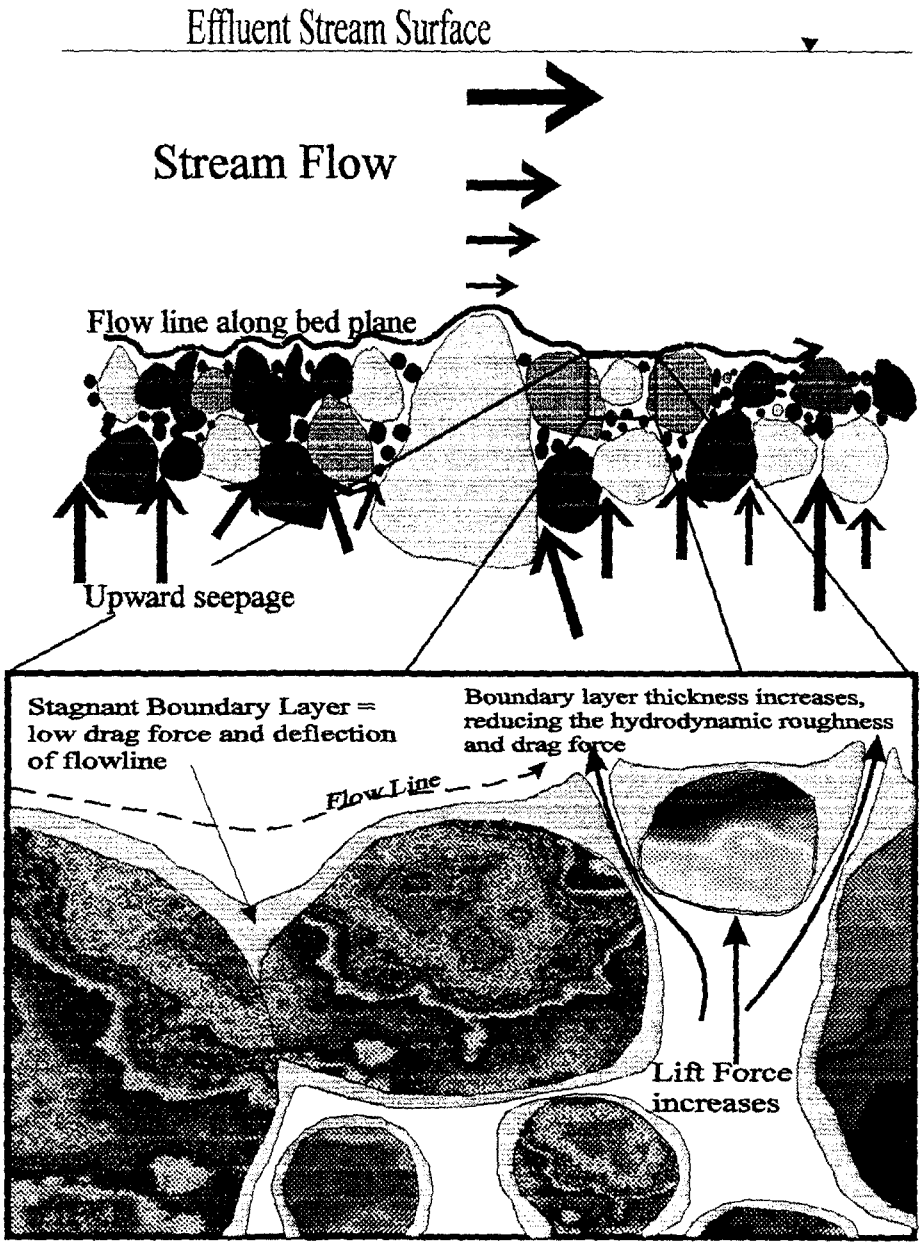

Figure 3.2 Effects of seepage and flow rate on drag and lift forces.

cobbles and gravel, which leads to the conclusion that the increase in lift force is dominant over the reduction in drag force. The first particles to move are the finest fraction and the hydraulic conductivity of the stream bottom increases, because fine material is no longer clogging up space in the interstitial voids of the coarser material. Toward the middle of the study area, the stream bed is primarily composed of sand grains with some cobbles and gravel. In this area the seepage rate is smaller than at upstream locations, consequently, the bed particles are inhibited in their motion.

Throughout the influent portion of the reach (lower half) the stream bed is covered with aquatic plants, which complicates the interpretation of the stream bed composition in terms of drag forces, lift forces, and seepage rates. The dense mat of aquatic plants creates a slow velocity zone along the stream bed which enhances the effects of downward vertical seepage on particle motion.

An anthropogenic effect may be present along the upstream portion, which counteracts the above ideas. Weir #2 is constructed to have a backwater pool in which the water is relatively stagnant compared to the normal flow rate. In this pool of water, the fine material normally being transported along in the stream may settle to the bottom of the backwater pool, and thus not be deposited further downstream. By cutting off the source of fine material, the downstream side of the weir could be stripped clean, thus resulting in a coarser composition, and therefore a higher hydraulic conductivity. The source of fine grained material that is deposited downgradient from the weir originates from two places: 1) from the stream bed directly below the weir, and 2) from the stream banks as storms or snowmelt wash sediment into the stream channel.

The relationship between the location of the aquatic plants and the downward gradient is not a coincidence. A downward seepage velocity holds the fine material in place along the stream bed, which the plants find conducive for root development. Areas of upward gradient do not have fine material present, which has resulted in little to no plant growth. A upward seepage can easily mobilize any fine grained material away from the stream bed, which prevents the aquatic plants from establishing a root system. If the vertical gradients where plants are currently established were to change from downward to upward, the hydraulic conductivity will change as the fine material is mobilized and swept away.

When determining hydraulic conductivity with the constant head permeameter, a downward gradient is imposed, regardless of the natural gradient present. This downward gradient increases the effective stress, which reduces the size of the pore openings in the stream bed material, thus lowers the hydraulic conductivity. An upward gradient may reduce the effective stress, which may increase the hydraulic conductivity. Consequently, even when sediment conditions are constant, the hydraulic conductivity at a point on the stream bed may be higher when an upward gradient prevails than when a downward gradient occurs. As a result, the values of hydraulic conductivity measured with the constant head permeameter may be underestimated. This underestimation will be larger for areas with upward gradient (as compared to areas with downward gradient).

3.4 Effects of Temperature on Hydraulic Conductivity

Changes in temperature of the water in the stream influence the hydraulic condu of the porous media. Hydraulic conductivity is a function of both the porous media an fluid. Intrinsic permeability is not a function of fluid properties. The density and visc of water are temperature sensitive. Temperature was not regularly measured in the fiel the measured temperature of the ground water on March 11, 1995 was 7.5°C, or 45.5° Table 3.1 uses a value of hydraulic conductivity from station 30 to obtain a value of int permeability. This value is then used at different temperatures to see the effects on hydraulic conductivity. As Table 3.1 demonstrates, a considerable temperature change water is required to affect hydraulic conductivity significantly. The temperature ranges in Table 3.1 are not likely to be experienced in the field. Even if they are, the resultin variations in hydraulic conductivity are not significant enough to explain the temporal variations determined from the constant head permeameter.

Temp. C°	15.5	10	5	1
Density (g/ml)	.999	.9997	1.000	.9999
Gravity (cm/sec^2)	981	981	981	981
Viscosity (mp)	11.3	13.1	15.19	17.32
k (cm^2)	$4.3x10^{-8}$	$4.3x10^{-8}$	$4.3x10^{-8}$	$4.3x10^{-8}$
K (cm/sec)	$3.77x10^{-3}$	$3.25x10^{-3}$	$2.81x10^{-3}$	$2.46x10^{-3}$

Table 3.1 Temperature effects on hydraulic conductivity.

Chapter 4. FLOW BETWEEN STREAM AND AQUIFER

The second objective of this project is to use the temporal variation of hydraulic conductivity along with the other hydraulic parameters to estimate the vertical flow rate between the stream and the underlying aquifer. The vertical flow rate is controlled by the hydraulic conductivity of the stream bed, the vertical gradient between the stream and the aquifer, and the cross sectional area.

4.1 Mass Balance

The vertical flow rate between the stream and the underlying aquifer is calculated by equating the difference in stream discharge between the top and the bottom of the reach to the net groundwater flow across the stream bottom. Weir #1 provides discharge data at the downstream end of the site and weir #2 provides discharge data at the upstream end of the site (Figure 2.6). Using a mass balance approach, vertical flow between the stream and the aquifer can be identified as follows:

$$Q_{stream\text{-}in} + Q_{precip} + Q_{gw\text{-}flow\text{-}in} + Q_{over} = Q_{stream\text{-}out} + Q_{gw\text{-}flow\text{-}out} + Q_{evap} + \Delta storage$$

where

$Q_{stream\text{-}in}$ = Stream discharge into the control area, weir #2.
$Q_{stream\text{-}out}$ = Stream discharge out of the control area, weir #1.
Q_{precip} = Flow due to precipitation falling into the control area.
$Q_{gw\text{-}flow\text{-}in}$ = Groundwater flow into stream
$Q_{gw\text{-}flow\text{-}out}$ = Stream flow into aquifer.
Q_{over} = Storm related overland flow.
Q_{evap} = Evaporation from the stream channel.
$\Delta storage$ = Change in storage in the stream channel.

To solve this equation several assumptions have to be made to eliminate the unknowns. These assumptions may limit the value of the analysis. Precipitation falling directly onto the stream is a storm related event. Stream discharge rates are not measured during storms, so effects from precipitation directly on site are neglected. The occasional precipitation events over the site are generally not torrential and measurements are not taken shortly after storms, so overland flow is assumed to be negligible. The annual free water surface evaporation rate is approximately 40 to 42 inches per year (Kohler et. al., 1959, Farnsworth et. al., 1982). Therefore, the amount of evaporation that occurs during the several minutes water takes to flow from weir #2 to weir #1 is insignificant, so evaporation is zero for this budget. Based on these assumptions, the mass balance equation is reduced to:

$$Q_{stream\text{-}in} - Q_{stream\text{-}out} = Q_{gw\text{-}flow\text{-}out} - Q_{gw\text{-}flow\text{-}in} \qquad (4.1)$$

The difference between the stream discharge equals the net amount of water flowing vertically through the stream bed.

4.2 Estimation of Groundwater In-flow and Out-flow

To estimate the net flow rate between the stream and the underlying aquifer, the stream is divided into 11 sections (Figure 4.1), and Darcy's Law is used for each sectior Darcy's Law is written as:

where:

$$Q = K\ i\ A \qquad (4.$$

Q = Flow rate (vertical) (L^3/T)
K = Hydraulic conductivity (L/T)
i = Gradient (unitless)
A = Cross sectional area of flow (L^2)

Each component of Darcy's Law is measured to solve for the vertical flow rate, (that section. The values for the eleven sections are summed to compare against the meas difference in stream discharge between the two weirs as in equation 4.1.

Values for hydraulic conductivity for each section are obtained from the constant l permeameter analysis. The division of the stream into eleven sections is based upon the locations of the constant head permeameter stations, so each section has a measured hydr conductivity. The eleven stations are positioned in areas where the cylinder of the consta head permeameter could be inserted into the stream bed. This means that areas between stations can have different hydraulic parameters than directly at the station itself. For example, if a riffle, or inclined section of the stream bed is between two stations, the gra at the riffle can be different than at either of the adjacent stations. Ideally, a finer discretization of the stream bed could identify these types of changes in the hydraulic parameter. Different schemes to weight the hydraulic conductivity values, other than by centering the permeameter station in each section, as done for this project, are possible.

Vertical gradients are determined from the difference in head between the static w level in the piezometers and the stage of the stream. The static water level in the piezom is measured, but the stream stage values are calculated as described in section 4.2.1. Calculations of vertical gradient are explained in section 4.2.2.

Using the physical dimensions of the particular section of stream as the cross secti area, Darcy's Law is used to solve for flow rate, which corresponds to the vertical flow r through the stream bed within that particular section. The section with the largest influen in the calculation was the section around station 179. This section has the largest gradien largest cross sectional area, and has a coarse composition of the stream bed compared wit the other sections. As a result, the hydraulic conductivity used in the calculation has a la

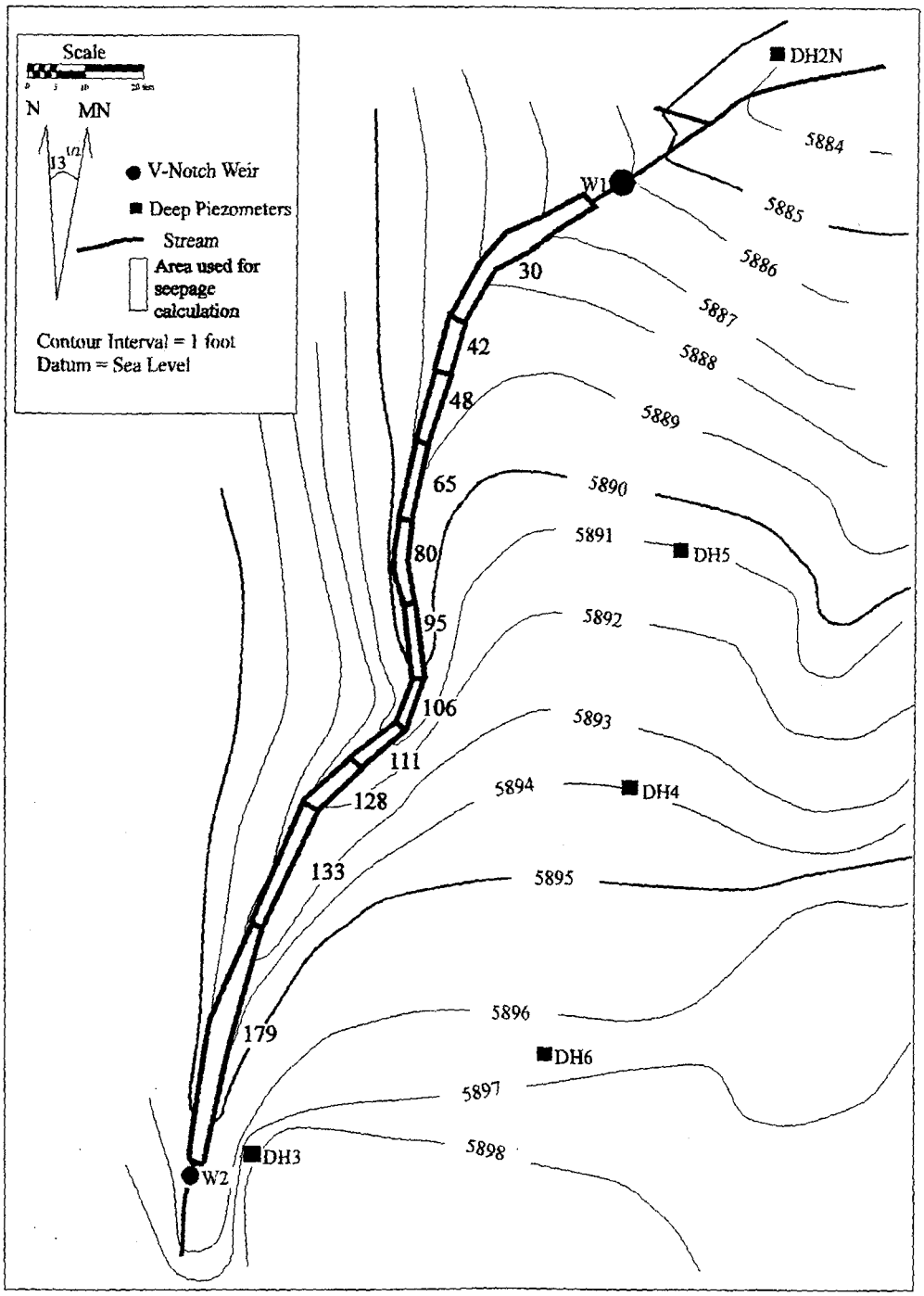

Figure 4.1 Stream divided into sections according to permeameter stations.

influence on the result.

Net vertical flow rate is compared with the difference in stream discharge betwee weir #1 and weir #2 in Table 4.1. The shaded bars indicate that the information is not available for that date, and the values are an approximation using data at the two closest dates. The shaded bar over station 179 indicates that the value of hydraulic conductivity is calculated and not measured. Without these data, the vertical flow can not be determi so a value of K for station 179 is calculated to force the equality in equation 4.1 to be tr The value for area and gradient for station 179 is measured, so the only unknown variabl hydraulic conductivity. The values obtained for hydraulic conductivity at station 179 ran from 2.0×10^{-2} to 4.9×10^{-2} cm/sec, which are reasonable for the clean sands at that locatio (Freeze and Cherry, 1979). The required hydraulic conductivity values at station 179 ar plotted as a function of time in Figure 4.2.

To physically measure hydraulic conductivity at station 179, an artificially saturat falling head permeameter test was done as described in section 2.2. However, in order t determine if the results from these falling head tests can be correlated to naturally saturat conditions, the falling head tests were performed at the same stations where the constant permeameter tests were performed. The results of each test are presented in Table 4.2 al with the range obtained during naturally saturated conditions and the hydraulic conductivi values for station 179 from Table 4.1. By comparison, these values do not appear to correlate well until some other factors are taken into account. At stations 30 through 65, artificially saturated conditions resulted in hydraulic conductivity values nearly an order o magnitude higher than those measured under naturally saturated conditions. However, th were the same locations where the plant growth was heavy while the stream was flowing. When the artificially saturated test was performed, the plants had dried up and the roots dormant, which changed the characteristics of the stream bed material. At station 80 and 106, a good comparison is made between the types of tests. No plants grew at either sta when the stream was flowing, so the character of the stream bed essentially remained the same after the stream dried up, thus the two tests produced similar results. At the locatic where the permeameter was cemented into place, plants never grew in the stream bed, so artificially saturated tests should yield the same K as the naturally saturated conditions an they do.

Relating an artificially saturated hydraulic conductivity to a saturated hydraulic conductivity can be difficult. Flow out of a small well point into an unsaturated soil achi steady state quickly, but within a finite wetting zone (Reynolds et al., 1985). Stephens a Neuman (1982(a), 1982(b)), found the wetted zone to consist of a small artificially satura volume surrounded by an envelope of partially saturated soil. The infiltration rates throu the artificially saturated zone are increased by the suction pressure in the unsaturated zon This suction pressure can influence the falling head and constant head permeameter tests performed with an artificially saturated soil, but this effect should have been minimized b artificially saturating a large volume of soil.

Date	Location	Hydraulic Cond. K (cm/sec)	Area A (ft^2)	Gradient i (-)= Losing	Q=KiA Estimated (cfs)	Seepage Measured (cfs)
3/23	30	3.3E-03	92.5	-0.62	-6.2E-03	
3/23	42	2.4E-03	16	-0.12	-1.5E-04	
3/23	48	7.2E-03	25	-0.21	-1.2E-03	
3/23	65	2.8E-03	45	-0.23	-9.8E-04	
3/23	80	1.5E-02	32.4	-0.16	-2.5E-03	
3/24	95	1.2E-02	19.8	0.11	8.1E-04	
3/24	106	2.7E-03	30	-0.25	-6.6E-04	
3/24	111	9.5E-03	20	0.19	1.2E-03	
3/24	128	6.2E-03	30	0.17	1.1E-03	
3/24	133	9.7E-03	80	0.31	8.0E-03	
	179	**3.1E-02**	**100**	**0.55**	**5.6E-02**	
3/30	30	2.3E-03	92.5	-0.91	-6.4E-03	
3/30	42	1.9E-03	17.6	-0.27	-3.0E-04	
3/31	48	5.3E-03	25	-0.23	-9.8E-04	
3/31	65	2.0E-03	45	-0.21	-6.3E-04	
3/31	80	7.4E-03	32.4	-0.16	-1.3E-03	
3/31	95	9.6E-03	19.8	0.02	1.1E-04	
	106	3.2E-03	30	-0.36	-1.1E-03	
3/31	111	9.7E-03	20	0.22	1.4E-03	
3/31	128	5.5E-03	30	0.31	1.7E-03	
3/31	133	1.2E-02	80	0.41	1.3E-02	
	179	**3.8E-02**	**100**	**0.51**	**6.4E-02**	
4/8	30	2.2E-03	92.5	-0.73	-4.9E-03	
4/8	42	1.6E-03	20	-0.27	-2.9E-04	
4/8	48	4.8E-03	29	-0.23	-1.0E-03	
4/8	65	2.9E-03	45	-0.04	-1.8E-04	
4/8	80	8.1E-03	32.4	-0.08	-6.7E-04	
4/8	95	5.1E-03	19.8	-0.03	-1.2E-04	
4/8	106	6.7E-03	30	-0.46	-3.0E-03	
	111	1.0E-02	20	0.19	1.3E-03	
4/8	128	5.9E-03	34	0.50	3.3E-03	
4/8	133	1.3E-02	80	0.54	1.8E-02	
	179	**4.2E-02**	**100**	**0.55**	**7.6E-02**	

Table 4.1 Flow calculations.

Date	Location	Hydraulic Cond. K (cm/sec)	Area A (ft^2)	Gradient i (-)= Losing	Q=KiA Estimated (cfs)	Seepage Measured (cfs)
4/22	30	1.1E-03	92.5	-0.91	-3.1E-03	
4/22	42	1.4E-03	24	-0.74	-8.1E-04	
4/22	48	1.9E-03	38	-0.22	-5.2E-04	
4/22	65	7.6E-04	45	0.03	3.3E-05	
4/23	80	6.6E-03	32.4	-0.01	-9.7E-05	
	95	3.0E-03	19.8	-0.17	-3.4E-04	
4/23	106	5.9E-03	35	0.09	5.8E-04	
4/23	111	6.0E-03	23	0.19	8.7E-04	
4/23	128	2.6E-03	34	1.14	3.3E-03	
4/23	133	1.7E-02	80	0.59	2.6E-02	
	179	**2.0E-02**	**100**	**0.46**	**3.0E-02**	
				SUM-->		

4/26	30	7.2E-04	92.5	-1.07	-2.4E-03	
4/26	42	1.1E-03	24	-0.91	-7.6E-04	
4/26	48	1.0E-03	38	-0.36	-4.5E-04	
4/26	65	1.2E-03	45	-0.04	-7.2E-05	
4/27	80	3.9E-03	32.4	-0.02	-6.5E-05	
4/27	95	2.3E-03	19.8	-0.53	-7.9E-04	
4/27	106	5.0E-03	35	-0.18	-1.0E-03	
4/27	111	2.5E-03	23	0.10	1.9E-04	
4/27	128	9.7E-04	34	0.49	5.3E-04	
4/27	133	5.7E-02	80	0.27	4.0E-02	
	179	**2.4E-02**	**100**	**0.46**	**3.7E-02**	
				SUM-->		

4/30	30	7.5E-04	92.5	-0.67	-1.5E-03	
4/30	42	9.6E-04	24	-0.32	-2.4E-04	
4/30	48	1.4E-03	38	0.18	3.0E-04	
4/30	65	1.0E-03	45	0.28	4.2E-04	
4/30	80	4.6E-03	32.4	0.07	3.2E-04	
4/30	95	5.9E-03	19.8	-0.08	-3.2E-04	
4/30	106	6.7E-03	35	0.07	5.3E-04	
4/30	111	3.6E-02	23	0.01	2.2E-04	
4/30	128	6.7E-03	34	0.88	6.6E-03	
	133	2.8E-02	90	0.40	3.3E-02	
	179	**2.2E-02**	**100**	**0.57**	**4.2E-02**	
				SUM-->		

Table 4.1 (continued) Flow calculations.

Date	Location	Hydraulic Cond. K *(cm/sec)*	Area A *(ft^2)*	Gradient i *(-)= Losing*	Q=KiA Estimated *(cfs)*	Seepage Measured *(cfs)*
5/3	30	7.8E-04	92.5	-0.67	-1.6E-03	
5/3	42	8.8E-04	24	-0.64	-4.4E-04	
5/3	48	1.7E-03	38	-0.22	-4.7E-04	
5/3	65	1.3E-03	45	0.16	2.9E-04	
5/3	80	5.0E-03	32.4	0.15	8.1E-04	
	95	4.2E-02	19.8	-0.09	-2.4E-03	
5/3	106	1.6E-02	38	0.17	3.3E-03	
	111	3.8E-02	23	0.20	5.6E-03	
5/3	128	8.2E-03	34	0.78	7.2E-03	
	133	4.5E-02	90	0.43	5.7E-02	
	179	**4.9E-02**	**100**	**0.49**	**8.0E-02**	
5/31	30	8.4E-04	92.5	0.06	1.6E-04	
5/31	42	7.1E-04	17.6	-1.04	-4.3E-04	
5/31	48	4.9E-04	25	-0.50	-2.0E-04	
5/31	65	1.1E-03	45	-0.22	-3.6E-04	
5/31	80	4.6E-03	32.4	0.09	4.6E-04	
	95	4.2E-02	19.8	-0.02	-5.4E-04	
	106	1.1E-02	25	0.03	3.1E-04	
	111	3.8E-02	15	0.11	2.0E-03	
5/31	128	5.0E-04	30	0.33	1.6E-04	
	133	2.2E-02	70	0.38	1.9E-02	
	179	**2.0E-02**	**100**	**0.66**	**4.3E-02**	
6/9	30	6.2E-04	92.5	-0.41	-7.7E-04	
6/9	42	3.9E-04	17.6	-0.75	-1.7E-04	
6/9	48	5.5E-04	25	-0.43	-2.0E-04	
6/9	65	7.6E-04	45	-0.24	-2.7E-04	
6/9	80	4.6E-03	32.4	0.03	1.3E-04	
	95	3.4E-02	19.8	-0.02	-4.4E-04	
6/9	106	1.0E-02	25	0.10	8.8E-04	
	111	3.8E-02	15	0.09	1.7E-03	
6/9	128	3.1E-04	30	0.19	5.7E-05	
	133	2.2E-02	60	0.38	1.7E-02	
	179	**3.1E-02**	**100**	**0.60**	**6.1E-02**	

Table 4.1 (continued) Flow calculations.

Date	Location	Hydraulic Cond. K *(cm/sec)*	Area A *(ft^2)*	Gradient i *(-)= Losing*	Q=KiA Estimated *(cfs)*	Seepage Measured *(cfs)*
6/20	30	5.0E-04	92.5	-0.28	-4.3E-04	
6/20	42	3.9E-04	16	-0.77	-1.6E-04	
6/20	48	5.1E-04	20	-0.47	-1.6E-04	
6/20	65	9.8E-04	45	-0.24	-3.5E-04	
6/20	80	4.2E-03	32.4	0.10	4.3E-04	
	95	3.4E-02	19.8	0.27	5.9E-03	
6/20	106	5.8E-03	20	0.24	9.4E-04	
	111	2.2E-02	15	0.42	4.5E-03	
6/20	128	9.4E-04	30	0.26	2.4E-04	
	133	1.0E-02	50	0.37	6.1E-03	
	179	**2.0E-02**	**100**	**0.26**	**1.7E-02**	

Table 4.1 (continued) Flow calculations.

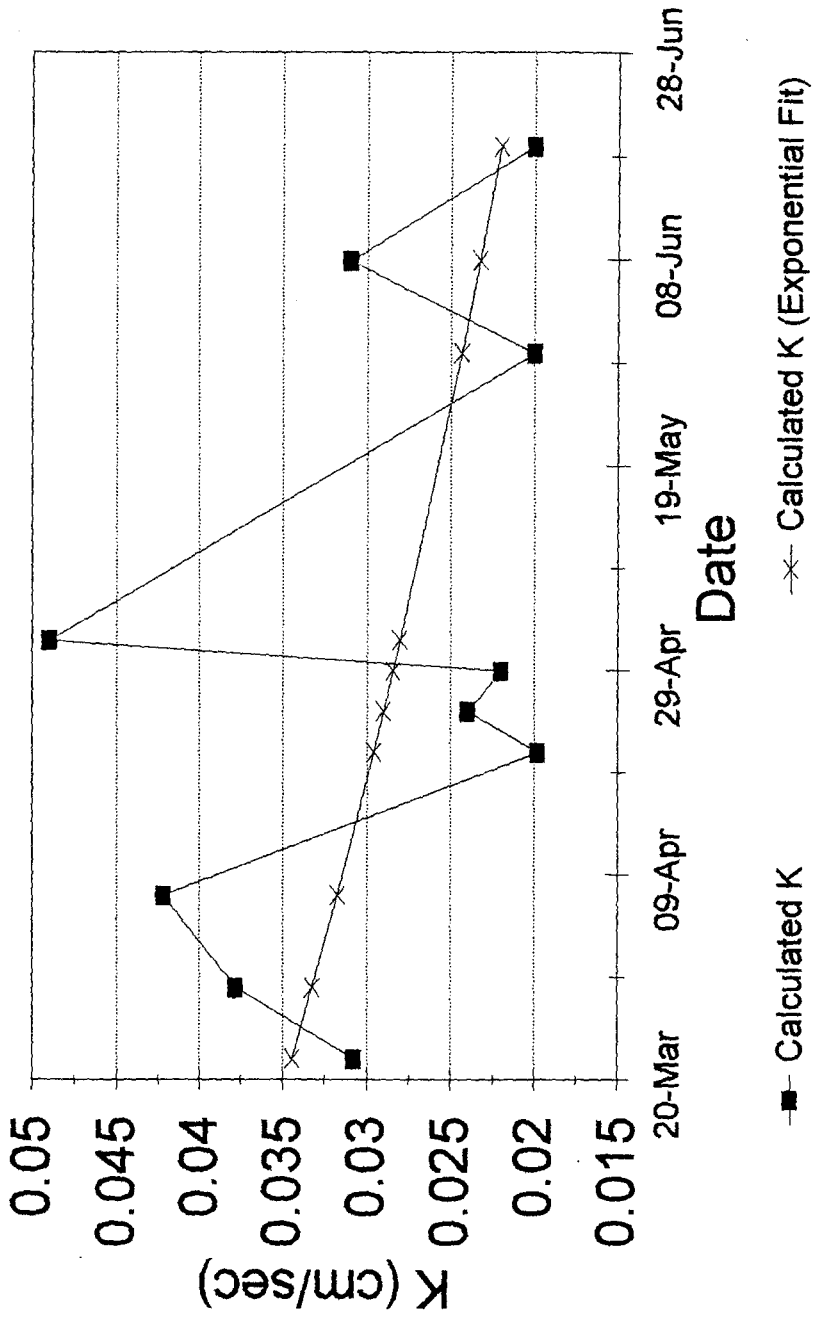

Figure 4.2 Hydraulic conductivity v. time (station 179).

Location	Hydraulic Conductivity (cm/sec)	Range of Ksat from Constant Head Permeameter (cm/sec)	Range of Ksat at Station 179 from Table 4.1 (cm/sec)
Cemented Pipe Aug. 10, 1994	$1.1x10^{-2}$ $1.0x10^{-2}$ $9.4x10^{-3}$ $8.3x10^{-3}$ $8.0x10^{-3}$ $7.5x10^{-3}$	None taken	$2.0x10^{-2}$ to $4.9x10^{-2}$
Cemented Pipe Oct. 2, 1994	$3.2x10^{-2}$ $2.5x10^{-2}$ $2.2x10^{-2}$ $2.0x10^{-2}$ $2.2x10^{-2}$ $2.4x10^{-2}$	None taken	
Station 30	$1.8x10^{-2}$ $1.8x10^{-2}$ $1.6x10^{-2}$ $1.6x10^{-2}$	$6x10^{-3}$ to $4x10^{-4}$	
Station 42	$2.0x10^{-2}$ $1.7x10^{-2}$ $1.7x10^{-2}$	$2x10^{-3}$ to $8x10^{-4}$	
Station 48	$4.8x10^{-2}$ $4.6x10^{-2}$ $4.4x10^{-2}$	$7x10^{-3}$ to $5x10^{-4}$	
Station 65	$3.0x10^{-2}$ $3.2x10^{-2}$ $3.0x10^{-2}$ $3.0x10^{-2}$	$3x10^{-3}$ to $6x10^{-4}$	
Station 80	$1.3x10^{-2}$ $1.2x10^{-2}$ $1.1x10^{-2}$ $1.1x10^{-2}$	$2x10^{-2}$ to $4x10^{-3}$	
Station 106	$2.6x10^{-2}$ $2.6x10^{-2}$ $2.5x10^{-2}$	$2x10^{-2}$ to $3x10^{-3}$	

Table 4.2 Results of artificially saturated permeameter tests.

4.2.1 Stream Stage v. Discharge

Mistakenly, stream stage measurements were not made over much of the study period. Stream stage was only measured at very low discharge rates before the stream completely dried up. Stream stage at times of peak discharge was determined by estimating the elevation to which the water rose along the bank. These stage and flow data were plotted and an empirical formula was fit to the observed data. These graphs were used to estimate stream stage for a given discharge rate. The resulting graphs are shown in Appendix D. Due to the non-prismatic nature of the stream channel and the extreme roughness of the stream bed, Mannings Equation was considered inappropriate and was not used. Table 4.3 shows the empirical relation between stream stage and discharge.

4.2.2 Determination of Vertical Gradients.

Vertical gradients are determined by dividing the difference in head by the distance along the flow path between the head measurements. Gradient can be written as:

$$Gradient = \frac{\Delta\ Head}{\Delta Length} = \frac{\Delta H}{\Delta L} \qquad (4.3)$$

The difference in head is the difference between the static water level in the piezometer and the stream stage. The length term is the distance between the stream bottom and the center of the open interval of the piezometer. Values of gradient are presented in Figure 4.3.

Location	Empirical Equation
30	$5888.51 + \frac{\log(weir1(cfs) * 10 + 0.01)}{7.4}$
42	$5888.95 + \frac{\log(weir1(cfs) * 8 + 0.03)}{6.9}$
48	$5889.09 + \frac{\log(weir1(cfs) * 5 + 0.001)}{8.1}$
65	$5889.455 + \frac{\log(weir1(cfs) * 2 + 0.0001)}{13.3}$
80	$5889.575 + \frac{\log(weir1(cfs) * 2 + 0.01)}{6.0}$
95	$5890.77 + \frac{\log(weir1(cfs) * 1.5 + 0.004)}{6.5}$

Table 4.3 Empirical equations of stream stage as a function of discharge.

Location	Empirical Equations
106	$5891.36 + \frac{\log(weir1(cfs) * 1.2 + 0.002)}{4.0}$
111	$5891.369 + \frac{\log(weir1(cfs) * 1.2 + 0.005)}{7.5}$
128	$5892.315 + \frac{\log(weir1(cfs) * 2.5 + 0.0001)}{13.0}$
133	$5892.475 + \frac{\log(weir1(cfs) * 1.7 + 0.01)}{7.0}$
173	$5894.06 + \frac{\log(weir1(cfs) * 1.2 + 0.006)}{4.0}$

Table 4.3 (continued) Empirical equations of stream stage as a function of discharge.

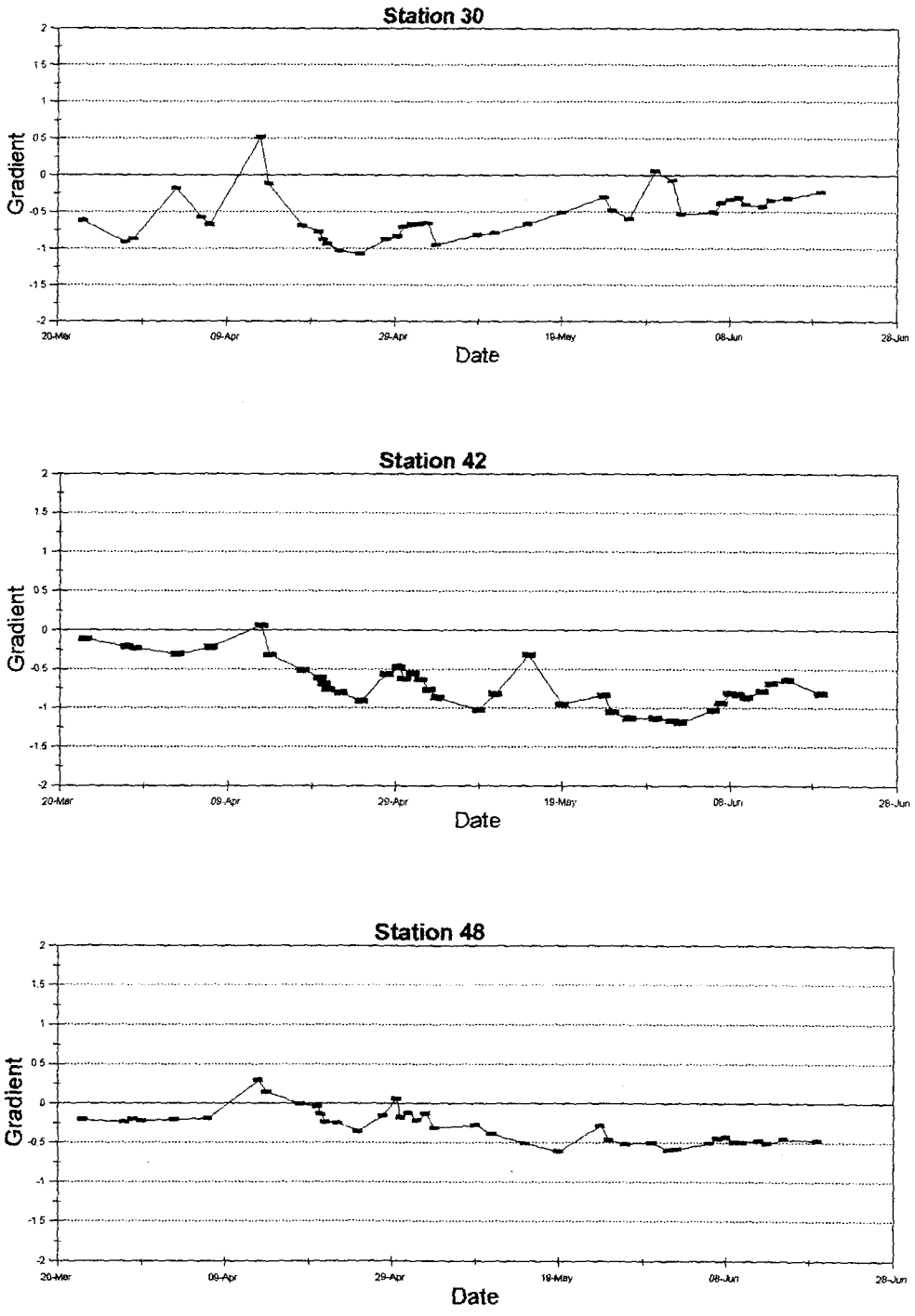

Figure 4.3 Vertical gradient.

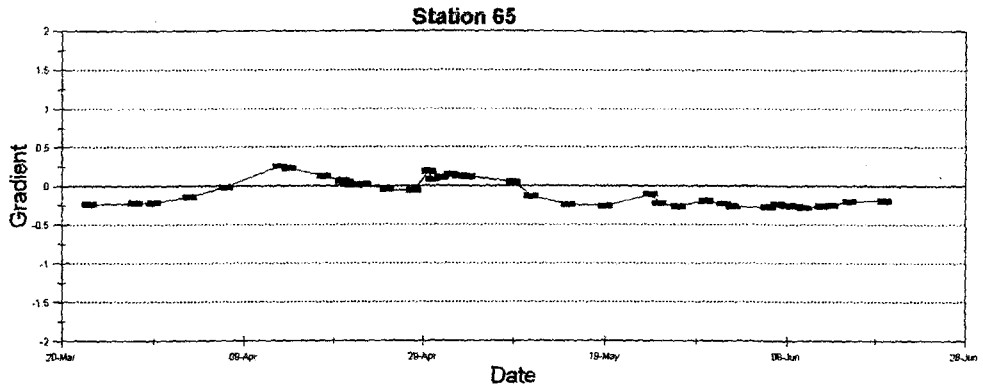

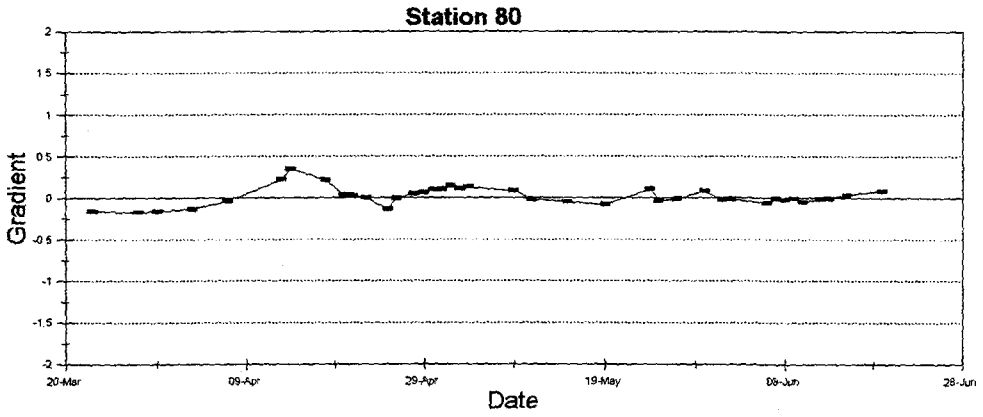

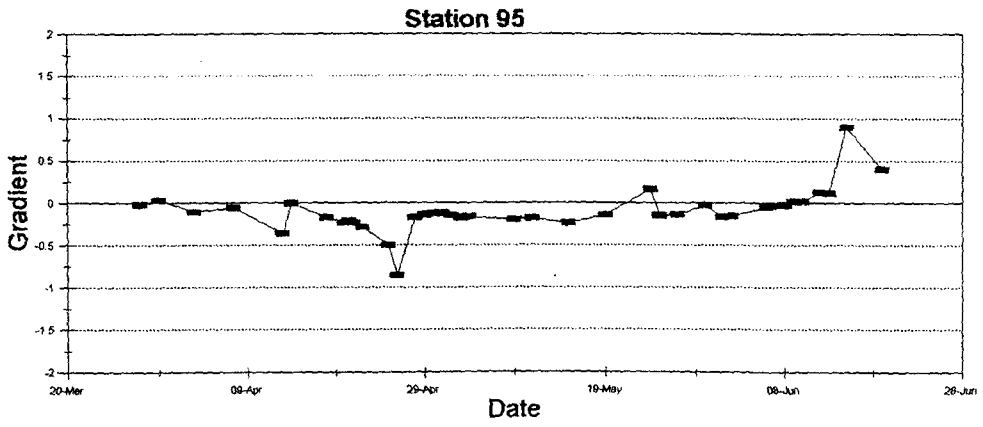

Figure 4.3 (continued) Vertical gradient.

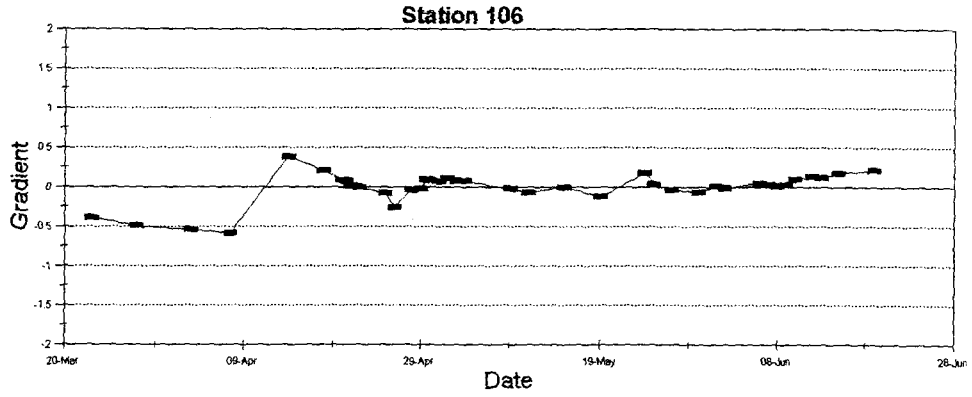

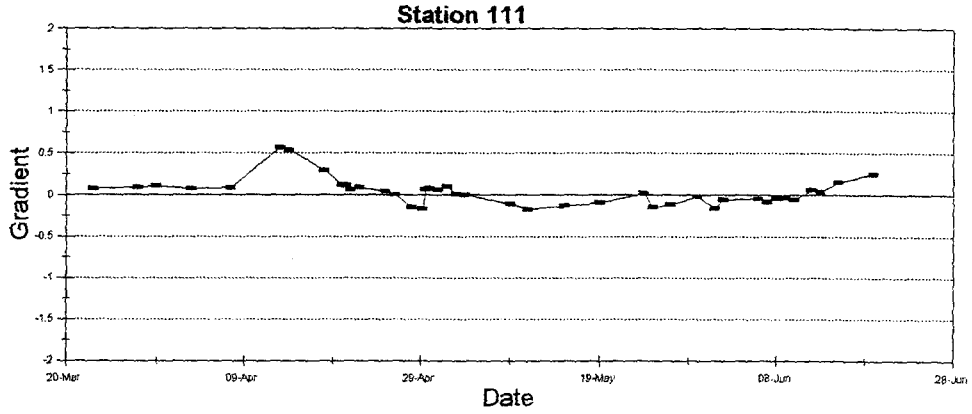

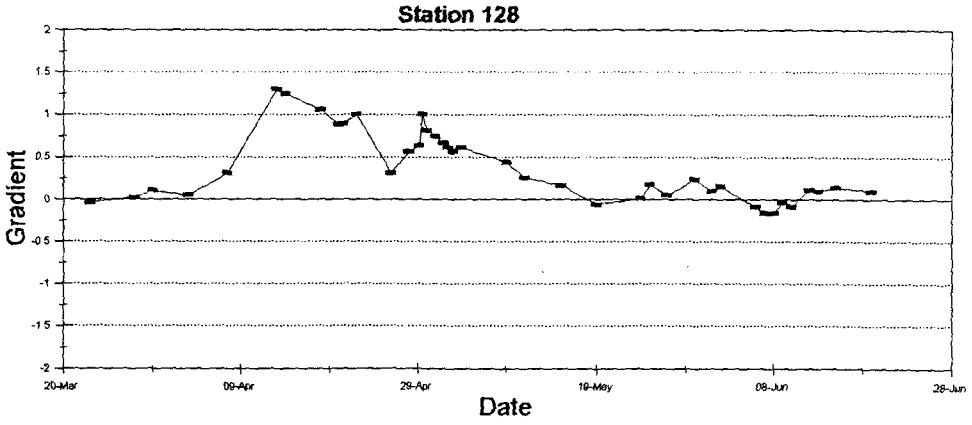

Figure 4.3 (continued) Vertical gradient.

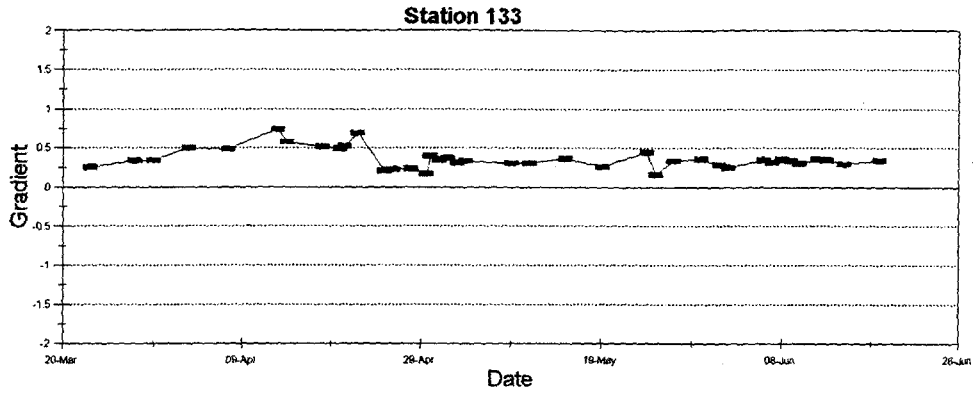

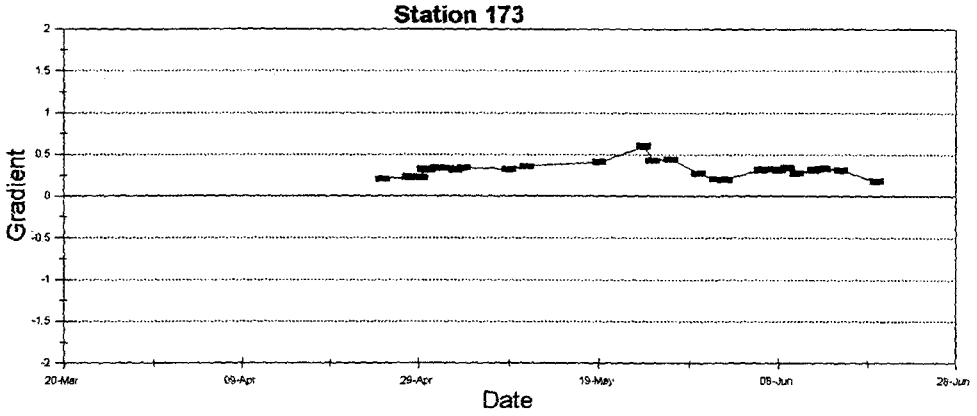

Figure 4.3 (continued) Vertical gradient.

Chapter 5. SITE HYDROGEOLOGY

The characterization of the site hydrogeology includes; the distribution of head direction of groundwater flow, saturated thickness in the alluvium, identification of the gaining and losing reaches of the stream, distribution of K within the alluvium, depth t bedrock, nature of the underlying bedrock, and distribution of recharge based on plant distribution.

Using head data collected from the four shallowest piezometers of the deep bor the two single piezometers (DH2 S & N), and the piezometers along the stream channe distribution map of head is made. A map of the head distribution on April 27, 1994 is presented in Figure 5.1. The direction of groundwater flow in the aquifer roughly par the stream channel. The static water levels in the deep borehole piezometers indicates t saturated thickness in the alluvium ranges from 14 feet to 20 feet thick during times of discharge in the stream to 7 feet to 10 feet during the dry season.

Based on data collected from the shallow piezometers in the stream channel, the identification of a gaining and a losing reach is made. The gaining reach begins at the upstream boundary of the field site and extends to approximately station 80. Supportin for this observation are found in the direction of vertical gradients established by the sh piezometers. Station 80 exhibits both upward groundwater flow and downward (Figure Station 80 is located at the base of an inclined section in the stream channel, which hap to be in the transition zone between the gaining reach and the losing reach. Station 95 l consistent downward gradient, which is probably the result of being located near the top inclined section of stream (Figure 5.2). Downstream from station 80 the vertical gradie are generally downwards indicating a losing reach that extends to the downstream bound

Results from the slug test analyses are presented in Table 4.4. These results are graphically presented in Figure 5.3. The question marks next to the piezometers indicat undetermined hydraulic conductivity values. Hydraulic conductivity at the question mar DH6 is not determined due to either a clogged sand pack or because the open interval is completed in an extremely low K zone. The unknown value of K at the DH5 wellbore i to the wellbore being dry. The large variations of K indicate heterogeneities are present the alluvium. A unique pattern cannot be resolved with the few data points available.

Depth to bedrock varies from 17 to 25 feet below ground surface. These variatio are attributed to different erosion rates of the bedrock prior to deposition of the alluvium This bedrock topography is considered a major hydraulic control to the groundwater and stream flow.

Variable geology is encountered at the base of the deep piezometers. Bedrock at t bottom of wells DH3, DH4, and DH5 is hard and competent. However, the bedrock be DH6 is clay. Based on field observations adjacent to the site and the geologic map of the Morrison Quadrangle, there are three geologic units beneath this site: the Morrison Formation, Ralston Creek Formation, and the Strain Shale Member of the Lykins Format A resistant layer of sandstone that is either lower Morrison Formation or upper Ralston C Formation is oriented near vertical and strikes approximately northwest-southeast directly through the field site (Weimer, personal communication).

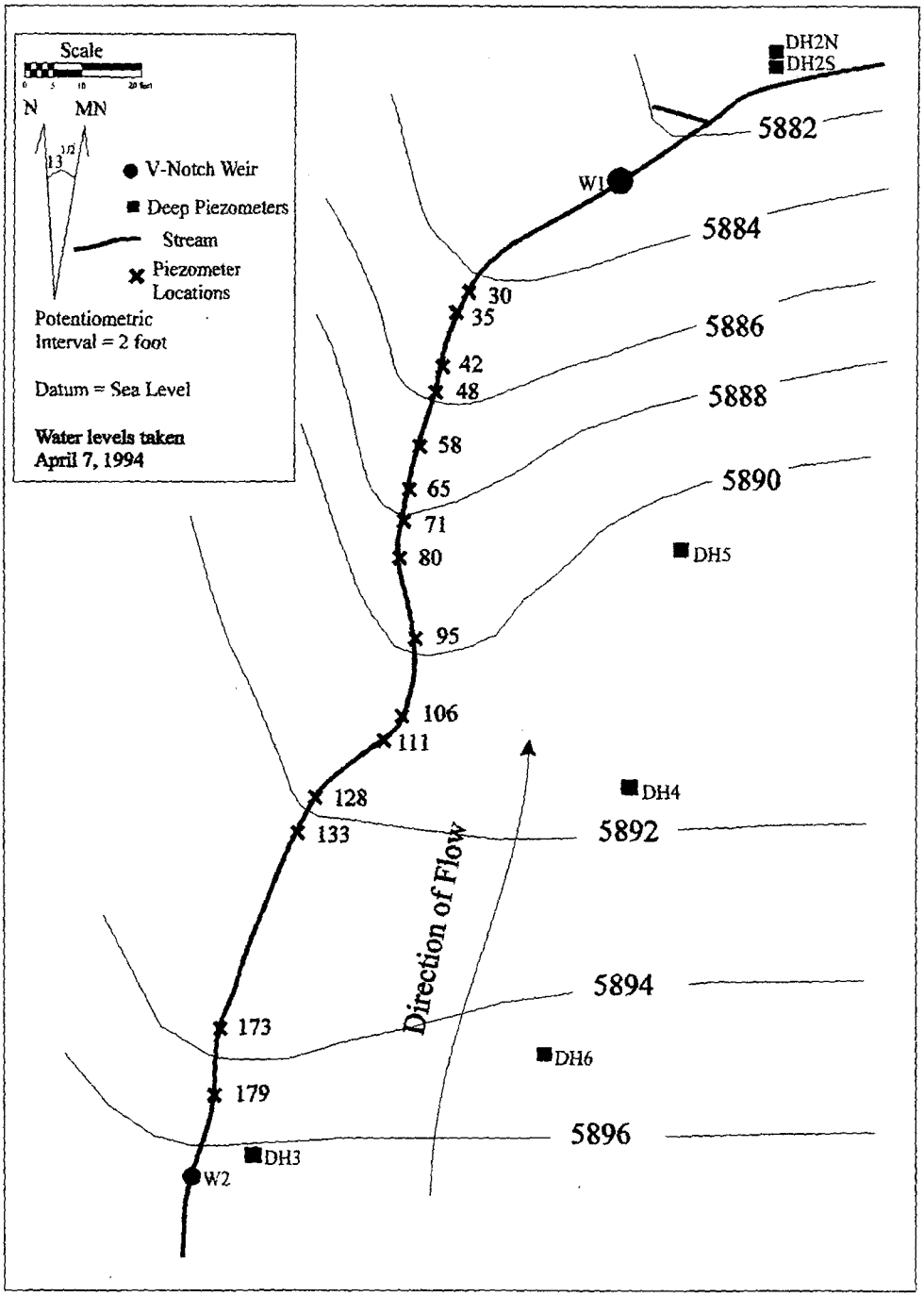

Figure 5.1 Head distribution and direction of flow.

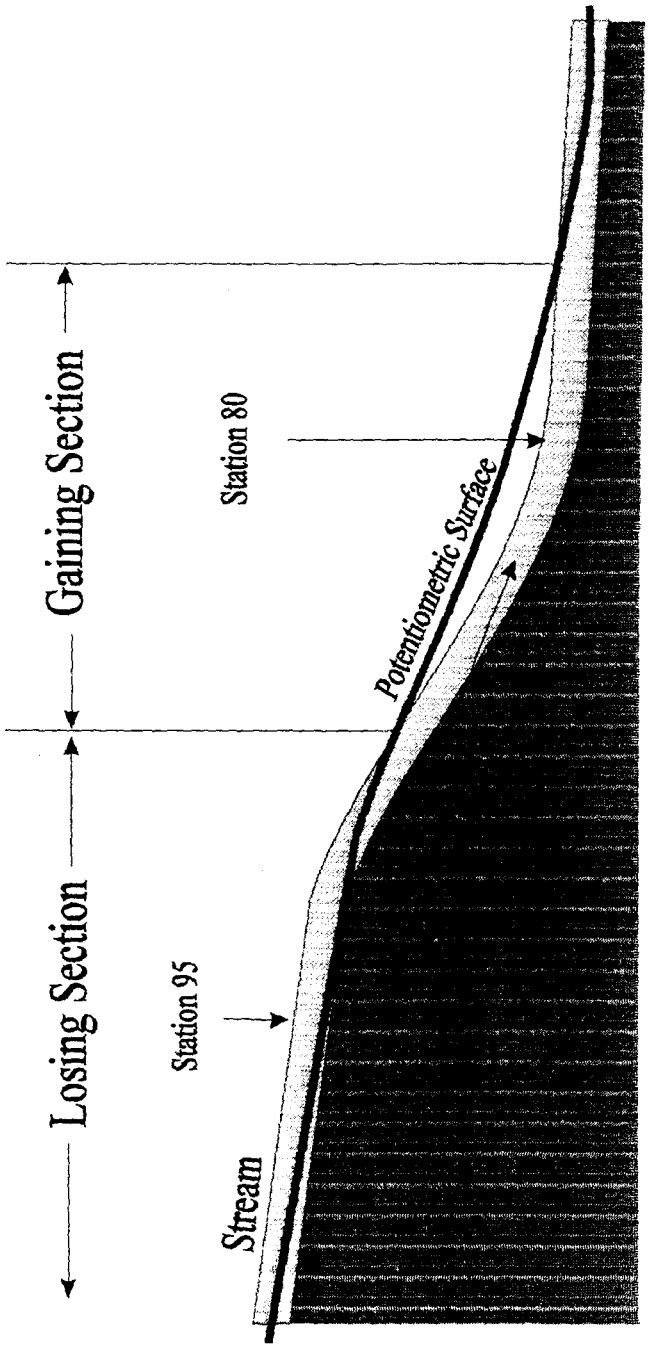

Figure 5.2 Inclined stream channel resulting in vertical gradients.

Location	Date	Hvorslev (cm/sec)	Bouwer & Rice (cm/sec)
DH3-16	June 11 June 27	$6x10^{-5}$ $1x10^{-4}$	$6x10^{-5}$ $1x10^{-4}$
DH3-12	June 27	$4x10^{-4}$	$2x10^{-4}$
DH3-8	June 27	$2x10^{-4}$	$6x10^{-5}$
DH4-16	June 10	$2x10^{-4}$	$3x10^{-4}$
DH4-13	June 10 June 11	$1x10^{-5}$ $7x10^{-5}$	$4x10^{-6}$ $2x10^{-5}$
DH4-8	June 11	$2x10^{-5}$	$3x10^{-5}$
DH5-17	June 10 June 27	$2x10^{-5}$ $2x10^{-4}$	$1x10^{-5}$ $1x10^{-4}$
DH5-14	June 10 June 27	$2x10^{-5}$ $1x10^{-4}$	$9x10^{-6}$ $1x10^{-4}$
DH6-20	June 27	$7x10^{-6}$	$3x10^{-6}$
DH6-15	June 27	$7x10^{-5}$	$3x10^{-5}$

Table 4.4 Slug test results.

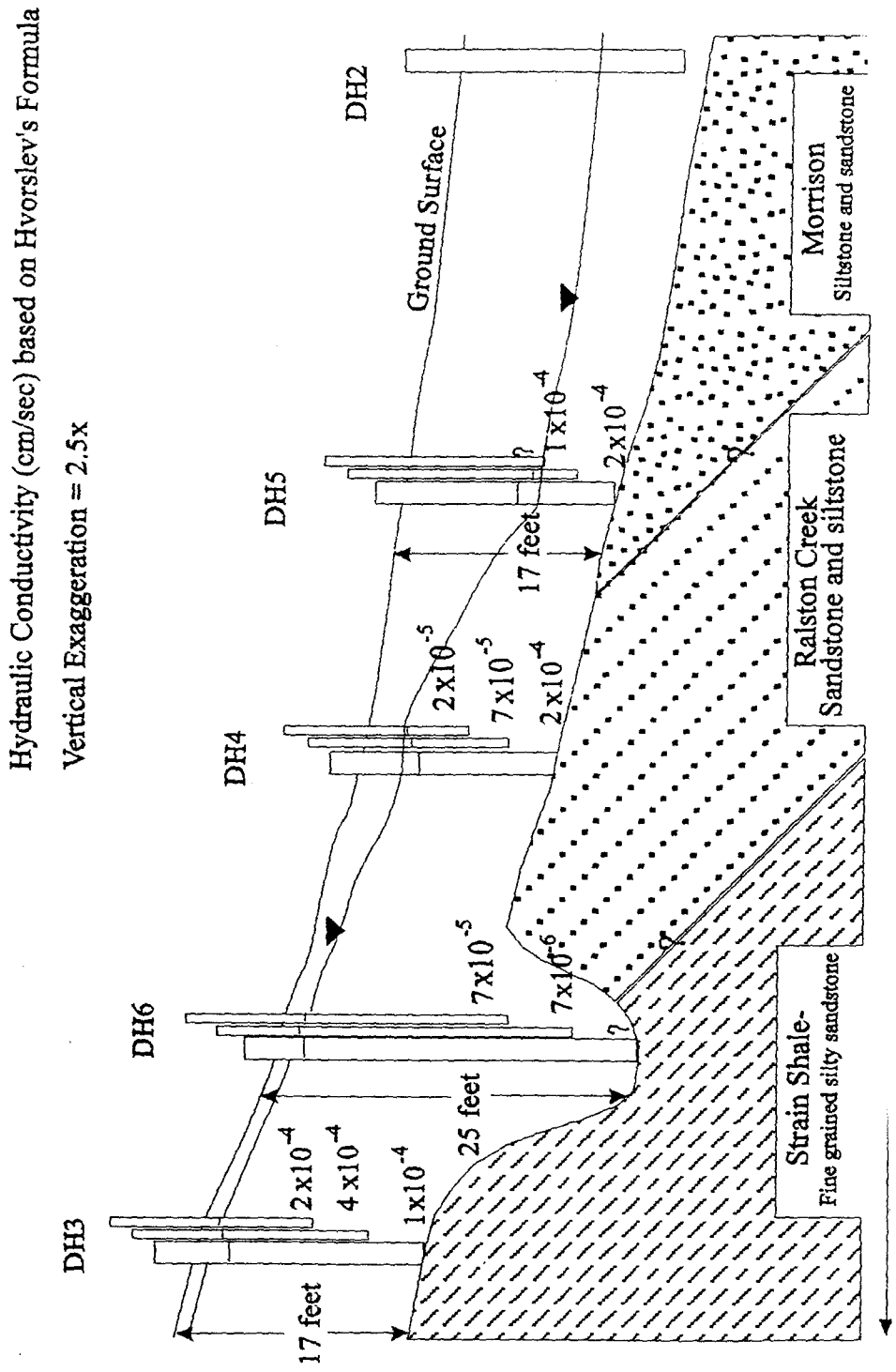

Figure 5.3 Distribution of hydraulic conductivity in the alluvium.

The distribution of the plants is a key to the geohydrology of this system. Many varieties of plant species are present at the site. Vegetation consists of yucca, optunia, and some grasses, all of which require little water for survival. Cottonwood trees, willows, reeds, scrub oak and other bushes are water loving species and are found along the stream channel (Bissett, 1994). With the presence of the large cottonwood trees, an easy inference can be made that the present hydrologic system has been very consistent. In order for the cottonwood trees to grow to their present size, a supply of water must have been available from year to year. The high concentration of phreatophytic plants along the stream channel is supporting evidence that the water table is close to the ground surface. Further from the stream channel, the nature of the plant species suggests that the water table is consistently beyond the reach of phreatophytic plants.

The proximity between water loving cottonwoods and cactus is a reflection of the variations in the recharge rate. Annual precipitation is approximately 18 to 23 inches, but the presence of cactus indicates that the amount of water available to the plants is low. Evidence for various conceptual models can be taken from this observation. Areas with cactus must shed the precipitation quickly either by surface runoff or by rapid infiltration. If this water is able to infiltrate rapidly, then this water can enter the groundwater system as recharge, rather than being removed through overland flow and/or evaporation.

The density and height of the grass species present suggest that the soils within the site have differing abilities to retain water (Emerick, personal communication). This capacity of soils to hold water can be attributed to either clay content or a caliche layer. Water retention is not the only factor controlling growth rate of the grass. For example, where the recessive Strain Shale Member crops out, the grass is sparse, indicating a lack of water and/or a lack of nutrients. Adjacent to the stream channel, the grass grows thick and tall, indicating a good supply of nutrients and water. These observations are an indicator of variable recharge across the site.

Chapter 6. CONCEPTUAL MODELS

The third objective of this project is to develop conceptual models that are suppor by the field observations. Ideally, the field data would support one unique conceptual m Realistically, the data are not sufficient to generate the ideal conceptualization, thus a nu of alternative conceptual models must be considered. Future work can be targeted towar eliminating some of the alternative models.

Using all of the information gathered, several conceptual models are developed. model accounts for the gaining reach and the losing reach as supported by the vertical gradient measured with the piezometers in the stream channel. Also, the models account the vertical gradients and the variations of K in the deep boreholes. According to the dat from the piezometers in the stream bottom, the gaining portion starts near weir #2 and extends downstream to approximately station 95. Downstream from station 95 the strean generally losing.

The nested piezometers in DH3 through DH6 consist of three piezometers, which provides two intervals for determination of vertical gradient. The borehole DH2 has one interval to use in calculating vertical gradient. Gradient calculations involving piezometer DH6-25 have questionable value as a result of either poor well development or extremely tight material around the open interval. In either case, the water levels in DH6-25 are ve slow to respond to respond to water level changes. The vertical gradients in DH2 throug DH6 are presented in Figure 6.1.

6.1 Conceptual Model #1.

The first conceptual model considers the underlying bedrock, which subcrops on b sides of the stream, to form a channel in which the alluvium was deposited. This bedrock of such low permeability that the leakage between it and the alluvium is negligible. In thi scenario, paleotopography in the bedrock causes the gaining and losing reaches as shown i Figure 6.2.

6.2 Conceptual Model #2.

The second conceptual model considers a low permeability layer within the alluviu A low permeability layer causes flow-divergence upgradient and convergence downgradien The low permeability layer also lowers the bulk hydraulic conductivity of the alluvium, w raises the gradient and hydraulic head. Ground water flows at a much slower rate through the low K material. If the water table rises until ground surface is intersected, a gaining stream is created. If this low permeability layer is not continuous throughout the alluvium

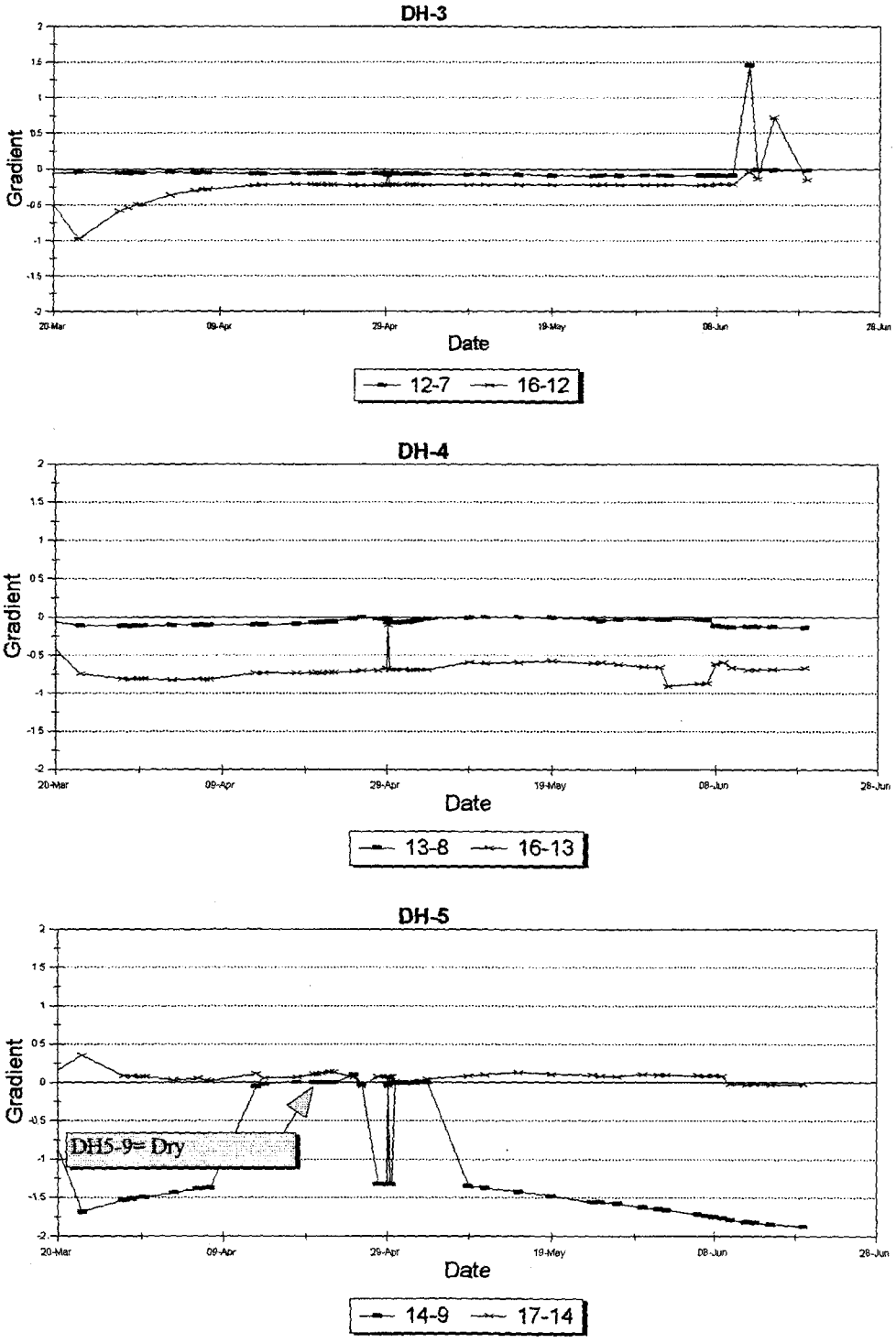

Figure 6.1 Vertical gradients in the deep boreholes.

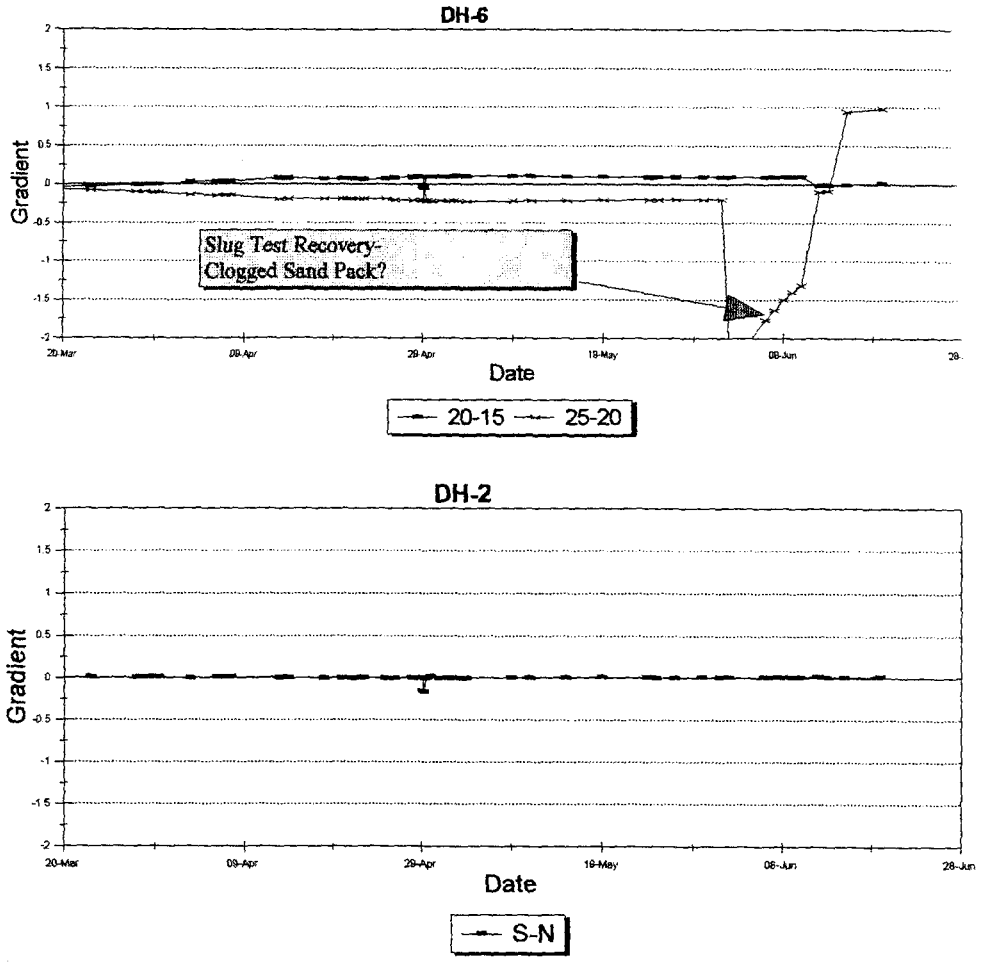

Figure 6.1 (continued) Vertical gradients in the deep boreholes.

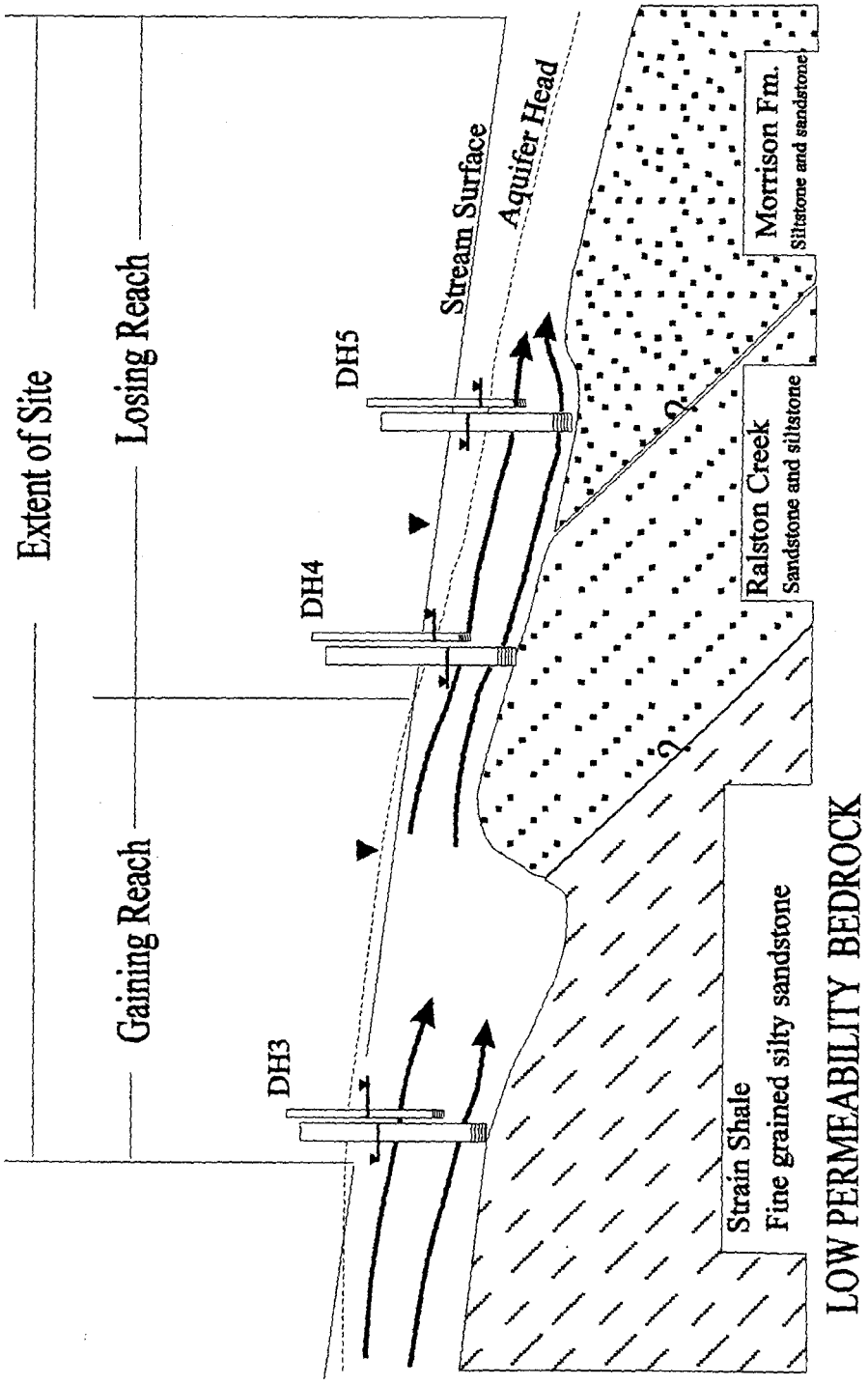

Figure 6.2 Gaining and losing reaches controlled by bedrock topography.

the bulk hydraulic conductivity increases where the layer is absent resulting in a decreas gradient and a lower head. A gaining and losing portion of a stream, as controlled by a impermeable layer within the alluvium, is illustrated in Figure 6.3. Evidence for low permeability zones within the alluvium is illustrated in Figure 5.3.

6.3 Conceptual Model #3.

The vertical gradients in the alluvium can be generated by considering that there i significant leakage into the bedrock. If there are moderately permeable zones with lower head in the bedrock then water flows from the alluvium to the bedrock in response to the downward gradient. The gradient in the lower interval of piezometer nest DH3 is downv The gradient in the lower interval of piezometer nest DH5 is upward. This scenario is illustrated in Figure 6.4. The same scenario can be created with a low permeability layer within the alluvium, illustrated by Figure 6.5.

6.4 Lateral Boundaries of the Conceptual Models

The lateral boundaries in Figures 6.2 through 6.5 are illustrated in Figure 6.6. Th water table in Figure 6.6 is shown to terminate at the bedrock-alluvium-water table contac Beneath this contact the bedrock is unsaturated. However, alternative hydrologic conditio may exist at these boundaries. The water table may exist above the bedrock-alluvium con along the side of the alluvial channel (Figure 6.7). The underlying bedrock could be eithe saturated or unsaturated.

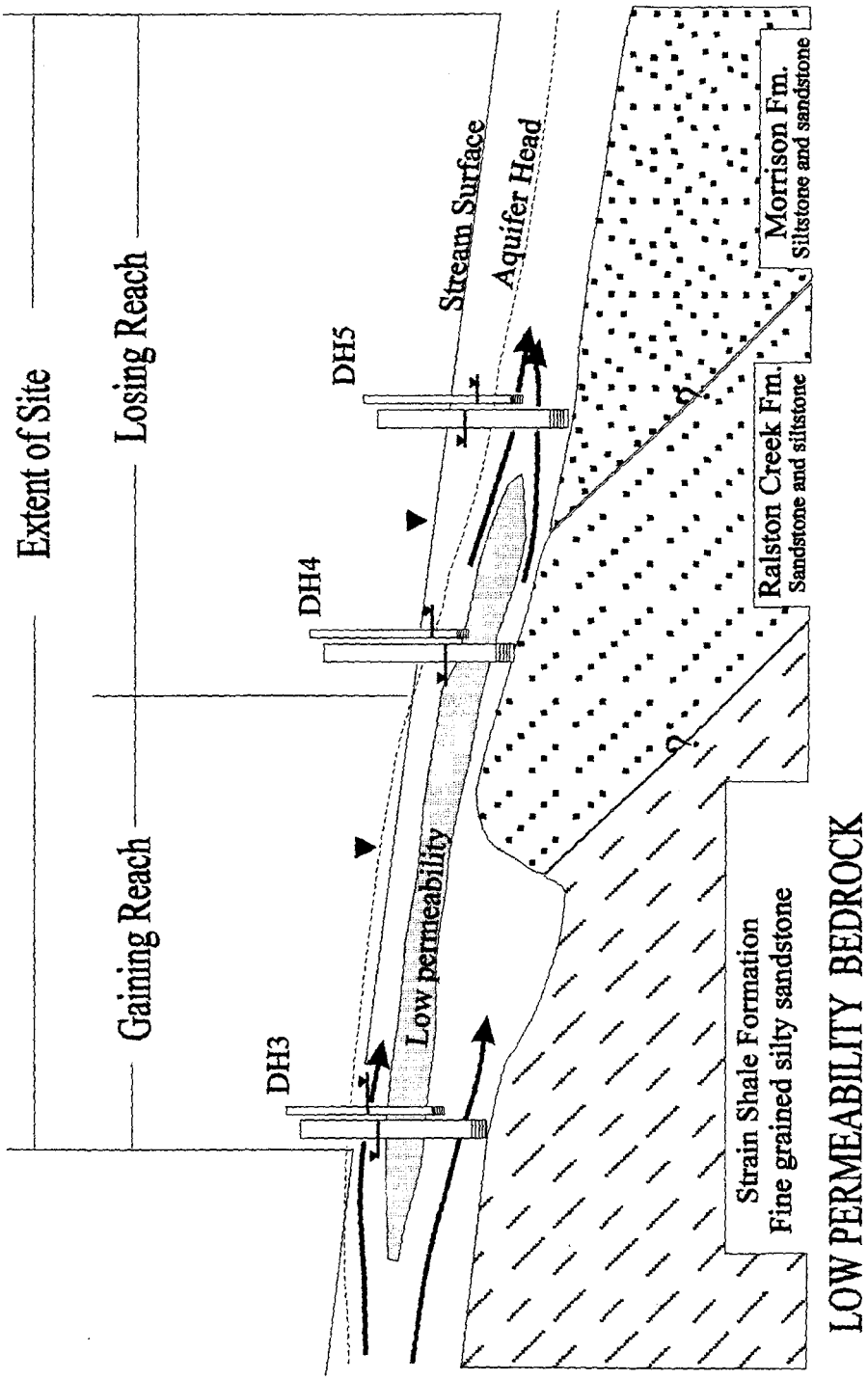

Figure 6.3 Gaining and losing reaches controlled by an impermeable layer.

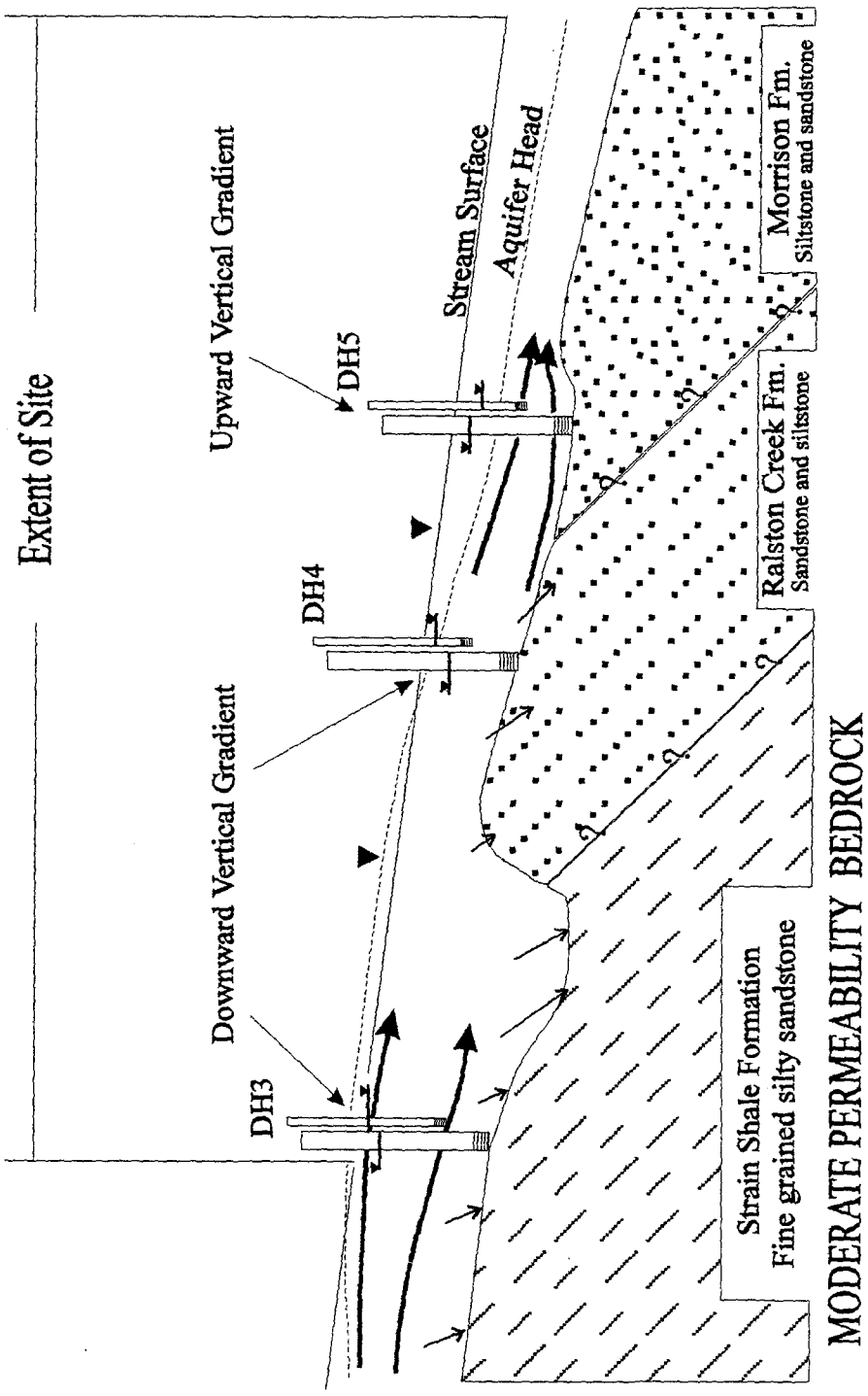

Figure 6.4 Vertical gradients with a varying bedrock topography.

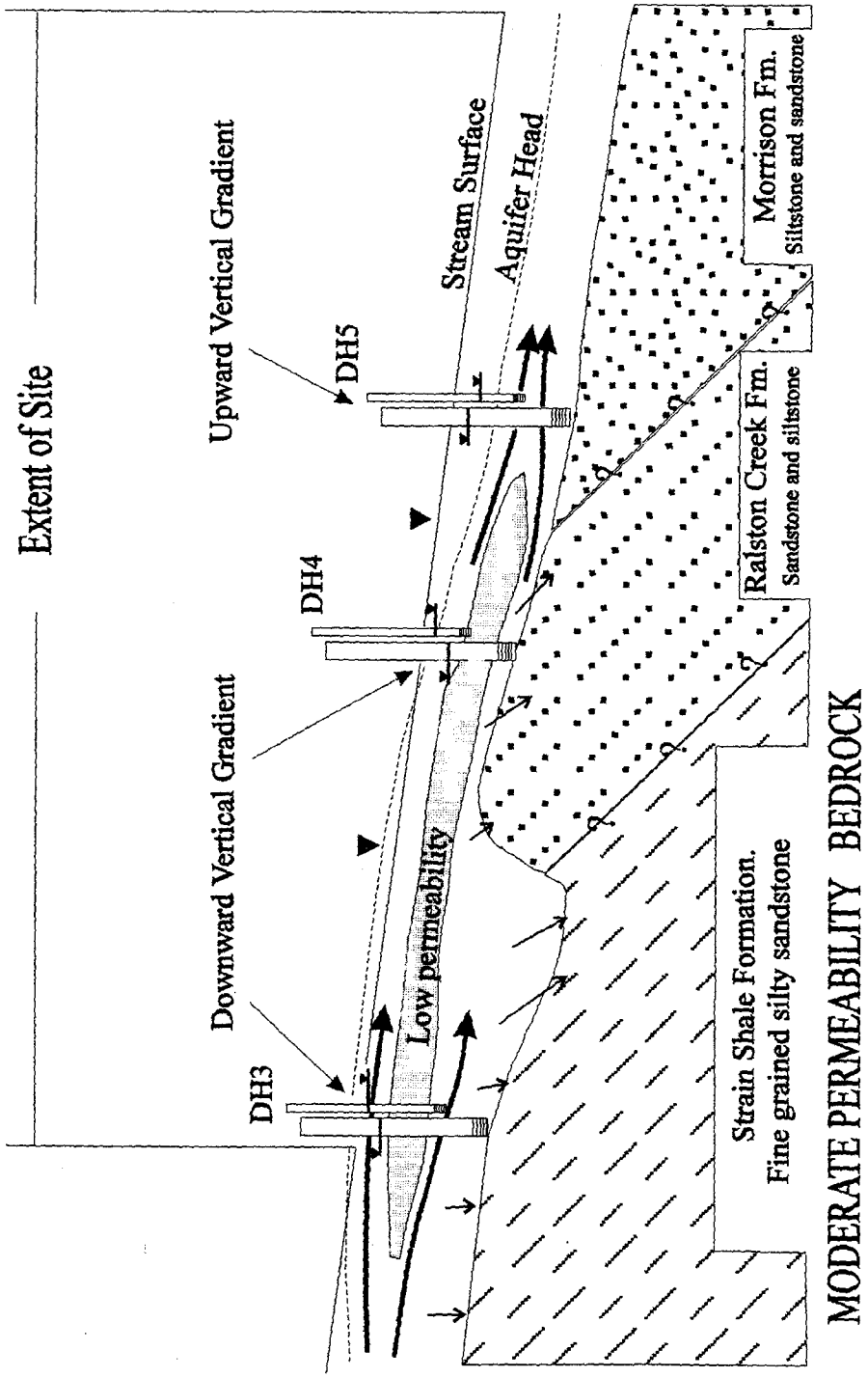

Figure 6.5 Vertical gradients with a low permeability layer.

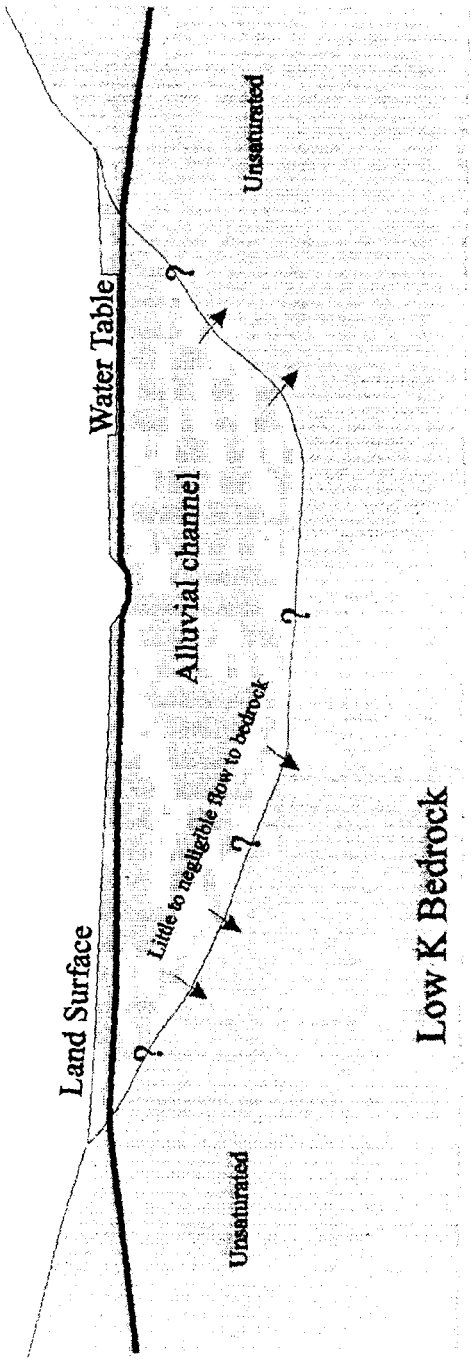

Figure 6.6 Lateral boundary model #1.

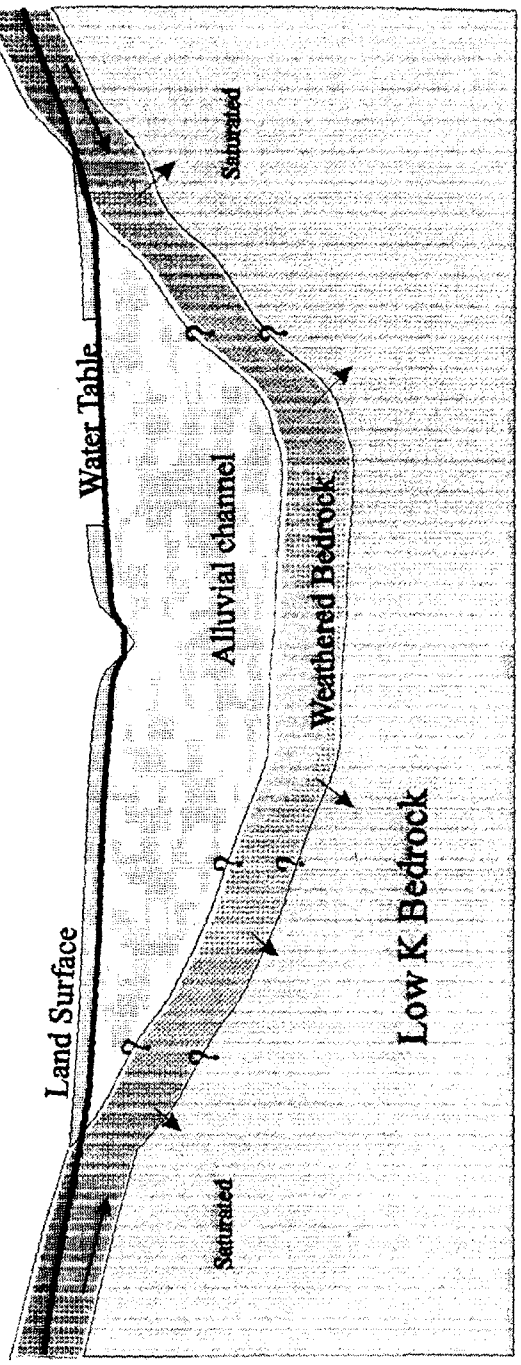

Figure 6.7 Lateral boundary model #2.

Chapter 7. SUMMARY AND CONCLUSIONS

The purpose of this project is to understand the nature of stream/aquifer interactic The methods used and the information gathered with this project have advanced the understanding of this system.

The first objective of this project is to quantify the temporal and spatial variabilit the hydraulic parameters of a stream bed. This objective is satisfied through the use of several field techniques. One of the field methods employed is the constant head permeameter. The constant head permeameter is well suited for this project because it is portable, easy to operate, and produces good results. The constant head permeameter is suitable in stony soils. The data obtained from the permeameter supports that hydraulic conductivity of the stream bed varies with time. A decrease in hydraulic conductivity ov the period of spring runoff was observed in sections of the stream bed where aquatic plan flourished. These plants act as filters in the stream to remove fine sediments from suspension. These fines collect at the water-sediment interface forming a layer that reduc the hydraulic conductivity. Hydraulic conductivity was erratic in sections where there are plants and no strong vertical gradients. Measurements along sections of stream that had a strong upward gradient indicate an increase in hydraulic conductivity over the period of spring runoff.

The second objective is to use the hydraulic parameters to calculate the flow rate between the stream and the aquifer. To complete this objective, hydraulic conductivity va are needed for the stream bed along the uppermost section. A range of hydraulic conductivity values was obtained by using a falling head permeameter under artificially saturated conditions. By comparison, the range of K values measured by the artificially saturated permeameter tests is similar to the range calculated indirectly with the mass balar equation. This leads to the conclusion that the hydraulic parameters used in the calculatior flow between the stream and aquifer are reasonable. The measured net vertical flow rates between the stream and the aquifer range from $3.4x10^{-2}$ to $1.5x10^{-1}$ cfs from March 23, 19 through June 20, 1994. The positive number represents a net increase in stream discharge along the 200 foot reach, signifying a gaining stream. The stream went dry during the firs week in July 1994. Stream flow rates range between 0 and 1.2 cfs. Peak discharge occur in late April during the spring thaw.

The third objective is to develop several conceptual models that characterize the hydrologic system. The distribution of large phreatophytic trees indicates the groundwater system is available to these plants from year to year. The distribution of cacti and grasses indicates a variable recharge rate across the site. The bedrock exhibits up to 8 feet of topographic relief as revealed during the drilling of the deep boreholes. The erosion resista layer of either lower Morrison Formation or upper Ralston Creek Formation is oriented nea vertically and strikes through the site. This resistant layer creates the topographic relief beneath the site. Subsurface controls on the hydrologic characteristics of the site could not uniquely resolved with the available data, therefore alternative conceptual models are developed.

Future work for this area could be directed to eliminate some of the conceptual models, or refine the interpretation of the current data. To support or eliminate the

conceptual model using an impermeable layer within the alluvium, a continuous soil core should be taken at several locations on the site. Analyzing the core may or may not reveal the presence of a clay-rich layer. To determine if the bedrock is permeable, samples should be collected and tested. A piezometer, completed in the bedrock could indicate if the bedrock is saturated, and/or permeable.

REFERENCES

Amoozegar, A., 1989, A compact constant-head permeameter for measuring saturated hydraulic conductivity of the vadose zone. Soil Sci. Soc. Am. J., Vol. 53:1356-1361, September-October 1989.

Anderman, E.R., 1993, Field verification of stream-aquifer interactions, Colorado School Mines Survey Field, Master of Engineering thesis, Department of Geology and Geological Engineering, Colorado School of Mines, Golden, Colorado.

Bissett, L.L., 1994, Field assessment of recharge and stream-aquifer interaction under aric conditions and comparison with computer representations, Master of Engineering thesis, Department of Geology and Geological Engineering, Colorado School of Mines, Golden, Colorado.

Bouwer, Herman, and Rice, R.C., 1976, A slug test for determining hydraulic conductivit of unconfined aquifers with completely or partially penetrating wells, Water Resources Research, 12(3), 423-428.

Bouwer, Herman, 1989, The Bouwer and Rice slug test - an update, Groundwater, 27(3), 304-309.

Demir, Z., and Narasimhan, T.N., 1994, Improved interpretation of Hvorslev Tests, Jourr of Hydraulic Engineering, 120(4), 477-494.

Emerick, John C., 1994, Personal communication, Associate Professor of Environmental Sciences and Engineering Ecology.

Farnsworth, Richard K., Thompson, E.S., and Peck, E.L., June 1982, Evaporation Atlas f the Contiguous 48 United States, NOAA Technical Report NWS 33.

Fetter, C.W., 1988, Applied Hydrogeology, Macmillan Publishing, Co., New York.

Freeze, R. Allan, Cherry, John A., 1979, Groundwater, Prentice-Hall, Inc., Englewood Cliffs, N.J.

Harza, L.F., 1935, Uplift and seepage under dams, Trans. Am. Soc. Civ. Eng., v 100, p 1352 - 1385.

Hvorslev, M. Juul, 1951, Time lag and soil permeability in ground-water observations, Bulletin No. 36, Waterways Experiment Station, Corps. of Engineers, U.S. Army.

Kohler, M.A., Nordenson, T.J., and Baker, D.R., 1959, Evaporation maps for the United States: U.S. Weather Bureau Technical paper No. 37, 13 p. [5 plates].

LeRoy, L.W., 1946, Stratigraphy of the Golden-Morrison area, Jefferson County, Colorado: Colorado School of Mines Quart., vol. 41, no. 2, 115 p.

Reynolds, W.D., D.E. Elrick, and G.C. Topp, 1983, A reexamination of the constant head well permeameter method for measuring saturated hydraulic conductivity above the water table, Soil Sci. 136:250-268.

Reynolds, W.D., D.E. Elrick, N. Baumgartner, and B.E. Clothier, 1984, The "Guelph Permeameter" for measuring the field-saturated soil hydraulic conductivity above the water table: 2. The apparatus Proc. Can. Hydrol. Symp. Quebec City, Quebec, 11-12 June 1984.

Reynolds, W.D., Elrick,D.E., Clothier, B.E., 1985, The constant head well permeameter: Effect of unsaturated flow., Soil Science, Vol. 139, No. 2.

Scott, G.R., 1972, Geologic map of the Morrison Quadrangle, Jefferson County, Colorado., U.S.G.S. I-790-A.

Stephens, D.B., Neuman, S.P., 1982(a), Vadose zone permeability tests: summary, Am. Soc. Civ. Eng. Proc. J. Hydrol. Div. 108:623-639.

Stephens, D.B., Neuman, S.P., 1982(b), Vadose zone permeability tests: steady state results., Am. Soc. Civ. Eng. Proc. J. Hydrol. Div. 108:640-659.

Taylor, Donald W., 1948, Fundamentals of soil mechanics, John Wiley & Sons, Inc.

Watters, Gary Z., Rao, Manam V.P., 1971, Hydrodynamic effects of seepage on bed particles, Journal of the Hydraulics division, Proceedings of the American Society of Civil Engineers, HY3, March 1971, pg 421-439.

Weimer, Robert J., Personal communication, (Professional Engineer); Professor Emeritus of Geological Engineering

APPENDIX A Constant Head Permeameter Construction

The constant head permeameter consists of four major components; 1) constant h bottle, 2) water reservoir, 3) flow measuring reservoir, and 4) a cylinder that is placed i the stream bottom. The constant head bottle, and the reservoirs, collectively known as t Mariotte Bottles, function to maintain a constant level of water in the cylinder using the Mariotte principle. Clear plastic pipes are used for the construction of the Mariotte Bott

The constant head bottle (bottle 1), is made from a 1 inch diameter clear pipe mounted on a water tight base. A two-hole rubber stopper seals the top. Two brass tub are pushed through the stopper for air flow. One of the air tubes, labeled 'A' on Figure is open to atmospheric pressure and ends below the water level. This tube is adjustable t allow variable levels of negative pressure above the water. The other air tube, 'B', conne the air pocket of bottle 1 to the water in the flow measuring reservoir with 1/4 inch diam rubber tubing and a quick connect.

The flow measuring reservoir (bottle 2), is a 2.5 inch diameter clear plastic pipe mounted on a water tight base. A two-hole #13.5 rubber stopper seals the top. Two bra rods are pushed through the stopper for air flow. One is the air flow tube, 'B' from abo The other tube, 'C' connects the air space of bottle 2 to the air space of the water reserv bottle 3.

The water reservoir, bottle 3, is made from a 4-inch diameter clear plastic pipe. T reservoir is used for highly permeable soils when the flow measuring reservoir has an insufficient volume of water to maintain flow for an adequate test. Bottle 3 is sealed with one holed #15 rubber stopper with a plexiglass back bolted on for support. This reservoi connected to the flow measuring reservoir by two tubes. One, labeled 'C', connects the a space to the air space in bottle 2 via a 1/4 inch diameter rubber tube and a valve. The wa in bottle 3 is connected to the water in bottle 2 with a 5/8 inch diameter rubber tube and a inline stopcock, labeled 'D' in the figure.

The cylinder inserted into the stream bed is made of an eight-inch PVC pipe. A th metal edge was riveted on the inside of the pipe, with one inch sticking out below the bott of the pipe to slice through the vegetation and sand of the stream bottom. A 5/8 inch rubb tube and an inline stopcock connects the cylinder to the flow measuring reservoir, labeled in the figure. The three bottles are mounted to a metal plate for support and portability.

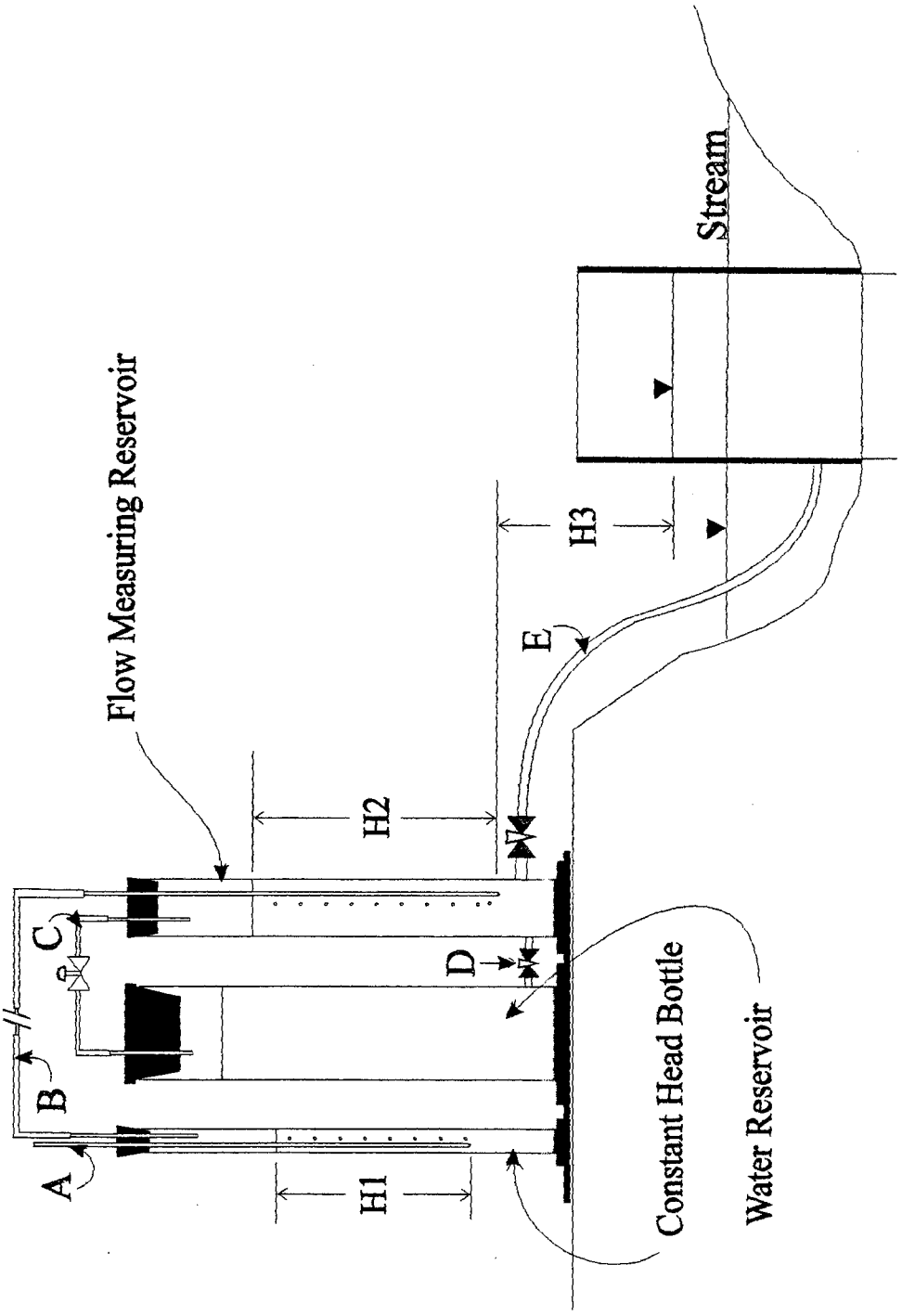

Figure A1 Constant head permeameter.

APPENDIX B Mariotte Bottle.

A discussion of the Mariotte principle applied to the constant head permeameter follows. In the constant head bottle (Figure A1), air passing through the air tube, 'A', h displace the water from inside. To do this, a sufficient vacuum is required in air tube 'B A sufficient vacuum is equivalent to a force large enough to displace the water column of length H1 out of brass tube 'A'. Air transfer through the bottles occurs when the water fully displaced from the brass tubes and bubbles flow out. The force required in the air space of bottle 1 is Pa - H1, where H1 is the distance from the water level in the bottle a the bottom of the brass tube, and Pa is atmospheric pressure.

The flow measuring reservoir, bottle 2, works in the same fashion, but rather than having a brass tube open to the atmosphere, it is connected to bottle 1. The outlet of bott is connected to the cylinder in the stream. In order for water to flow out of the reservoir volume of air is required to replace to lost volume of water. The sole source of this air comes from bottle 1. Additional vacuum is required to pull the air from bottle 1 through water in bottle 2. This additional vacuum is the equivalent of the displaced water column length H2, as shown in Figure A1. The pressure in the air space in the flow measuring reservoir is Pa - H1 - H2. By summing the forces from bottle 2 to the cylinder's water le one finds that the distance from the cylinder's water level to the bottom of the brass tube i bottle 2, H3, is the same as H1 in bottle 1.

Assumptions made for the permeameter are; the head in the cylinder is constant, th seal between the metal edge and the soil is good, the sphere of influence below the cylinde at steady state when piezometer levels stabilize, and only vertical K is being measured.

APPENDIX C Completion Diagrams.

DH-3

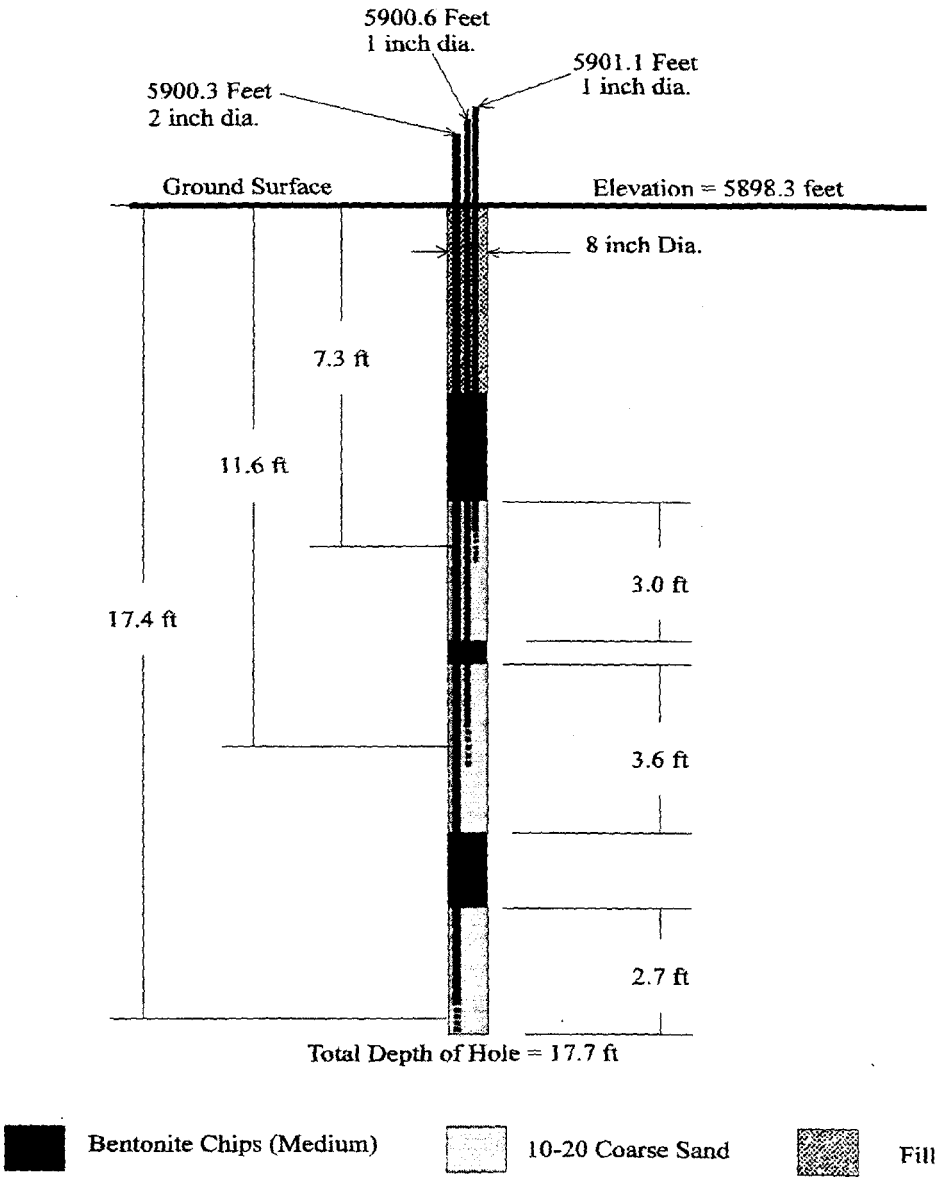

Figure C1 Completion diagram for DH-3.

DH-4

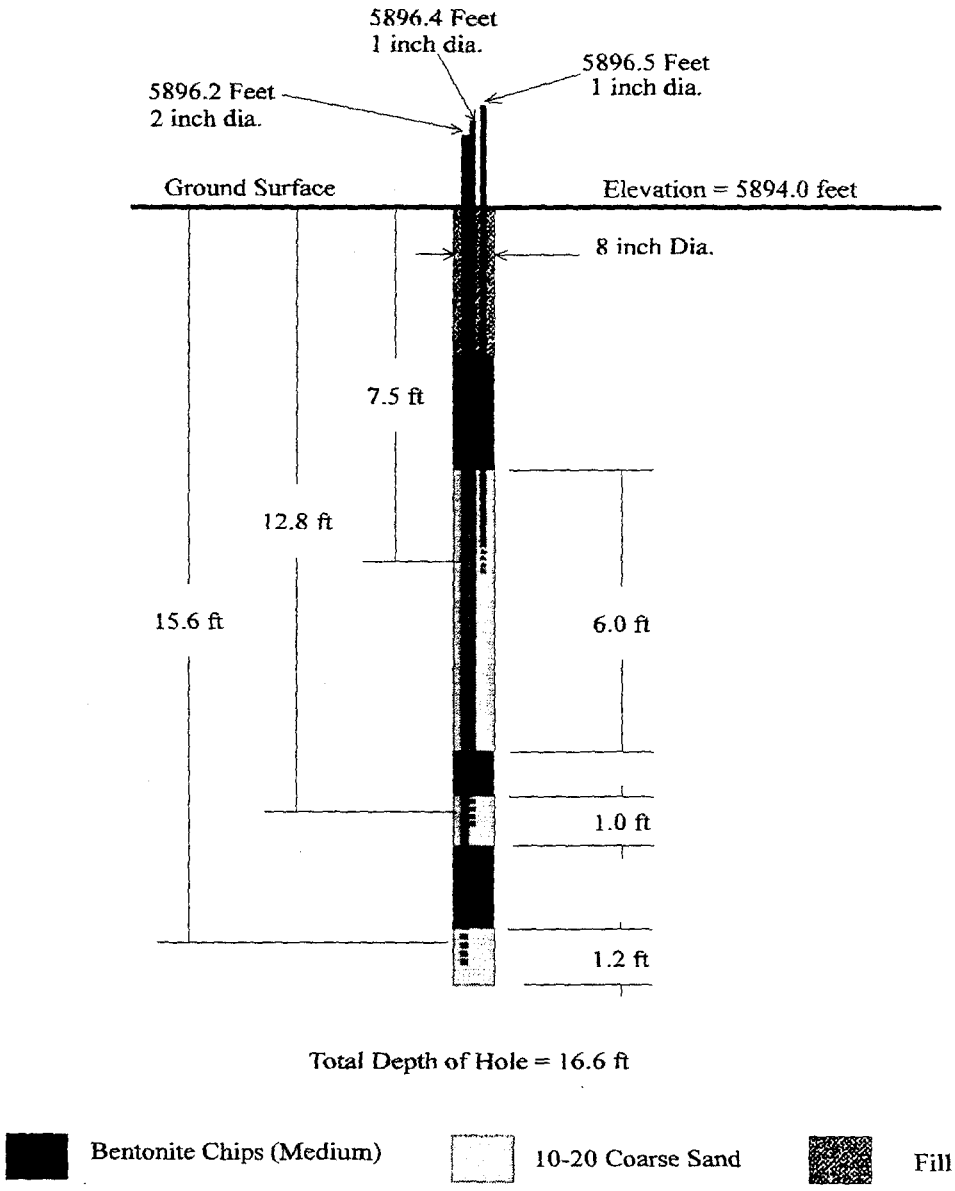

Figure C2 Completion diagram for DH-4.

DH-5

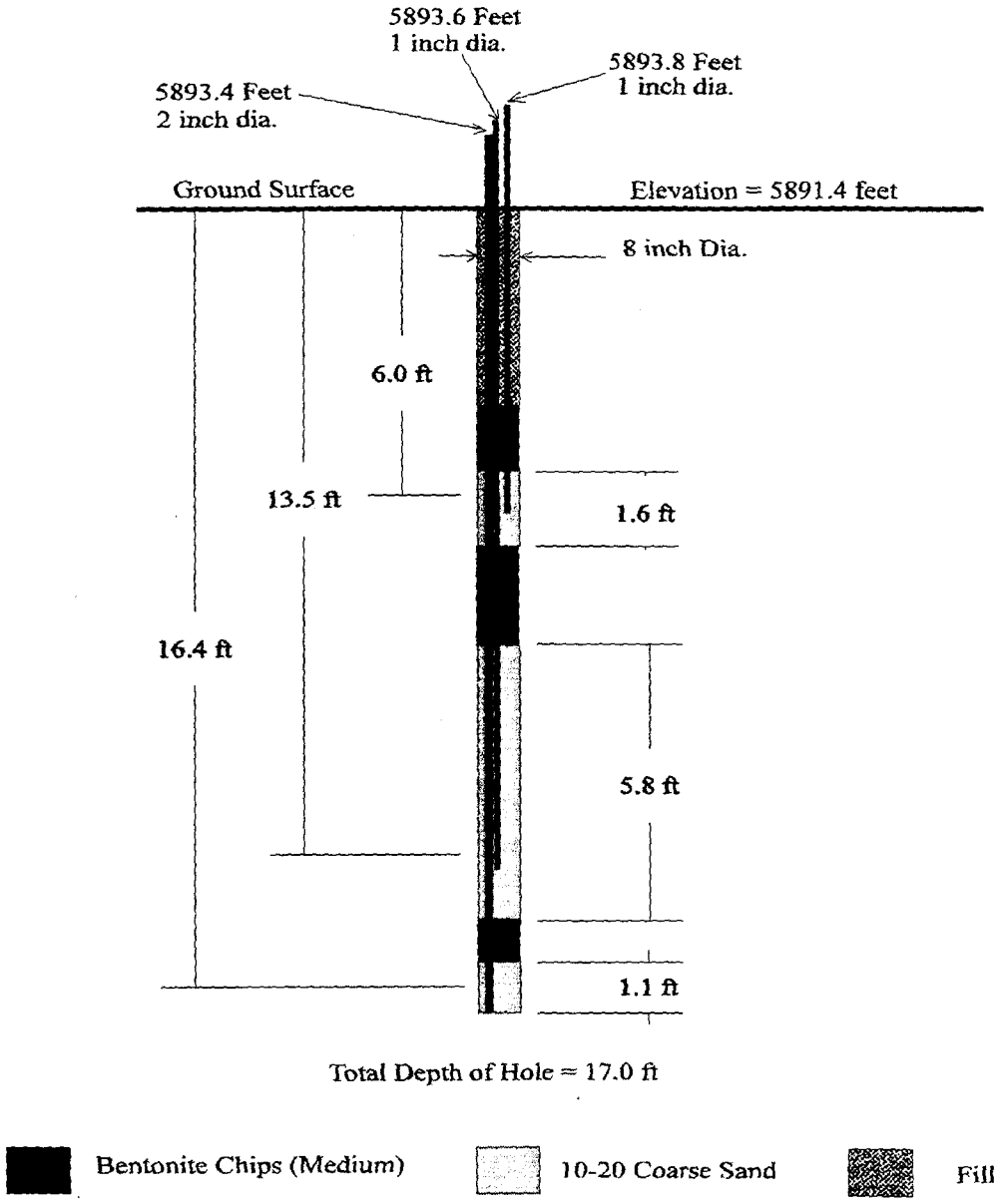

Figure C3 Completion diagram for DH-5.

DH-6

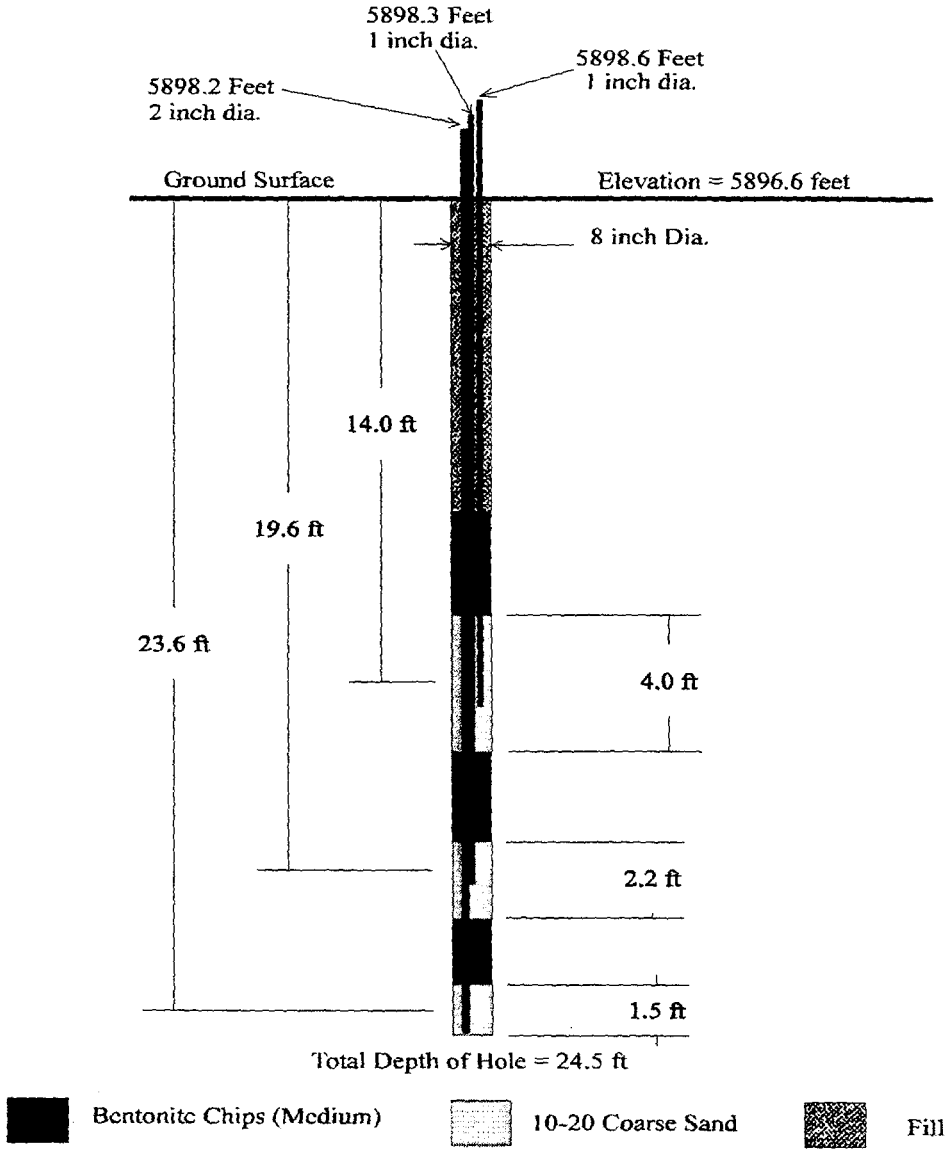

Figure C4 Completion diagram for DH-6.

APPENDIX D Stream Stage v. Discharge.

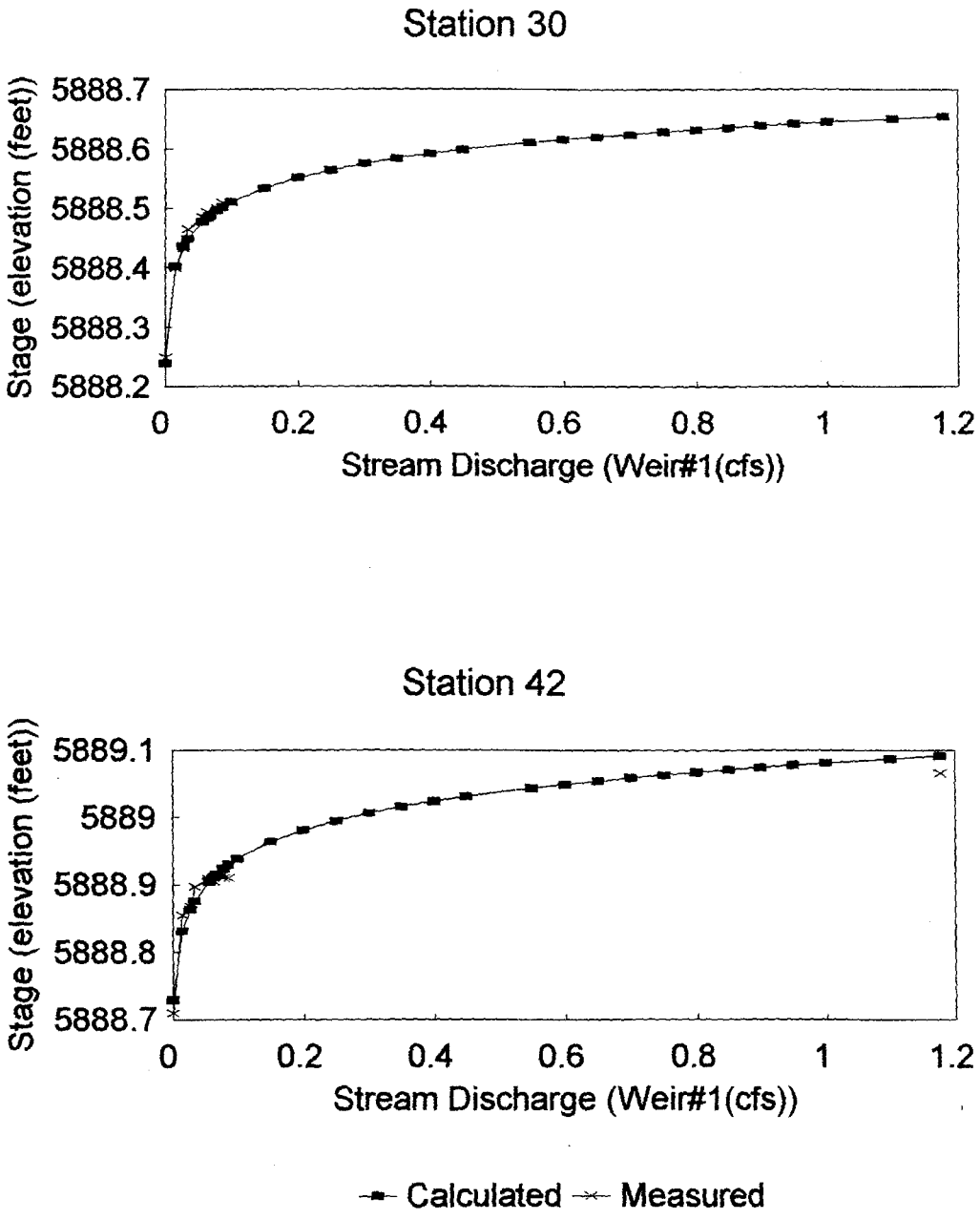

Figure D1 Stream stage v. discharge.

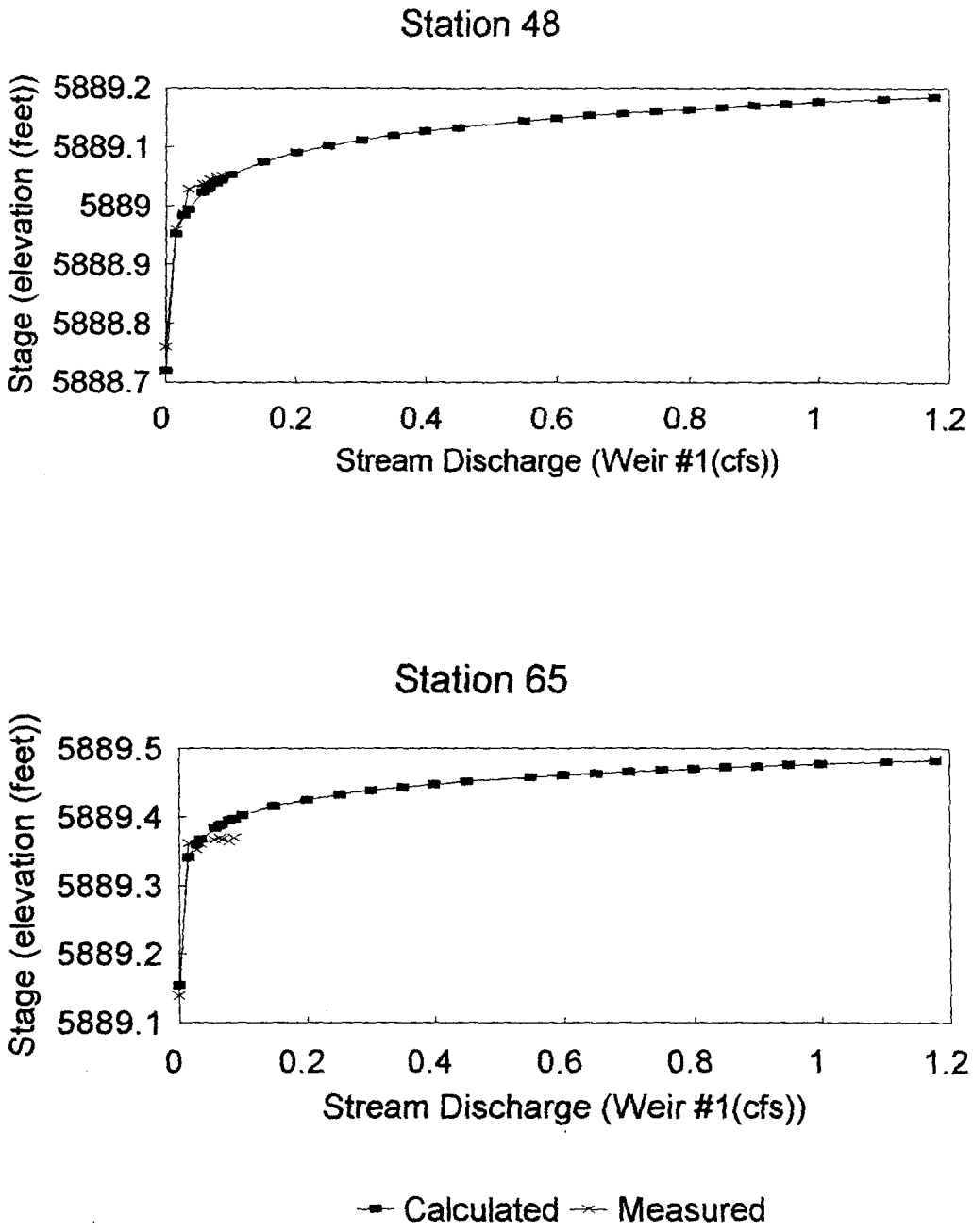

Figure D1 (continued) Stream stage v. discharge.

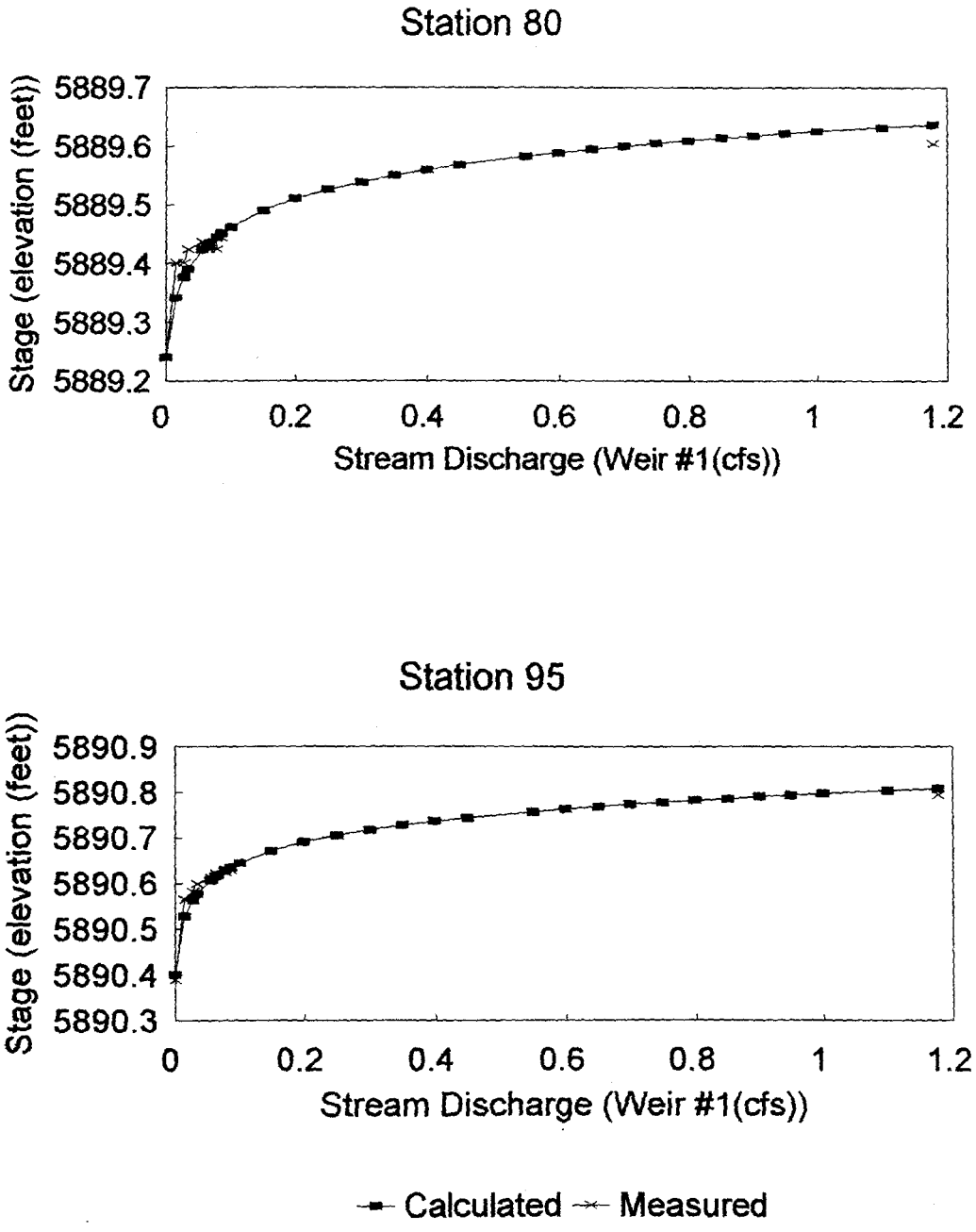

Figure D1 (continued) Stream stage v. discharge.

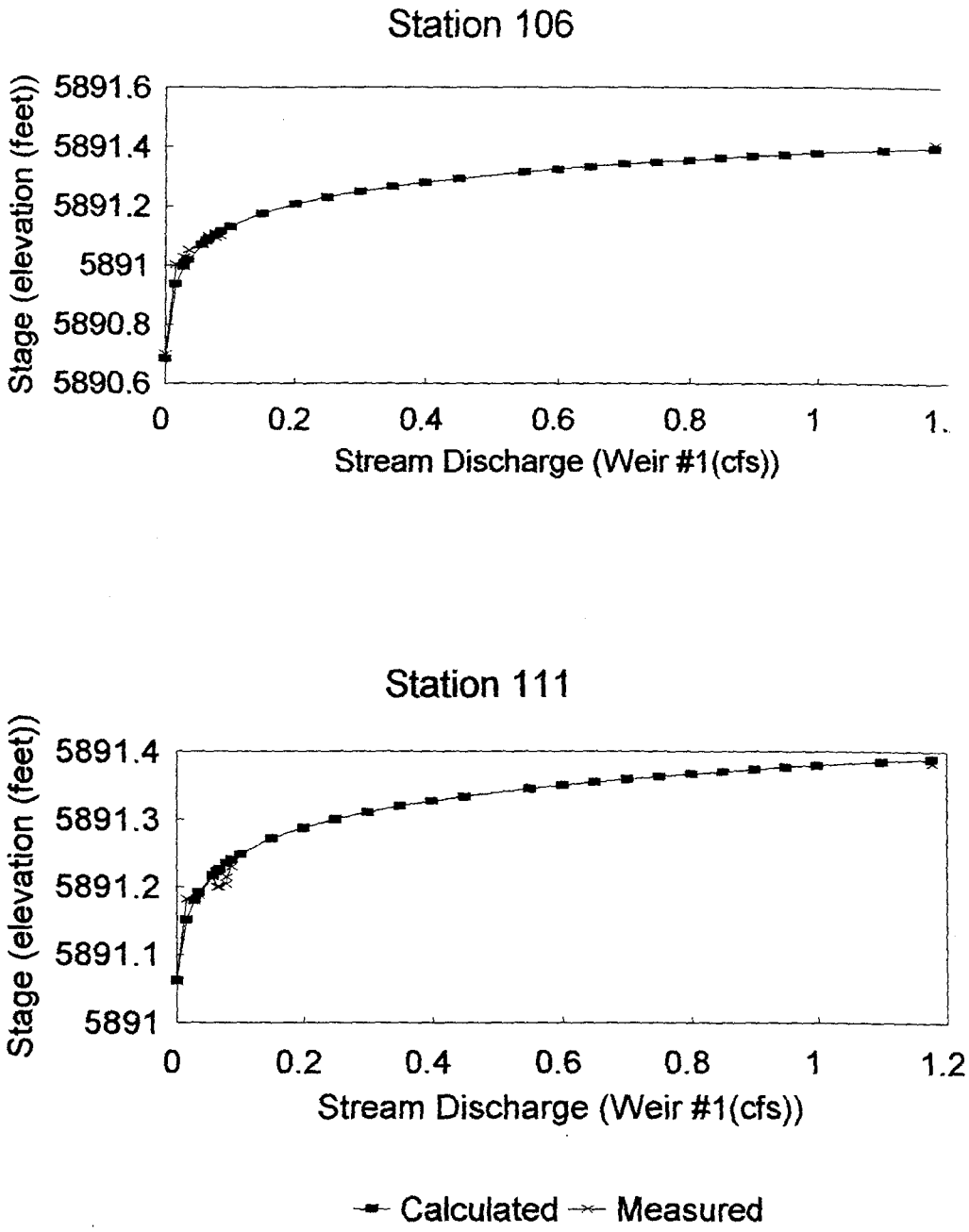

Figure D1 (continued) Stream stage v. discharge.

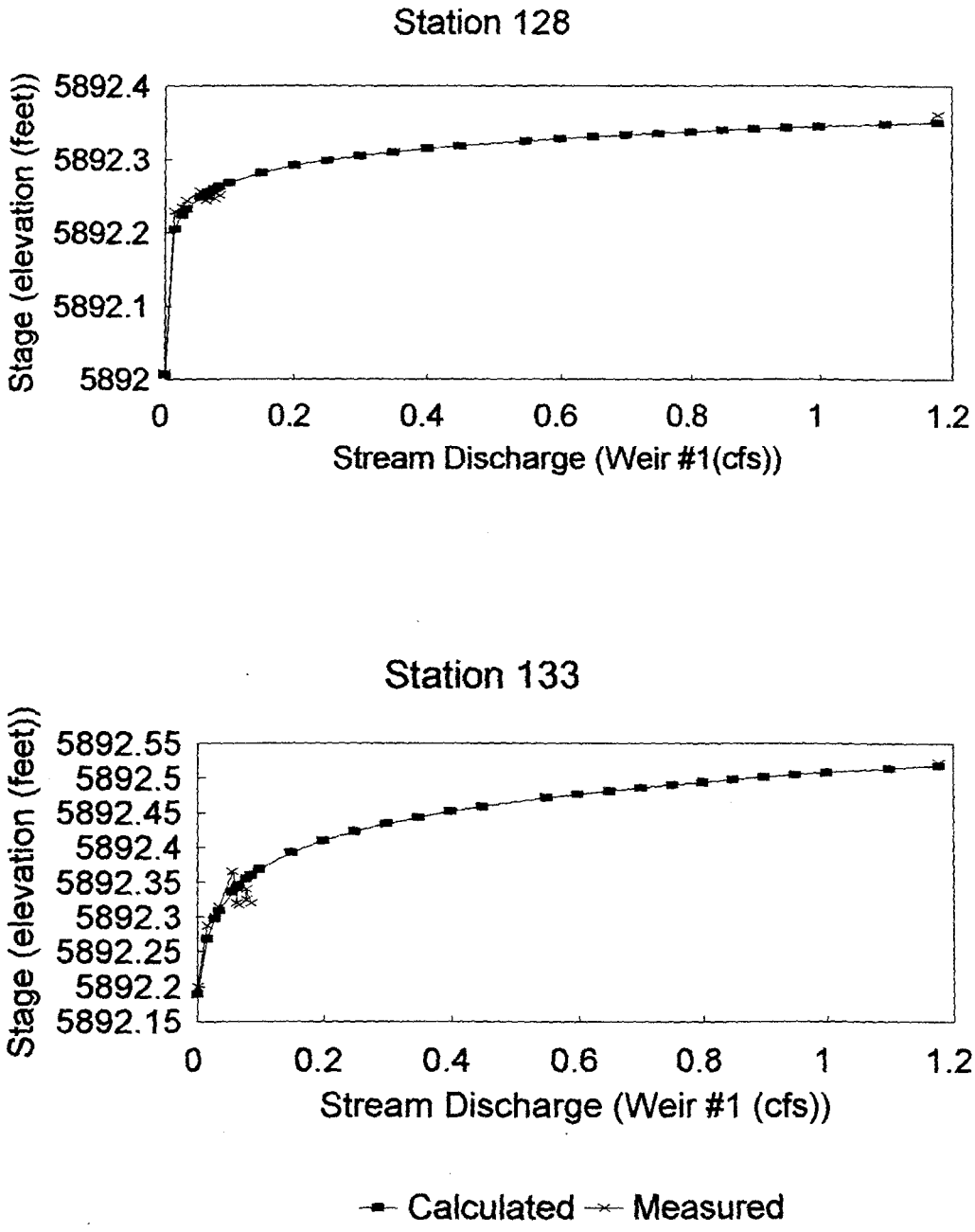

Figure D1 (continued) Stream stage v. discharge.

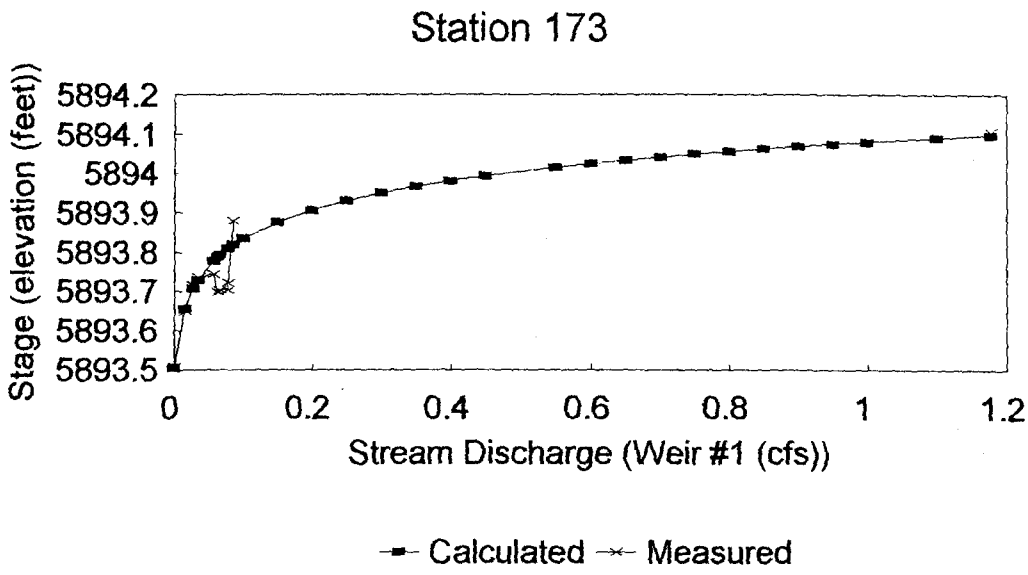

Figure D1 (continued) Stream stage v. discharge.